Accepted Manuscript

Indole Based Peptidomimetics as Anti-inflammatory and Anti-hyperalgesic Agents: Dual Inhibition of 5-LOX and COX-2 Enzymes

Palwinder Singh, Parteek Prasher, Parvirti Dhillon, Rajbir Bhatti

PII: S0223-5234(15)30007-6

DOI: 10.1016/j.ejmech.2015.04.044

Reference: EJMECH 7859

To appear in: *European Journal of Medicinal Chemistry*

Received Date: 5 February 2015

Revised Date: 10 April 2015

Accepted Date: 20 April 2015

Please cite this article as: P. Singh, P. Prasher, P. Dhillon, R. Bhatti, Indole Based Peptidomimetics as Anti-inflammatory and Anti-hyperalgesic Agents: Dual Inhibition of 5-LOX and COX-2 Enzymes, *European Journal of Medicinal Chemistry* (2015), doi: 10.1016/j.ejmech.2015.04.044.

Indole Based Peptidomimetics as Anti-inflammatory and Anti-hyperalgesic Agents: Dual Inhibition of 5-LOX and COX-2 Enzymes

Palwinder Singh,[a] Parteek Prasher,[a] Parvirti Dhillon,[b] Rajbir Bhatti[b]*

[a]UGC Sponsored Centre for Advanced Studies, Department of Chemistry, Guru Nanak Dev University, Amritsar – 143005, India; [b]Department of Pharmaceutical Sciences, Guru Nanak Dev University, Amritsar – 143005, India

Graphical Abstract

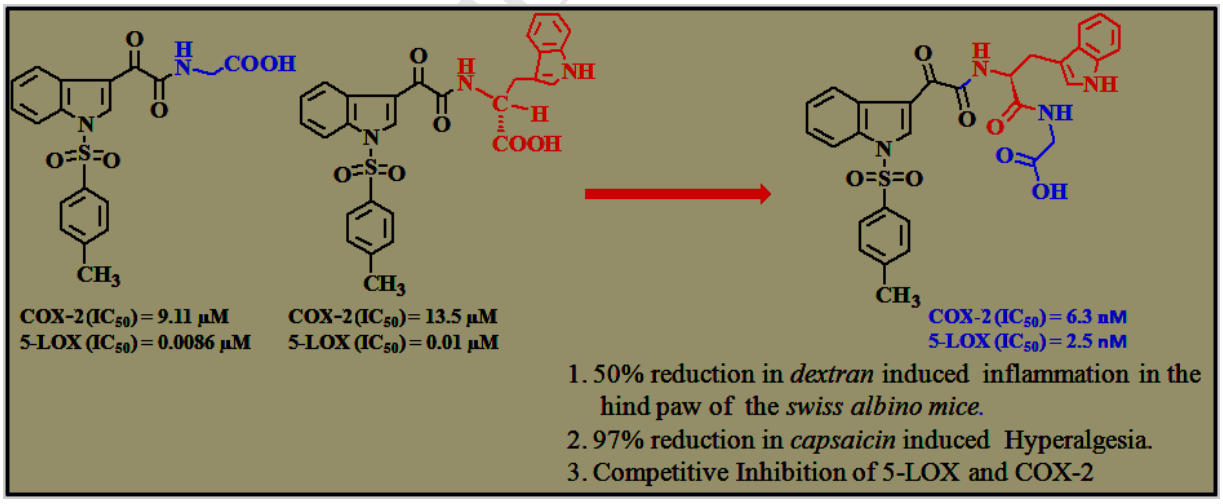

Presence of both Gly and Trp residues at C-3 substituent of N-tosylated indole increased the anti-inflammatory activity of the molecules.

Indole Based Peptidomimetics as Anti-inflammatory and Anti-hyperalgesic Agents: Dual Inhibition of 5-LOX and COX-2 Enzymes

Palwinder Singh,[a] Parteek Prasher,[a] Parvirti Dhillon,[b] Rajbir Bhatti[b]*

[a]UGC Sponsored Centre for Advanced Studies, Department of Chemistry, Guru Nanak Dev University, Amritsar – 143005, India

[b]Department of Pharmaceutical Sciences, Guru Nanak Dev University, Amritsar – 143005, India

KEYWORDS. Peptidomimetics; Anti-inflammatory; Anti-hyperalgesic; COX-2, 5-LOX inhibitors.

ABSTRACT. The indoles bearing a tosyl group at N-1 and a dipeptide substituent at C-3 were screened for anti-inflammatory and anti-hyperalgesic activities. Some of the compounds made significant reduction in the dextran induced swelling and capsaicin induced pain in the albino mice. About 95% reversal in capsaicin induced pain occurred in the presence of 5 mg Kg^{-1} of compound **7b**, **7d** and **7h** while diclofenac showed 90% reversal when its 10 mg Kg^{-1} dose was used. In order to examine the mode of action of these compounds; COX-1, COX-2 and 5-LOX enzyme immunoassays were performed. The IC_{50} of compound **7b** for COX-2 and 5-LOX were in the nM range: 5-LOX, IC_{50} = 2.0 nM; COX-2, IC_{50} = 6.3 nM, selectivity for COX-2 over COX-1 was 351. The interactions of the compounds with COX-2 and 5-LOX were supported by

the physical parameters including K_i, K_a and ΔG. The most potent compounds **7b**, **7d** and **7h** showed no toxicity to the animals and were identified as the promising leads for anti-inflammatory drugs.

INTRODUCTION

The discovery of arachidonic acid metabolism [1] helped in understanding the root cause for several inflammatory diseases [2]. The arachidonic acid cascade catalyzed by the enzymes lipoxygenases [3] and cyclooxygenases [4] for the biosynthesis of leukotrienes [5] and prostaglandins [6], respectively is responsible for the chronic inflammation in humans. The consequent ailments are expressed in the form of asthma [7], atherosclerosis [8], irritable bowel syndrome [9], rheumatoid arthritis [10] and cancer [11]. Hence, the continuous threat of the severe inflammation problems is making the medicinal research to focus on exploiting new treatment strategies. Targeting the induced isoform of cyclooxygenase, viz. cyclooxygenase-2 (COX-2), the anti-inflammatory medication [12] made a long journey from SAIDs' and NSAIDs' to COXIBS [13]. Likewise, the consistent efforts have made zileuton [14], MK885 and MK0591 [15] (Chart 1) to reach to the market for the treatment of inflammatory diseases through the inhibition of LOX enzymes. Irrespective of the development of a number of new chemical entities targeting COX-2 and LOX enzymes, the progress of these compounds towards clinical stage is hampered by their severe cardiovascular side effects [16]. Rofecoxib and valdecoxib were even withdrawn from the market due to these limitations [17].

Recently, we reported cyclic amine / amino acid appended indoles as highly effective 5-LOX inhibitors [18, 19]. Compounds **4** and **5** (Chart 1) have shown appreciable IC_{50} for 5-LOX and also exhibited significant anti-inflammatory activities. Compound **5** was also found to inhibit COX-2 enzymatic activity with IC_{50} 9 – 13 μM. The advantage of developing the new drugs by the modification of the existing ones [20] and the benefits of the practice of polypharmacology [21] made us to refine the structures of compounds **4** and **5** so that their anti-inflammatory activity gets improved. Since the activity of compounds **5**, carrying one amino acid at C-3

substituent, was improved over that of compounds **4**; it was planned to extend the amino acid chain at the C-3 substituent of compound **5** and thereby compounds **6** and **7** (Chart 1) were designed. Care was taken that LogP and total polar surface area (TPSA) of the compounds are within the range of Lipinski values when amino acids were chosen for the extension of C-3 substituent in compounds **6**.

<Chart 1>

2. Results and Discussion

2.1. Selection of the compounds

Amongst the previous set of compounds [18], those having Gly and Trp residues as a part of their C-3 substituent showed appreciable inhibition of 5-LOX. It was envisaged that the combination of these amino acids in one molecule may increase its anti-inflammatory potency. Hence, introducing Gly – Trp dipeptide at the C-3 substituent and the possible stereoisomers led to the design of compounds **6a** – **d**. In order to increase the variation, His and Glu based dipeptide was also introduced at C-3 position of indole, thus compounds **6e – h** were synthesized. Compounds **7**, the respective acids of compounds **6**, were also included for the biological screening (Chart 2).

<Chart 2>

Compounds **6a – h** and **7a – h** were docked in the active site of 5-LOX and COX-2 (Table S1 – S3). Also, the LogP and TPSA of these compounds were calculated [22] (Table S4) which were found to be within the limits of Lipinski values. It was noticed that the isomers of compounds **6** and **7** with *S*- configuration at the C_α position of amino acid/s exhibited better interactions (docking score) when docked in the active site of 5-LOX and COX-2 enzymes (Table S1 – S3). Hence, compounds **6b**, **6d**, **6h** and their corresponding acids **7b**, **7d**, **7h** were selected as the

potential candidates for the present studies. For making the comparison, compounds **6a**, **6c**, **6e**, **6i** and **7a**, **7c**, **7e**, **7i** were also synthesized and included in the biological assays.

2.2. Synthesis

Oxalyl chloride was slowly added to the ice cooled solution of indole (**8**, Scheme 1) in dry ether. The yellow colored solid (**9**) was filtered and dissolved in dry acetonitrile (ACN) followed by the addition of K_2CO_3. The appropriate L-amino acid ester hydrochloride, after neutralization with triethylamine, was added to the ACN solution of compound **9**. All additions to the reaction mixture were made at 0 ^oC. C-3 Substituted indoles **10 – 12** (Scheme 1) were purified through column chromatography using ethyl acetate – hexane as the eluent.

<Scheme 1>

After washing with dry hexane, NaH (1 mmol) was suspended in dry ACN. Compound **10** (1 mmol) and p-toluenesulphonyl chloride (1.2 mmol) were added to the NaH suspension in ACN keeping the reaction temperature 0 – 5 ^oC. On usual work up of the reaction mixture, compound **13** was isolated. Using the same reaction conditions, tosyl group was introduced at N-1 of compounds **11** and **12** and respective compounds **14** and **15** were procured (Scheme 2). Further treatment of compounds **13 – 15** with 1N NaOH in acetone – H_2O (1:1) provided compound **16 – 18** (Scheme 2)**.**

<Scheme 2>

In order to introduce second amino acid; the solution of compound **16**, triethyl amine and ethyl chloroformate in dry DCM at 0 ^oC was treated with neutralized solution of glycine methyl ester hydrochloride. The coupling reaction was completed in 25 – 30 min and compound **6i** was isolated (Scheme 3**)**. Similarly, compound **6d**, **6b** and **6h** were synthesized from compound **16**, **17** and **18**, respectively.

<Scheme 3>

Compounds **6** were converted into corresponding compounds **7** by hydrolyzing the ester component with 1N NaOH (Scheme 4). The optical purity of compounds **7** was checked by recording their LC-MS using chirobiotic® T 10 μm chiral HPLC column. Synthesis of compounds **6a**, **6c**, **6e** and their corresponding acids **7** is given in the supplementary data.

<Scheme 4>

3. Biological studies

3.1. Anti-inflammatory and anti-hyperalgesic activity

The anti-inflammatory and anti-hyperalgesic activities of the compounds were checked on Swiss albino mice (25-35 g) of either sex [23, 24]. The animals were divided into different groups of five each. Group I, the control, comprised of animals treated with vehicle, and group II was treated with standard reference drug – diclofenac (10 mg kg^{-1}). All the test compounds were administered at two doses of 5 and 10 mg Kg^{-1}. Compound **7i** was given to groups III, IV; **7d** to groups V, VI; **7b** to groups VII, VIII and groups IX, X were given **7h** at both doses, intraperitoneally. Dextran was administered at a dose of 1% by subplantar injection 30 min after the respective treatments and paw thickness was measured using vernier calipers after 1, 2, 3, 4, 6 and 24 h of dextran injection.

Anti-inflammatory activity of **7b** and **7h** was observed to be most significant in comparison to the control. For **7b**, the dose of 5 mg Kg^{-1} produced 47% reduction in the paw thickness (w.r.t. control) which further improved to 49% on increasing the dosage to 10 mg Kg^{-1} at 4h (Figure 1). Similar to the effect shown by compound **7b**, 5 mg Kg^{-1} dose of compound **7h** caused 45% reduction in the paw thickness after 4h which was improved to 48% when 10 mg Kg^{-1} dose was used. The effect of both **7b** and **7h** was comparable to that of diclofenac (42%).

<Figure 1>

For studying the anti-hyperalgesic effect of the compounds, 20 μL of capsaicin was injected into the plantar surface of the right hind paw. Animals were observed individually for 10 min after capsaicin administration and the number of paw lickings and twitchings was recorded as an indicator of hyperalgesia. Animals were divided into 10 groups of 5 each. All treatments were administered intraperitoneally 30 min before capsaicin injection. Group I was the control group in which the animals were injected vehicle; in group II, the animals were injected diclofenac at a dose of 10 mg Kg^{-1}. Group III and IV animals were injected compound **7i** at doses of 5 and 10 mg Kg^{-1}, respectively; group V and VI animals were injected compound **7d** at doses of 5 and 10 mg Kg^{-1}, respectively; group VII and VIII animals were given compound **7b** at doses of 5 and 10 mg Kg^{-1}, respectively and group IX and X animals were injected compound **7h** at doses of 5 and 10 mg Kg^{-1}, respectively.

Compounds **7b**, **7d**, **7h** and **7i** were found to have a significant anti-hyperalgesic effect at dose of 5 mg Kg^{-1} and a further increase in dose (10 mg Kg^{-1}) of compound **7i**, **7b** and **7h** did not result in corresponding increase in anti-hyperalgesic effect whereas compound **7d** showed an appreciable increase in the anti-hyperalgesic effect at dose 10 mg Kg^{-1} (Figure 2). The number of paw lickings was remarkably reduced by 96% (w.r.t. control) on treatment with compound **7b**. A similar effect was observed in the presence of compound **7h** (95%) and **7i** (90%). Unlike other compounds, amplification in the analgesic effect when increasing the dose was observed for compound **7d** which made 88% reduction in paw lickings at 5 mg Kg^{-1} and 96% reduction at 10 mg Kg^{-1}. Interestingly, all the compounds showed slightly better but not statistically significant anti-hyperalgesic response as compared to diclofenac (90%).

<Figure 2>

3.2. Toxicity

Studies for checking acute toxicity of the most active compound **7b** were conducted as per OECD guidelines- 423 (OECD, 2001) [25]. Three groups of three animals in each group were administered compound **7b** at 5 mg, 50 mg and 300 mg dose. The animals were observed continuously for the first 4 h for any signs of toxicity. Thereafter, the animals were observed at regular intervals for the first 24h followed by once daily for the next 14 days. After 14 days, the histological studies on the liver, kidney and heart did not show any signs of behavioural abnormality. The histological studies also did not show any gross structural variations as compared to the control (Figure S113).

4. Mechanistic investigation for the mode of action of the compounds

Prostaglandins and leukotrienes, the metabolites of arachidonic acid, generated by the cyclooxygenase (COX) and lipooxygenase (LOX), respectively are amongst the major culprits in mediating pain and inflammation. With due support from the results of the docking studies, the compounds which showed best anti-inflammatory and anti-hyperalgesic activities were checked for the inhibition of COX and LOX enzymes.

4.1. 5-LOX inhibitory activities

Compounds **6** and **7** at 10^{-4} M – 10^{-8} M concentrations were examined for the inhibition of 5-LOX enzymatic activity [26]. Similar to the previous observations [18]; compounds **7**, the corresponding acids of compounds **6**, exhibited better IC_{50} for 5-LOX. Compounds **7b** and **7d** having Gly-Trp dipeptide exhibited IC_{50} 0.002 μM and 0.004 μM, respectively against 5-LOX which was considerably improved with comparison to compounds **16** and **17** [18]. Compound **7h** with His-Glu dipeptide has IC_{50} 0.08 μM which was also improved over the parent compound **18**, the single amino acid homologue of **7h** having His as a part of its C-3

substituent. Compound **7i**, containing Gly-Gly dipeptide showed IC_{50} 0.005 μM – better than that of compound **16** (Table 1). Hence, supporting the design of the molecules, the combination of those amino acids which were part of the previous active compounds (**5/16, 17**), into a single molecule resulted in considerable increase in the 5-LOX inhibitory activity. Additionally, compound **7h** having His-Glu combination showed appreciable enzyme inhibition activity. Overall, we observed that 5-LOX inhibitory activities of compounds **6** and **7** were comparable/better than the commercially available drugs zileuton and MK0591. Remarkably, compounds **6a**, **6c**, **6e**, **7a**, **7c** and **7e,** which exhibited poor docking score for 5-LOX, were found to be less potent than their corresponding enantiomer/diastereomer for the inhibition of 5-LOX enzymatic activity.

<Table 1>

4.2. COX-1/2 inhibitory activities

Compounds **6a-e**, **6h**, **6i**, and **7a-e**, **7h**, **7i** were screened for COX-1 and COX-2 inhibition at five different molar concentrations (10^{-4} M – 10^{-8} M) [27]. As evidenced by the IC_{50} and selectivity index data, these compounds displayed higher efficacy towards the inhibition of COX-2 enzyme over COX-1 enzyme (Table 1). Compound **7b**, with IC_{50} 0.0063 μM for COX-2 and 2.21 μM for COX-1 and selectivity index 351 (for COX-2 over COX-1), was found to be the most active. Compound **7d** with IC_{50} 0.099 μM against COX-2 and a selectivity index 440 was another potent and selective COX-2 inhibitor. Compound **7h** also displayed appreciable IC_{50} 0.54 μM for COX-2 enzyme but its selectivity over COX-1 was poor. The IC_{50} of compounds **7b** and **7d** against COX-2 was much better than that of commercially available drugs wogonin [28], indomethacin [29], celecoxib [30], SC-558 and diclofenac [31].

Intriguingly, these compounds were identified with highest anti-inflammatory and anti-hyperalgesic activities amongst the compounds investigated here. In this enzyme immunoassay, compound **6b** exhibited IC_{50} 0.047 for COX-2 with selectivity index 210. The enzyme inhibitory activities of compounds **6a**, **6c**, **6e**, **7a**, **7c** and **7e** were found to be less than the other isomeric compounds.

Therefore, it seems that 5-LOX and COX-2 are the cellular targets of these compounds and inhibition of their enzymatic activity imparts anti-inflammatory features to the compounds. The interactions of the compounds with these enzymes were also supported by the other physical experiments.

4.3. Kinetic Studies: UV-vis and isothermal calorimetric experiments.

In order to support the results of enzyme immunoassays and for checking the extent of interactions between the compounds and COX-2/5-LOX enzymes, the kinetic and thermodynamics of the enzyme – ligand interactions were investigated.

4.3.1 K_a and K_i of compounds 6 and 7 for 5-LOX and COX-2.

K_a (association constant) quantifies the strength of the enzyme inhibitor complex ($E + I \overset{Ka}{\rightleftharpoons} EI$) while K_i is the concentration of the inhibitor which is required to decrease the maximum rate of reaction by half. Smaller the K_i, lesser is the concentration of inhibitor required to decrease the enzymatic activity. For non-competitive or uncompetitive kinetics, K_i equals IC_{50} whereas for competitive kinetics, K_i is different from IC_{50}. Hence, it is a relevant parameter for not only determining the effectiveness of the compound (inhibitor) against the enzyme but also hints towards the mode of inhibition of the enzyme. K_a and K_i of compounds **6** and **7** for 5-LOX and COX-2 were calculated from the UV spectral data with the aid of Benesi Hildebrand equation 1 [32].

$1/(A_f - A_{obs}) = 1/(A_f - A_{fc}) + 1/K_a(A_f - A_{fc})[L]$ (1)

A_f = absorbance of free host, A_{obs} = absorbance observed, A_{fc} = absorbance at saturation

The K_i (inhibitor concentration required to produce half maximum inhibition) was calculated with equation 2.

$K_i = IC_{50}/(1+[L]/K_d)$ (2), K_d = dissociation constant

Using K_a, ΔG (Gibbs free energy) for the enzyme-compound complex was also calculated from the equation 3.

$\Delta G = -2.303\ RT \log K_a$ (3), K_a = association constant

<Table 2>

It is evident from the data given in table 2 that the compounds **7b** and **7d**, with best IC_{50} for 5-LOX, are showing ΔG -37.20 and -36.02 KJ mol^{-1} K^{-1}, respectively; K_a 3.36 x 10^6 M^{-1} and 2.06 x 10^6 M^{-1}, respectively and K_i 0.042 and 0.064 μM, respectively against 5-LOX. Compounds **6i** and **7h** also exhibited appreciable free energy change while interacting with the enzyme, having respective ΔG -30.33 and -32.22 KJ $mol^{-1}K^{-1}$; K_a 2.08 x 10^5 M^{-1} and 1.99 x 10^5 M^{-1} and K_i 0.097 and 0.536 μM for 5-LOX. The K_a and K_i values were also calculated for COX-2 enzyme. Compound **7d** was having ΔG -37.15 KJ mol^{-1} K^{-1}; K_a and K_i 3.25 x 10^6 M^{-1} and 0.005 μM, respectively while the same parameters for compound **7b** and **7h** were ΔG -31.48, -33.60 KJ mol^{-1} K^{-1} ; K_a and K_i 3.29 x 10^5 M^{-1}, 0.109 μM and 7.76 x 10^5 M^{-1}, 0.012 μM (Table 2). A comparison of the IC_{50} and K_i values indicated that these compounds exhibit competitive inhibition of the enzymes which was also verified by the Lineweaver-Burk plots.

4.3.2. Isothermal calorimetric data for free energy change (ΔG) during interaction of compounds 6 and 7 with the enzymes.

Regarded as a method of choice for characterizing the thermodynamics and stoichiometry of the molecular interactions with high sensitivity, the isothermal calorimetry (ITC) experiments were performed. The binding constant (K), standard molar enthalpy (ΔH), standard molar entropy (ΔS) and stoichiometry (N) of binding of compounds **7b**, **7d**, **7h** and **7i** with 5-LOX and COX-2 were determined. The compound solution was titrated into the sample cell (containing the enzyme) using a 250 µL rotating stirrer syringe set at 500 rpm. The reference cell contained HEPES buffer. Each experiment consisted of 19 consecutive injections of 2 µL of 10 µM of the compound to the enzyme contained in the sample cell after regular time intervals of 120 s to guarantee the equilibrium in each titration point. Control experiments were performed for comparison. The total heat Q produced or absorbed in the active cell volume V_0 determined at fractional saturation Θ after the i^{th} injection is given by equation 4

$$Q = n \Theta M_t \Delta H V_0 \qquad (4)$$

Where, M_t is the total concentration of the macromolecule

n is the total number of binding sites in the macromolecule and

ΔH is the molar heat of ligand binding

The enthalpy change for the i^{th} injection ΔH(i) for an injection volume dVi is defined by equation 5.

$$\Delta H(i) = Q(i) + dV_i/V_0 [Q(i) – Q(i-1)/2] – Q(i-1) \qquad (5)$$

The various parameters determined from ITC experiments are given in table 3 and table 4 (Figure 3, Figure S112). Remarkably, the isothermal calorimetric data was quite in agreement with the physical constants calculated from the UV-vis spectral data. It was evident from all the four experiments that 5-LOX and COX-2 have one binding site for the test compound.

<Table 3>

<Table 4>

<Figure 3>

4.3.3. Competitive/non-competitive interaction of compounds 7 with 5-LOX and COX-2

In addition to the information obtained from the comparison of K_i and IC_{50}, the double reciprocal plots were also used for further confirmation about competitive/non-competitive inhibition of the enzymes by compounds **7**. The rate of change in absorbance on incremental addition of the substrate (arachidonic acid) to a fixed concentration of the enzyme during the progress of the reaction was plotted in the form of a double reciprocal plot (green trail). Similarly, the change in absorbance of the enzyme – inhibitor solution on incremental addition of arachidonic acid was recorded. The red and blue trails in figure 4 correspond to the solutions containing 10 μM and 20 μM of the inhibitor, respectively. The point where the three trails meet on extrapolation indicates the nature of inhibition: competitive or non competitive. Compounds **7b**, **7d, 7i** and **7h** displayed competitive inhibition of both 5-LOX and COX-2 (Figure 4).

<Figure 4>

4.4. Further evidences in support of mode of action of the compounds

Experiments were designed to see the effect of compound **7** on misoprostol and substance P stimulated reversal of paw lickings. Misoprostol is a synthetic prostaglandin E analogue while substance P is known to stimulate lipooxygenase and increase the production of LTB_4 [33] and also substance P has been reported to stimulate PGE_2 production by increasing the expression of COX-2 in human colonic epithelial cells [34]. Each of the seven groups having five animals were given all the treatments intraperitoneally 30 min before the capsaicin injection. Group I was control wherein the animals were injected normal saline. In group II and III animals were injected compound **7b** and **7h**, respectively at a dose of 5 mg Kg^{-1}; in group IV and V, animals were injected with misoprostol (200 μg) 30 min before compound **7b** and **7h**, respectively (5 mg

Kg^{-1}) followed by capsaicin after 30 min. In group VI and VII, animals were injected with substance-P (10 µg) 30 min before compound **7b** and **7h**, respectively (5 mg Kg^{-1}) followed by capsaicin after 30 min.

The treatment with compound **7b** and **7h** was found to produce a marked decrease in the number of paw lickings after capsaicin injection. Pretreatment of the animals with misoprostol increased the number of paw lickings slightly but not significantly. However, pretreatment with substance P was found to reverse the antihyperalgesic effect of compounds **7b** and **7h** completely (Figure 5). Therefore, these findings corroborate to the fact that compounds **7b** and **7h** decrease the hyperalgesic effect of capsaicin by inhibiting COX-2 and 5-LOX and not by COX pathway alone as misoprostol could not reverse the antinociceptive effect of compounds **7b** and **7h**.

<Figure 5>

5. Docking of compounds 7b in the active site of 5-LOX and COX-2. In order to support the experimental results, interactions of compound **7b** in the active site of 5-LOX and COX-2 were investigated with the help of molecular docking. Compound **7b** sits in the active site of COX-2 (Figure 6A, B) and interacts with Ser516 (2.14Å, 2.20Å) and Tyr371 (2.50 Å) amino acid residues through the carbonyl oxygen of amide group and carboxylic group, respectively. When docked in the active site of 5-LOX, compound **7b** exhibited H-bond interactions with Phe177 (2.61 Å, 3.57 Å) and Asn554 (1.10 Å) (Figure 7A, B).

<Figure 6>

<Figure 7>

6. Conclusions

We have performed a stepwise modification of the compounds for developing highly efficacious anti-inflammatory agents. Improved over the previous set of compounds, presence of

a dipeptide unit in the C-3 substituent of N-tosylated indole and a careful selection of the stereoisomers enabled us to identify compounds with significant anti-inflammatory and anti-hyperalgesic activities. Significant reversal in the dextran induced swelling and capsaicin induced lickings in the hind paw of the mice were observed in the presence of compounds **7b** and **7h**. Remarkably, the analgesic effectiveness of these compounds was as good as shown by diclofenac. IC_{50} of compound **7b** for COX-2 and 5-LOX was 2 nM and 6.3 nM respectively and these results indicated that COX-2 and 5-LOX might be the cellular targets of **7b**. Similar results were shown by compound **7d**. The physical parameters including K_a, K_i and ΔG of compounds **7b**, **7d** and **7h** for both COX-2 and 5-LOX enzymes were compromising for the possible hit-to-lead development. Other general observations during this work are supporting the fact that stereochemistry of the molecule play critical role during its interaction with the cellular target. Moreover the compounds with free carboxyl group at the end of C-3 substituent (**7**) were more potent than their corresponding esters **6**.

7. EXPERIMENTAL PROCEDURES

7.1. Chemistry

All reactions were performed in oven-dried glassware with magnetic stirring. Diethyl ether was distilled over activated anhydrous calcium chloride and further dried by passing sodium wire. Acetonitrile was dried by refluxing over anhydrous P_2O_5, then over anhydrous K_2CO_3 and stored over activated 4 Å molecular sieves. The reactions were monitored by thin-layer chromatography using silica gel GF254; visualization of the developed chromatogram was performed by UV and staining with iodine. Column chromatography was performed with silica gel of 100-200 mesh using hexane and ethyl acetate as eluents. ^1H and ^{13}C NMR spectra were recorded at 500 MHz and 125 MHz NMR spectrometer using $CDCl_3$ and DMSO as solvents and

TMS as internal standard. Data for ^{1}H NMR spectra are reported as chemical shift (δ ppm), multiplicity (s = singlet, d = doublet, t = triplet, m = multiplet, dd = double doublet, br s = broad singlet) and coupling constant (*J* in Hz). Data for ^{13}C and DEPT-135 NMR spectra are given in terms of chemical shift; +ve signals correspond to CH_3 and CH carbons, -ve signals correspond to CH_2 carbons while absent means a quaternary carbon. Infrared spectra were examined in KBr pallets using SP 300 PYE UNI CAM Infrared Spectrophotometer. Mass spectra were acquired using Bruker micrOTOF-Q-II mass spectrometer in +ve ESI mode.

General method of preparation of compounds 10-12:

Oxalyl chloride was slowly added to the ice cooled solution of indole **(8)** in dry ether. The yellow colored solid **(9)** was filtered and dissolved in dry ACN followed by the addition of K_2CO_3. L-Amino acid ester hydrochloride was neutralized with K_2CO_3 and added to the ACN solution of compound **9**. All the additions were done at 0 ^{o}C. C-3 Substituted indoles **10-12** were purified through column chromatography using ethyl acetate -hexane as eluent.

General method of preparation of compounds 13-18:

Compounds **10-12** (1 mmol) and NaH (1.2 mmol) (after washing with dry hexane) were taken in dry ACN. Keeping the reaction temperature 0 – 5 ^{o}C, p-toluene sulphonyl chloride (1.2 mmol) was added and the reaction mixture was stirred for 30 min. After filtration, the filtrate was concentrated under vacuum and purified by column chromatography to procure compounds **13-15** (Scheme 2). Compounds **13-15** were further treated with 1N NaOH in acetone – H_2O (1:1) to get compound **16 – 18**. All the compounds were characterized with NMR, IR, mass spectral data.

General method of preparation of compounds 6:

Solution of compound **16** and triethylamine in dry DCM was stirred at 0 ^{o}C. After 2-3 min of stirring, ethylchloroformate was added to the reaction mass. Eventually, the neutralized solution

of glycine methyl ester hydrochloride (neutralized with 1.5 equivalent solution of triethylamine) was added to the reaction mass. The coupling reaction was completed in 25 – 30 min to provide the product in 50-60% yield (Scheme 3). It should be taken into consideration that all the additions to the reaction mixture were done at 0 ^{o}C. The crude product was purified through column chromatography using ethyl acetate-hexane as eluent to get compound **6i**. Similarly, compound **6d** was synthesized from **16**. Through the same reaction procedure as depicted in scheme 5, compounds **6b** and **6h** were procured

General method of preparation of compounds 7:

Compounds **6** were dissolved in acetone-water (2:1). 1N NaOH was eventually added to this solution. The hydrolysis reaction was completed in 15-20 min to yield compounds **7** (Scheme 4). The crude product was purified through column chromatography using ethyl acetate-hexane as eluent. The optical purity of compounds **7** was checked by recording their LC-MS using chirobiotic® T 10 µm chiral HPLC column. All the compounds were characterized with NMR and high resolution mass spectra (Supporting information).

[2-(1*H*-Indol-3-yl)-2-oxo-acetylamino]-acetic acid methyl ester (10). Indole (1 mmol) was dissolved in dry ether (10 ml) and allowed to stir in an ice bath for a while till a clear solution is obtained. Afterwards, dropwise addition of oxalyl chloride (1.2 mmol) was done to this solution which immediately gives a yellow solid through an exothermic reaction. This yellow solid was filtered under vacuum and dissolved in dry ACN (25 ml) followed by the addition of K_2CO_3 (1.5 mmol). Eventually, the neutralized solution of glycine methyl ester hydrochloride (1.2 mmol) (neutralized with 1.5 equivalents of triethyl amine) was added to the reaction mass. The progress of the reaction was monitored with TLC. Reaction completes in 15-20 min. The reaction mass was washed with a minimum amount of water and extracted with ethyl acetate. Finally, the ethyl

acetate was distilled off to leave behind a crude product which was washed with absolute ethanol to get the product. Yield 95%. White solid. Mp 167 ^{o}C. IR ν_{max} (KBr, cm^{-1}): 1681 (C=O), 1750 (C=O), 2857 (C-H), 3487 (NH). ^{1}H NMR (500 MHz, $CDCl_3$) δ: 3.83 (s, 3H, OCH_3), 4.20 (d, *J*=1.5 Hz, 2H, CH_2), 7.39-7.43 (m, 2H, ArH), 7.82-8.01 (m, 2H, ArH), 8.35 (s, 1H, ArH), 8.78 (s, 1H, NH). ^{13}C NMR (normal/DEPT- 135) (125 MHz, $CDCl_3$) δ: 41.09 (CH_2, -ve), 52.74 (OCH_3), 122.79 (CH), 125.17 (CH), 125.98 (CH), 128.04 (C), 130.27 (CH), 134.43 (C), 138.48 (CH), 161.30 (C=O), 169.30 (C=O), 180.63 (C=O). ESI-MS (HRMS) calcd for $C_{13}H_{12}N_2O_4Na$ 283.0689. Found *m/z* 283.0670 $[M+H]^+$.

3-(1*H*-Indol-3-yl)-2-[2-(1*H*-indol-3-yl)-2-oxo-acetylamino]-propionic acid methyl ester (11). Indole (1 mmol) was dissolved in dry ether (10 ml) and allowed to stir in an ice bath for a while till a clear solution is obtained. Afterwards, dropwise addition of oxalyl chloride (1.2 mmol) is done to this solution which immediately gives a yellow solid through an exothermic reaction. This yellow solid was filtered under vacuum and dissolved in dry ACN (25 ml) followed by the addition of K_2CO_3 (1.5 mmol). Eventually, the neutralized solution of L-tryptophan methyl ester hydrochloride (1.5 mmol) (neutralized with 1.5 equivalents of triethyl amine) was added to the reaction mass. The progress of the reaction was monitored with TLC. Reaction completes in 15-20 min. The reaction mass was washed with a minimum amount of water and extracted with ethyl acetate. Finally, the ethyl acetate was distilled off to leave behind a crude product which was further refined through column chromatography using ethyl acetate-hexane as eluents to get the product. Yield 89%. Grey solid. Mp 146 ^{o}C. IR ν_{max} (KBr, cm^{-1}): 1681 (C=O), 1759 (C=O), 2987 (CH), 3307 (NH). ^{1}H NMR (500 MHz, $CDCl_3$) δ: 3.44-3.47 (dd, *J* = 7.5 Hz, *J* = 1.5 Hz, 1H, CH_2), 3.58-3.63 (dd, *J* = 9.0 Hz, *J* = 1.0 Hz, 1H, CH_2), 3.88 (s, 3H, OCH_3), 4.51 (m, 1H, CH), 6.70 (d, *J*=3.5 Hz, 1H, ArH), 7.16-7.28 (m, 5H, ArH), 7.32-7.50 (m, 4H, ArH), 8.160 (s,

1H, NH). ^{13}C NMR (normal/DEPT- 135) (125 MHz, $CDCl_3$) δ: 26.06 (CH_2, -ve), 51.41 (CH), 54.75 (OCH_3), 117.61 (CH), 117.84 (CH), 120.45 (CH), 121.51 (CH), 123.23 (CH), 123.53 (CH), 124.74 (CH), 126.10 (C), 126.11 (CH), 126.75 (C), 129.98 (CH), 130.72 (C), 134.63 (C), 134.73 (C), 136.53 (C), 145.40 (C), 160.72 (C=O), 161.41 (C=O), 169.56 (C=O). ESI-MS (HRMS) calcd for $C_{22}H_{19}N_3O_4$ 390.1448. Found *m/z* 390.1444 $[M+H]^+$.

3-(3*H*-Imidazol-4-yl)-2-[2-(1*H*-indol-3-yl)-2-oxo-acetylamino]-propionic acid methyl ester (12). Indole (1 mmol) was dissolved in dry ether (10 ml) and allowed to stir in an ice bath for a while till a clear solution is obtained. The yellow solid obtained after dropwise addition of oxalyl chloride (1.2 mmol) to this solution was filtered under vacuum and dissolved in dry ACN (25 ml) followed by the addition of K_2CO_3 (1.5 mmol). Eventually, the neutralized solution of L-histidine methyl ester hydrochloride (1.34 mmol) (neutralized with 1.5 equivalents of triethyl amine) was added to the reaction mass. The progress of the reaction was monitored with TLC. Reaction completes in 15-20 min. The reaction mass was washed with a minimum amount of water and extracted with ethyl acetate. Finally, the ethyl acetate was distilled off to leave behind a crude product which was further refined through column chromatography using ethyl acetate-hexane as eluents to get the product. Yield 90%. Yellow solid. Mp 118 ^{o}C. IR ν_{max} (KBr, cm^{-1}): 1688 (C=O), 1750 (C=O), 2857 (C-H), 3537 (NH). ^{1}H NMR (500 MHz, DMSO-d_6) δ: 3.33 (d, *J*= 6.5 Hz, 2H, CH_2), 3.77 (s, 3H, OCH_3), 4.46 (m, 1H, CH), 6.82 (s, 1H, ArH), 6.83-7.28 (m, 3H, ArH), 7.28-7.33 (m, 2H, ArH), 7.33-7.39 (m, 2H, ArH, NH), 7.58 (s, 1H, NH), 9.10 (s, 1H, NH); ^{13}C NMR (normal/DEPT- 135) (125 MHz, DMSO- d_6) δ: 25.56 (CH_2, -ve), 51.51 (CH), 53.51 (OCH_3), 109.89 (CH), 113.53 (CH), 118.57 (CH), 122.02 (CH), 123.88 (CH), 125.10 (CH), 127.12 (C), 127.15 (CH), 127.39 (CH), 130.65 (CH), 130.98 (C), 134.49 (C), 134.52

(CH), 169.07 (C=O), 174.51 (C=O), 179.89 (C=O); ESI-MS (HRMS) calcd for $C_{17}H_{16}N_4O_4$ 341.1244. Found *m/z* 341.1241 $[M+H]^+$.

{2-Oxo-2-[1-(toluene-4-sulfonyl)-1*H*-indol-3-yl]-acetylamino}-acetic acid methyl ester (13). NaH (1.2 mmol) was washed with dry hexane (5 ml) and suspended in a solution of dry ACN (20 ml). Compound **10** (1 mmol) was added to this suspension and allowed to stir at 0 ^oC for 2-3 min until the whole reactant gets dissolved. Eventually, the p-toluyl sulphonylchloride (1.2 mmol), recrystallized over warm hexane, was added to the reaction mass. The progress of the reaction was monitored with TLC. On completion, the reaction was quenched by adding a minimum amount of ice cold water. The crude product was extracted from aqueous layer by ethyl acetate. The organic layer was dried over Na_2SO_4 and concentrated under vacuum. The crude residue was purified with column chromatography using ethyl acetate-hexane as eluents to procure the product. Yield 68%. Yellow solid. Mp 180 ^oC. IR ν_{max} (KBr, cm^{-1}): 1130 (S=O), 1661 (C=O), 1757 (C=O), 2957 (C-H), 3407 (NH). ^1H NMR (500 MHz, $CDCl_3$) δ: 2.38 (s, 3H, CH_3), 3.83 (s, 3H, OCH_3), 4.20 (d, J = 5.5 Hz, 2H, CH_2), 7.28-7.43 (4H, ArH), 7.82-7.84 (m, 1H, ArH), 7.89-8.01 (m, 2H, ArH), 8.35-8.36 (m, 2H, ArH), 9.39 (s, 1H, NH). ^{13}C NMR (normal/DEPT- 135) (125 MHz, $CDCl_3$) δ: 21.66 (CH_3), 41.06 (CH_2, -ve), 52.62 (OCH_3), 113.27 (CH), 115.93 (C), 122.81 (CH), 125.17 (CH), 125.98 (CH), 127.38 (CH), 128.11 (C), 130.30 (CH), 134.23 (C), 134.43 (C), 138.48 (CH), 146.09 (C), 161.27 (C=O), 169.34 (C=O), 180.74 (C=O). ESI-MS (HRMS) calcd for $C_{20}H_{18}N_2O_6S$ 437.0778. Found *m/z* 437.0855 $[M+Na]^+$.

3-(1*H*-Indol-3-yl)-2-{2-oxo-2-[1-(toluene-4-sulfonyl)-1*H*-indol-3-yl]-acetylamino}-propionic acid methyl ester (14). NaH (1.2 mmol) was washed with dry hexane (5 ml) and suspended in dry ACN (20 ml). Compound **11** (1mmol) was added to this suspension and allowed to stir at 0 ^oC for 2-3 min until the whole reactant gets dissolved. Eventually, p-toluyl sulphonylchloride

(1.2 mmol), recrystallized from warm hexane, was added to the reaction mass. The progress of the reaction was monitored with TLC. On completion, the reaction was quenched by adding a minimum amount of ice cold water. The crude product was extracted from aqueous layer by ethyl acetate. After drying over anhydrous Na_2SO_4, the organic layer was concentrated under vacuum. The crude residue was purified through column chromatography by using ethyl acetate-hexane as eluents to procure the product. Yield 79 %. Brown solid. Mp 131 ^oC. IR ν_{max} (KBr, cm^{-1}): 1135 (S=O), 1651 (C=O), 1741 (C=O), 2927 (CH), 3411 (NH). ^1H NMR (500 MHz, $CDCl_3$) δ: 2.36 (s, 3H, CH_3), 3.44-3.49 (dd, *J* = 15.0 Hz, *J* = 7.5 Hz, 1H, CH_2), 3.59-3.63 (dd, *J* = 15.0 Hz, *J*=2.7 Hz, 1H, CH_2), 3.88 (s, 3H, OCH_3), 4.51 (m, 1H, CH), 6.70 (d, *J* = 3 Hz, 1H, ArH), 7.16-7.18 (m, 2H, ArH), 7.22-7.28 (m, 5H, ArH), 7.32-7.35 (m, 3H, ArH), 7.41 (d, *J* = 10 Hz, 1H, ArH), 7.49 (d, *J* = 10 Hz, 1H, ArH), 7.56 (m, 1H, NH), 7.77 (d, *J* = 10 Hz, 1H, ArH), 7.97 (m, 1H, NH). ^{13}C NMR (normal/DEPT- 135) (125 MHz, $CDCl_3$) δ: 21.47 (CH_3), 26.11 (CH_2, -ve), 54.09 (CH), 54.11 (CH), 105.46 (C), 109.56 (CH), 110.93 (C), 111.92 (CH), 113.19 (C), 113.43 (CH), 115.46 (C), 117.63 (CH), 117.72 (C), 120.45 (CH), 121.51 (CH), 123.23(CH), 123.53 (CH), 124.71 (CH), 124.74 (CH), 126.10 (C), 126.16 (CH), 126.75 (CH), 129.98 (CH), 130.84 (C), 134.63 (C), 134.76 (C), 136.56 (C), 145.41 (C), 169.61 (C=O). ESI-MS (HRMS) calcd for $C_{29}H_{25}N_3O_6S$ 566.1356. Found *m/z* 566.1366 $[M+Na]^+$.

3-(3*H*-Imidazol-4-yl)-2-{2-oxo-2-[1-(toluene-4-sulfonyl)-1*H*-indol-3-yl]-acetylamino}-propionic acid methyl ester (15) NaH (1.2 mmol) was washed with dry hexane (5 ml) and suspended in a dry ACN (20 ml). Compound **12** (1 mmol) was added to this suspension and allowed to stir at 0 ^oC for 2-3 min until the whole reactant gets dissolved. Eventually, p-toluyl sulphonylchloride (1.2 mmol), recrystallized from warm hexane, was added to the reaction mass. The progress of the reaction was monitored with TLC. On completion, the reaction was

quenched by adding a minimum amount of ice cold water. The crude product was extracted from aqueous layer by ethyl acetate. After drying over anhydrous Na_2SO_4, the organic layer was concentrated under vacuum. The crude product was purified through column chromatography by using ethyl acetate-hexane as eluents to procure the product. Yield 85%. Grey solid. Mp 121 ^oC. IR ν_{max} (KBr, cm^{-1}): 1087.19 (S=0), 1628 (C=O), 1744 (C=O), 2925 (CH), 3401 (N-H). ^1H NMR (300 MHz, DMSO-d_6) δ: ^1H NMR (500 MHz, DMSO d_6): 2.29 (s, 3H, CH_3), 3.33-3.35 (d, *J* = 7.0 Hz, 2H, CH_2), 3.72 (s, 3H, OCH_3), 4.49 (t, *J* = 7.0 Hz, 1H, CH), 6.82 (d, *J*= 5 Hz, 1H, ArH), 7.23 (t, *J* = 5 Hz, 1H, ArH), 7.31 (s, 1H, ArH), 7.35 (t, *J* = 10 Hz, 3H, ArH), 7.54 (s, 1H, ArH), 7.59 (d, *J* = 10 Hz, 1H, ArH), 7.77 (d, *J* = 5 Hz, 1H, ArH), 7.84 (d, *J* = 10 Hz, 1H, ArH), 7.92 (d, *J* = 10 Hz, 1H, ArH), 9.10 (s, 1H, NH). ^{13}C NMR (normal/DEPT- 135) (125 MHz, $CDCl_3$) δ: 21.46 (CH_3), 25.51 (CH_2, -ve), 51.49 (CH), 53.51 (OCH_3), 109.88 (CH), 113.53 (CH), 118.57 (CH), 122.07 (CH), 123.89 (CH), 125.10 (CH), 127.12 (C), 127.15 (CH), 127.38 (CH), 127.39 (C), 130.68 (CH), 130.93 (C), 134.52 (CH), 134.56 (C), 134.63 (C), 145.92 (C), 169.02 (C=O), 174.65 (C=O), 179.82 (C=O). ESI-MS (HRMS) calcd for $C_{24}H_{22}N_4O_6S$ 495.1323. Found *m/z* 495.1333 $[M+H]^+$.

{2-Oxo-2-[1-(toluene-4-sulfonyl)-1*H*-indol-3-yl]-acetylamino}-acetic acid (16). Compound **13** (1 mmol) was dissolved in 10 ml acetone - water (2:1) and allowed to stir at room temperature. Eventually 1N solution of NaOH was added to the reaction mass. The progress of reaction was monitored with TLC. The reaction completes in 15-20 min. On completion, the reaction mass was heated to evaporate acetone. On dropwise addition of 0.1N HCl to the aqueous part, the solid product precipitates out which was filtered and purified through column chromatography using ethyl acetate - hexane as eluents. Yield 80%. Brown solid. Mp 140 ^oC. IR ν_{max} (KBr, cm^{-1}): 1120 (S=O), 1630 (C=O), 1764 (C=O), 3412 (NH); ^1H NMR (500 MHz, $CDCl_3$) δ: 2.38 (s,

3H, CH_3), 4.20 (d, *J*= 4.5 Hz. 2H, CH_2), 7.13-7.15 (d, *J* = 10 Hz, 2H, ArH), 7.26-7.28 (t, *J* = 5 Hz, 2H, ArH), 7.50 (m, 2H, ArH), 7.54 (m, 1H, ArH), 8.25 (m, 1H, ArH), 8.76 (m, 1H, ArH), 8.95 (s, 1H, NH), 12.35 (s, 1H, OH). ^{13}C NMR (normal/DEPT- 135) (125 MHz, $CDCl_3$) δ: 21.98 (CH_3), 41.07 (CH_2 -ve), 113.30 (CH), 115.79 (C), 122.81 (CH), 125.17 (CH), 125.74 (CH), 127.38 (CH), 128.11 (CH), 134.24 (C), 134.43 (C), 138.48 (CH), 146.09 (C), 161.27 (C=O), 169.35 (C=O), 180.66 (C=O). ESI-MS (HRMS) calcd for $C_{19}H16N_2O_6S$ 423.0621. Found *m/z* 423.0641 $[M+Na]^+$.

3-(1*H*-Indol-3-yl)-2-{2-oxo-2-[1-(toluene-4-sulfonyl)-1*H*-indol-3-yl]-acetylamino}-propionic acid (17). Compound **14** (1 mmol) was taken in 10 ml acetone - water (2:1) to which 1N NaOH was added. On completion of the reaction (TLC), the reaction mass was heated to evaporate acetone. On dropwise addition of 0.1N HCl to the aqueous part, the solid product precipitates out which was vacuum filtered and purified through column chromatography using ethyl acetate - hexane as eluents. Yield 69%. Cream solid. Mp 110 ^{o}C. IR ν_{max} (KBr, cm^{-1}): 1110 (S=O), 1632 (C=O), 1735 (C=O), 3421 (NH). ^{1}H NMR (500 MHz, DMSO-d_6) δ: 2.30 (s, 3H, CH_3), 3.25 (d, *J* = 5 Hz, 2H, CH_2), 4.17 (m, 1H, CH), 6.82 (d, *J* = 5 Hz, 1H, ArH), 7.01 (t, *J* = 5 Hz, 1H, ArH), 7.10 (t, *J* = 5 Hz, 1H, ArH), 7.24 (t, *J* = 5 Hz, 1H, ArH), 7.32-7.39 (m, 3H, ArH), 7.56-7.60 (m, 3H, ArH), 7.78 (d, *J* = 5 Hz, 1H, ArH), 7.85 (d, *J* = 10 Hz, 2H, ArH), 7.93 (d, *J* = 10 Hz, 1H, ArH), 8.19 (s, 2H, NH), 11.058 (s, 1H, OH). ^{13}C NMR (normal/DEPT- 135) (125 MHz, DMSO-d_6) δ: 21.44 (CH_3), 26.61 (CH_2, -ve), 53.05 (CH), 107.07 (C), 109.85 (CH), 111.98 (CH), 112.29 (C), 113.53 (CH), 114.60 (C), 116.90 (C), 118.66 (CH), 119.09 (CH), 119.20 (C), 121.65 (CH), 122.05 (CH), 123.88 (CH), 125.08 (CH), 125.41 (CH), 127.15 (CH), 127.38 (CH), 127.47 (C), 130.67 (CH), 130.93 (C), 134.57 (C), 134.66 (C), 136.76 (C), 145.92 (C), 171.35 (C=O). ESI-MS (HRMS) calcd for $C_{28}H_{23}N_3O_6S$ 552.1200. Found *m/z* 552.1243 $[M+Na]^+$.

3-(3*H*-Imidazol-4-yl)-2-{2-oxo-2-[1-(toluene-4-sulfonyl)-1*H*-indol-3-yl]-acetylamino}-propionic acid (18). Compound **15** (1 mmol) was dissolved in 10 ml acetone - water (2:1) and allowed to stir at room temperature. Eventually 1N NaOH was added to the reaction mass. The progress of the reaction was monitored with TLC. On completion, the reaction mass was heated to evaporate acetone. On dropwise addition of 0.1N HCl to the aqueous part, the solid product precipitates out which was vacuum filtered and purified by column chromatography using ethyl acetate - hexane as eluents. Yield 65%. Yellow solid. Mp 135 ^{o}C. IR ν_{max} (KBr, cm^{-1}): 1065 (S=O), 1630 (C=O), 1735 (C=O), 3395 (NH). ^{1}H NMR (500 MHz, DMSO-d_6) δ: 2.29 (s, 3H, CH_3), 3.28 (d, *J* = 6.0 Hz, 2H, CH_2), 4.12 (t, *J* = 5.5 Hz, 1H, CH), 7.00 (t, *J*= 5 Hz, 1H, ArH), 7.09-7.12 (m, 3H, ArH), 7.14 (s, 1H, ArH), 7.24 (d, *J* = 5 Hz, 1H, ArH), 7.37 (d, *J* = 10 Hz, 1H, ArH), 7.50 (d, *J* = 10 Hz, 2H, ArH), 7.57 (d, *J* = 5 Hz, 1H, ArH), 7.59 (d, *J* = 10 Hz, 1H, ArH), 8.30-8.33 (b, 2H, NH), 11.08 (s, 1H, OH). ^{13}C NMR (normal/DEPT- 135) (125 MHz, DMSO-d_6) δ: 21.24 (CH_3), 26.54 (CH_2, -ve), 53.04 (CH), 107.08 (C), 111.97 (CH), 116.64 (C), 118.71 (CH), 119.05 (CH), 121.59 (CH), 125.46 (CH), 125.96 (CH), 127.49 (C), 128.61 (CH), 136.73 (C), 138.36 (C), 145.77 (C=O), 158.64 (C=O), 158.95 (C=O), 171.27 (C=O). ESI-MS (HRMS) calcd for $C_{23}H_{20}N_4O_6S$ 481.1176. Found *m/z* 481.1171 $[M+Na]^+$.

(2-{2-Oxo-2-[1-(toluene-4-sulfonyl)-1*H*-indol-3-yl]- acetylamino}-acetylamino)-acetic acid methyl ester (6i). Compound **16** (1 mmol) was dissolved in dry DCM (25 ml) and stirred for 2-3 min to make a clear solution. Triethylamine and ethylchloroformate were added to this solution. Eventually, neutralized solution of glycine methyl ester hydrochloride in triethylamine was added to the reaction mass at 0 ^{o}C. The progress of the reaction was monitored with TLC. On completion, the reaction mass was neutralized with 0.1N HCl and washed repeatedly with 1M $NaHCO_3$ till the effervescence persists. Eventually, the crude organic product was extracted with

ethyl acetate. Further purification of the crude material was done through column chromatography using ethyl acetate-hexane as eluent. Yield 68%. Brown solid. Mp 171 ^{o}C. IR ν_{max} (KBr, cm^{-1}): 1135 (S=O) 1666 (C=O), 1717 (C=O), 2950 (C-H), 3477 (NH). ^{1}H NMR (500 MHz, $CHCl_3$ + TFA) δ: 2.29 (s, 3H, CH_3), 3.34 (d, *J* = 7.0 Hz, 2H, CH_2), 3.72 (s, 3H, OCH_3), 4.49 (t, *J* = 7.0 Hz, 2H, CH_2), 6.82 (s, 1H, ArH), 7.31-7.36 (m, 4H, ArH), 7.58-7.60 (m, 1H, ArH), 7.54 (s, 1H, ArH), 7.77-7.78 (m, 1H, ArH), 7.83-7.85 (m, 1H, ArH), 7.91-7.93 (m, 1H, ArH), 9.10 (s, 1H, NH). (normal/DEPT- 135) (125 MHz, $CHCl_3$ + TFA) δ: 21.40 (CH_3), 25.78 (CH_2, -ve), 29.66 (CH_2, -ve), 51.78 (OCH_3), 109.82 (CH), 113.53 (CH), 114.55 (CH), 116.85 (CH), 122.03 (CH), 123.86 (CH), 125.06 (CH), 127.14 (CH), 127.35 (CH), 130.93 (CH), 130.65 (CH), 134.57 (CH), 134.66 (CH), 145.90 (CH), 171.23 (C=O), 173.70 (C=O). ESI-MS (HRMS) calcd for $C_{22}H_{21}N_3O_7S$ 471.1100. Found *m/z* 471.1103 $[M+H]^+$.

(2-{2-Oxo-2-[1-(toluene-4-sulfonyl)-1*H*-indol-3-yl]-acetylamino)-acetic acid (7i). Compound **6i** was dissolved in acetone - water (2:1) and stirred for 2-3 min to make a homogeneous solution. Eventually, 1N NaOH was added to the reaction mass and allowed to stir at room temperature. The progress of the reaction was monitored through TLC. The reaction mass was heated to evaporate acetone. On dropwise addition of 0.1N HCl to the reaction mass, the crude product precipitated out which was filtered under vaccum and washed repeatedly with diethyl ether to procure pure product. Yield 59%. Brown solid. Mp 191 ^{o}C. IR ν_{max} (KBr, cm^{-1}): 1099 (S=O), 1610 (C=O), 1717 (C=O), 2885 (C-H), 3402 (NH); ^{1}H NMR (500 MHz, DMSO-d_6 + TFA) δ: 2.29 (s, 3H, CH_3), 3.28 (d, *J* = 6.0 Hz, 2H, CH_2), 4.12 (d, *J* = 5.5 Hz, 2H, CH_2), 6.99-7.07 (m, 2H, ArH), 7.09-7.14 (m, 3H, ArH), 7.24 (d, *J* = 5 Hz, 1H, ArH), 7.36-7.58 (m, 3H, ArH), 8.30-8.33 (b, 2H, ArH), 11.08 (s, 1H, COOH); ^{13}C NMR (normal/DEPT- 135) (125MHz, DMSO-d_6 + TFA) δ: 21.54(CH_3), 41.07 (CH_2, -ve), 43.20 (CH_2, -ve), 112.28 (C), 113.94 (CH),

120.33 (CH), 122.79 (CH), 123.85 (CH), 125.16 (CH), 127.84 (CH), 128.00 (C), 129.98 (C), 130.26 (CH), 134.98 (C), 143.99 (C=O), 145.23 (C=O), 167.75 (C=O), 169.81 (C=O). $[\alpha]_D + 22^0$ (c 1, MeOH), ESI-MS (HRMS) calcd for $C_{21}H_{19}N_3O_7S$ 457.0944. Found *m/z* 457.0955 $[M+H]^+$.

3-(1*H*-indol-2-yl)-2-(2-{2-oxo-2-[1-toluene-4-sulfonyl)-1*H*-indol-3-yl]-acetylamino}-acetylamino)-propionic acid methyl ester (6b). Compound **17** was dissolved in dry DCM and stirred for 2-3 min to make a clear solution. Triethylamine and ethylchloroformate were added to this solution. Eventually, neutralized solution of glycine methyl ester hydrochloride in triethylamine was added to the reaction mass at 0 ^oC. The progress of the reaction was monitored with TLC. On completion, the reaction mass was neutralized with 0.1N HCl and washed repeatedly with 1M $NaHCO_3$ till the effervescence persists. Eventually, the crude product was extracted with ethyl acetate. Further purification of the crude material was done through column chromatography using ethyl acetate-hexane as eluent. Yield 78 %. Yellow solid. Mp 181 ^oC. IR ν_{max} (KBr, cm^{-1}): 1139 (S=O), 1695 (C=O), 1721 (C=O), 2999 (CH), 3415 (N-H). ^1H NMR (500 MHz DMSO-d_6 + TFA) δ: 2.33 (s, 3H, CH_3), 3.26 (t (dd), *J* = 5.5 Hz, 2H, CH_2), 3.70 (s, 3H, OCH_3), 4.04 (d, *J* = 6.0 Hz, 1H, CH), 4.15 (t, *J* = 5.5 Hz, 1H, CH), 6.99-7.98 (m, 10H, ArH), 8.00-8.26 (m, 4H, ArH), 9.11 (s, 1H, NH), 9.31 (t, *J* = 5Hz, 1H, NH), 11.04 (s, 1H, NH). (normal/DEPT- 135) (125 MHz, DMSO-d_6 + TFA) δ: 21.45 (CH_3), 26.57 (-ve, CH_2), 41.12 (-ve, CH_2), 52.35 (CH), 53.05 (OCH_3), 107.04 (C), 111.96 (CH), 112.09 (C), 113.61 (CH), 116.14 (C), 116.67 (C), 118.63 (CH), 118.97 (C), 119.06 (CH), 121.62 (CH), 122.62 (CH), 125.39 (CH), 125.75 (CH), 126.66 (CH), 127.45 (C), 127.76 (C), 127.83 (CH), 129.06 (C), 131.11 (CH), 133.57 (C), 133.93 (C), 136.76 (C), 137.69 (CH), 162.85 (C=O), 171.01 (C=O), 171.34 (C=O), 182.78 (C=O). ESI-MS (HRMS) calcd for $C_{31}H_{28}N_4O_7S$ 600.1678 Found *m/z* 600.1680 $[M+H]^+$.

3-(1*H*-indol-2-yl)-2-(2-{2-oxo-2-[1-(toluene-4-sulfonyl)-1*H*-indol-3-yl]-acetylamino}-acetylamino)-propionic acid (7b). Compound **6b** was dissolved in acetone-water (2:1) and stirred for 2-3 min to make a homogeneous solution. Eventually, 1N NaOH was added to the reaction mass and allowed to stir at room temperature. After completion of the reaction (TLC), the reaction mixture was heated to evaporate acetone. On dropwise addition of 0.1N HCl to the aqueous part, the crude product precipitated out which was filtered under vacuum and washed repeatedly with diethyl ether to procure the product. Yield 65%. Cream solid. Mp 190 ^{o}C. IR ν_{max} (KBr, cm^{-1}): 1111 (S=O); 1602 (C=O), 1730 (C=O), 3420 (NH). ^{1}H NMR (500 MHz, DMSO-d_6 + TFA) δ: 2.28 (s, 3H, CH_3), 2.64 (s, 2H, CH_2), 3.30 (d, *J* = 6.5 Hz, 2H, CH_2), 4.11 (t, *J* = 6.0 Hz, 1H, CH), 6.80-6.98 (m, 1H, ArH), 7.00-7.38 (m, 4H, ArH), 7.56-7.69 (m, 6H, ArH), 7.70-7.92 (m, 4H, ArH, NH), 8.31 (m, 2H, NH), 11.12 (s, 1H, COOH), (normal/DEPT- 135) (125MHz, DMSO-d_6 + TFA) δ: 21.34 (CH_3), 26.57 (CH_2, -ve), 40.08 (CH_2, -ve), 53.16 (CH), 107.17 (C), 109.82 (C), 111.95 (C), 113.50 (CH), 113.77 (C), 116.13 (C), 118.49 (C), 118.64 (CH), 119.00 (CH), 120.85(C), 121.54(CH), 122.02(CH), 123.86(CH), 125.06(CH), 125.40 (CH), 127.11 (CH), 127.29 (CH), 127.50 (C), 129.08 (C), 130.61 (CH), 130.92 (C), 131.99 (C), 134.54 (C), 134.62 (C), 136.76 (C), 145.93 (C), 159.61 (C=O), 169.40 (C=O), 171.28 (C=O). $[\alpha]_D$ + 21^0 (c 1, MeOH), ESI-MS (HRMS) calcd for $C_{30}H_{26}N_4O_7S$ 587.1522. Found *m/z* 587.1520 $[M+H]^+$.

2-(3-(3*H*-imidazol-4-yl)-2-{2-oxo-2-[1-(toluene-4-sulfonyl)-1*H*-indol-3-yl]-acetylamino}-propionylamino)-pentanedioic acid dimethyl ester (6h). Compound **18** was dissolved in dry DCM and stirred for 2-3 min to make a clear solution. Triethylamine and ethylchloroformate were added to the above solution. Eventually, neutralized solution of L-glutamic dimethyl ester hydrochloride in triethylamine was added to the reaction mass at 0 ^{o}C. The progress of the

reaction was monitored with TLC. On completion, the reaction mass was neutralized with 0.1N HCl and washed repeatedly with 1M solution of $NaHCO_3$ till the effervescence persists. Eventually, the crude product was extracted with ethyl acetate and purified through column chromatography using ethyl acetate-hexane as eluent. Yield 72%. Yellow solid. Mp 141 ^{o}C. IR ν_{max} (KBr, cm^{-1}): 1080 (S=O), 1632 (C=O), 1699 (C=O), 2906 (C-H), 3434 (NH). ^{1}H NMR (500 MHz, DMSO-d_6) δ: 2.08-2.13 (m, 2H, CH_2), 2.28 (s, 3H, CH_3), 2.48-2.62 (m, 4H, 2xCH_2), 3.33 (d, *J* = 6.0 Hz, 1H, CH), 3.60 (s, 3H, OCH_3), 3.73 (s, 3H, OCH_3), 4.08 (m, 1H, CH), 6.82 (s, 1H, ArH), 7.00-7.10 (m, 1H, ArH), 7.21-7.35 (m, 3H, ArH), 7.38-7.58 (m, 3H, ArH), 7.83-7.94 (m, 3H, ArH), 8.45 (s, 1H, NH), 8.76 (s, 1H, NH). ^{13}C NMR (normal/DEPT- 135) (125MHz, DMSO-d_6) δ: 21.39 (CH_3), 25.58 (CH_2, -ve), 26.50 (CH_2, -ve), 29.32 (CH_2, -ve), 51.94 (OCH_3), 53.06 (CH), 53.20 (OCH_3), 107.12 (C), 109.84 (CH), 111.94 (CH), 113.52 (CH), 114.81 (C), 117.12 (C), 118.75 (CH), 119.00 (CH), 121.52 (CH), 122.03 (CH), 123.86 (CH), 125.0 (CH), 125.49 (CH), 127.12 (CH), 127.33 (CH), 127.53 (C), 130.63 (CH), 130.93 (C), 134.57 (C), 134.64 (C), 136.73 (C), 145.88 (C), 169.98 (C=O), 171.22 (C=O), 172.63 (C=O). ESI-MS (HRMS) calcd for $C_{30}H_{31}N_5O_9S$ 637.1843. Found *m/z* 637.1856 $[M+H]^+$.

2-(3-(3H-imidazol-4-yl)-2-{2-oxo-2-[1-(toluene-4-sulfonyl)-1H-indol-3-yl]-acetylamino}-propionylamino)-pentanedioic acid (7h) Compound **6h** was dissolved in acetone-water (2:1) and stirred for 2-3 min to make a homogeneous solution. Eventually, 1N NaOH was added to the reaction mass and allowed to stir at room temperature. The progress of the reaction was monitored through TLC. On completion, the reaction mass was heated to evaporate acetone. On dropwise addition of 0.1N HCl to the aqueous part, the crude product precipitated out which was filtered under vaccum and washed repeatedly with diethyl ether to procure the product. Yield 85%. Orange solid. Mp 175 ^{o}C. IR ν_{max} (KBr, cm^{-1}): 1099 (S=O), 1611 (C=O), 1797 (C=O),

3455 (NH). ^{1}H NMR (500 MHz, DMSO-d_6) δ: 1.97-2.07 (m, 2H, CH_2), 2.29 (s, 3H, CH_3), 2.35-2.47 (m, 2H, CH_2), 3.27 (t (dd), *J* = 6.0 Hz, 2H, CH_2), 3.94 (t, *J* =5.5 Hz, 1H, CH), 4.15 (t, *J* = 5.5 Hz, 1H, CH), 7.01-7.10 (m, 2H, ArH), 7.23-7.58 (m, 3H, ArH), 7.75-7.93 (m, 2H, ArH), 7.80-7.99 (m, 2H, ArH), 8.20-8.28 (m, 4H, ArH, 2NH), 11.04 (s, 1H, COOH), 11.16 (s, 1H, COOH). (normal/DEPT- 135) (125 MHz, DMSO-d_6) δ: 21.32 (CH_3), 25.76 (CH_2, -ve), 26.56 (CH_2, -ve), 29.63 (CH_2, -ve), 51.79 (CH), 55.18 (CH), 107.05 (C), 109.75 (C), 111.95 (CH), 112.21 (C), 113.51 (CH), 114.51 (C), 116.81 (C), 118.63 (CH), 119.05 (CH), 119.10 (C), 121.59 (CH), 121.98 (CH), 123.80 (CH), 125.00 (CH), 125.39 (CH), 127.10 (CH), 127.27 (CH), 127.46 (C), 130.58 (CH), 130.92 (C), 134.57 (C), 134.69 (C), 136.77 (C), 145.85 (C=O), 171.23 (C=O), 171.33 (C=O), 173.70 (C=O). $[\alpha]_D + 16^0$ (c 1, MeOH), ESI-MS (HRMS) calcd for $C_{28}H_{27}N_5O_9S$ 609.1530. Found *m/z* 609.1540 $[M+H]^+$.

(3-(1*H*-indol-3-yl)-2-{2-oxo-2-[1-(toluene-4-sulfonyl)-1*H*-indol-3-yl]-acetylamino}-propionylamino)-acetic acid methyl ester (6d). Compound **16** was dissolved in dry DCM and stirred for 2-3 min to make a clear solution. Triethylamine and ethylchloroformate was added to the above solution. Eventually, neutralized solution of L-tryptophan methyl ester hydrochloride in triethylamine was added to the reaction mass at 0 ^oC. The progress of the reaction was monitored with TLC. On completion, the reaction mass was neutralized with 0.1N HCl and washed repeatedly with 1M $NaHCO_3$ till the effervescence persists. Eventually, the crude product was extracted with ethyl acetate and purified through column chromatography using ethyl acetate-hexane as eluent. Yield 59%. Cream solid. Mp 170 ^oC. IR ν_{max} (KBr, cm^{-1}): 1140 (S=O), 1636 (C=O), 1775 (C=O), 3441 (NH); ^{1}H NMR (500 MHz, DMSO d_6 + TFA) δ: 2.34 (s, 3H, CH_3), 3.26 (d, *J* = 6.0 Hz, 2H, CH_2), 3.71 (s, 3H, OCH_3), 4.04 (d, *J* = 6.0 Hz, 2H, CH_2), 4.16 (m, 1H, CH), 7.00-7.23 (m, 3H, ArH), 7.37-7.49 (m, 5H, ArH), 7.57 (d, *J* = 10 Hz, 1H,

ArH), 8.01-8.26 (m, 5H, ArH, NH), 9.11 (s, 1H, ArH), 9.33 (t, *J* = 5 Hz, 1H, NH), 11.06 (s, 1H, NH). ^{13}C NMR (normal/DEPT- 135) (125 MHz, DMSO-d_6 + TFA, δ): 14.29 (CH_3), 21.53 (CH_2, -ve), 40.17 (CH_2, -ve), 52.42 (OCH_3), 107.07 (C), 111.97 (CH), 112.31 (C), 113.64 (CH), 114.62 (C), 116.15 (C), 116.92 (C), 118.65 (CH), 119.08 (CH), 121.63 (C), 122.64 (CH), 125.41 (CH), 125.80 (CH), 126.72 (CH), 127.47 (C), 127.75 (C), 127.87 (C), 128.56 (CH), 131.16 (CH), 133.55 (C), 133.93 (C), 136.76 (C), 137.68 (CH), 147.19 (C), 162.88 (C=O), 170.02 (C=O), 171.34 (C=O), 182.82 (C=O). ESI-MS (HRMS) calcd for $C_{31}H_{28}N_4O_7S$ 600.1678. Found *m/z* 600.1670 $[M+H]^+$.

(3-(1*H*-indol-3-yl)-2-{2-oxo-2-[1-(toluene-4-sulfonyl)-1*H*-indol-3-yl]-acetylamino}-propionylamino)-acetic acid (7d). Compound **6d** was dissolved in acetone:water (2:1) and stirred for 2-3 min to make a homogeneous solution. After the addition of 1N NaOH, the reaction mixture was further stirred at room temperature. The progress of the reaction was monitored through TLC. On completion, the reaction mass was heated to evaporate acetone. On dropwise addition of 0.1N HCl to the aqueous part, the crude product precipitated out which was filtered under vacuum and washed repeatedly with diethyl ether to procure the product. Yield 70%. Cream colored solid. Mp 189 ^{o}C. IR ν_{max} (KBr, cm^{-1}): 1109 (S=O), 1649 (C=O), 1718 (C=O), 3491 (NH). ^{1}H NMR (500 MHz, DMSO-d_6 + TFA) δ: 2.29 (s, 3H, CH_3), 3.28 (d, *J* = 6.0 Hz, 2H, CH_2), 3.68 (dd, *J* = 5.5 Hz, J= 5.5 Hz, 2H, CH_2), 4.11 (m, 1H, CH), 6.98-7.14 (m, 4H, ArH), 7.24-7.38 (m, 2H, ArH), 7.51-7.50 (m, 4H, ArH), 7.58-7.57 (m, 3H, ArH), 8.23-8.32 (m, 3H, ArH, 2NH), 11.18 (s, 1H, COOH). ^{13}C NMR (normal/DEPT- 135) (125 MHz, DMSO d_6 + TFA) δ: 21.22 (CH_3), 26.52 (CH_2, -ve), 40.13 (CH_2, -ve), 45.66 (C=O), 53.05 (CH), 107.07 (C), 111.96 (CH), 114.48 (C), 116.78 (C), 118.71 (CH), 119.03 (CH), 121.56 (CH), 125.47 (CH), 125.96 (CH), 127.49 (C), 128.62 (CH), 136.72 (C), 138.42 (C), 158.97 (C=O), 169.39 (C=O), 171.25

(C=O). $[\alpha]_D$ + 16^0 (c 1, MeOH), ESI-MS (HRMS) calcd for $C_{30}H_{26}N_4O_7S$ 587.1522. Found 587.1520 *m/z* $[M+H]^+$.

7.2 Biology

7.2.1. Anti-inflammatory studies.

The animals were housed at 25 ± 2 ºC under 12 h light/ 12 h dark cycle with free access to food and water in the central animal house at Guru Nanak Dev University, Amritsar, Punjab. Animals were acclimatized to the laboratory conditions before testing and were used once throughout the experiments. All the protocols have been duly approved by the Institutional Ethics Committee for the purpose of Control and Supervision of Experiments on Animals (CPSCEA), Ministry of Environment and Forests, India.

Swiss albino mice were divided into different groups each comprising of five animals. Group I, the control, comprised of animals treated with vehicle, and group II was treated with standard reference drug – diclofenac (10 mg kg^{-1}). All the test compounds were administered at two doses 5 mg Kg^{-1} and 10 mg Kg^{-1}. Compound **7i** was given to groups III, IV; **7d** to groups V, VI; **7b** to groups VII, VIII and groups IX, X were given **7h** at both doses, intraperitoneally. Dextran was administered at a dose of 1% by subplantar injection 30 min after the respective treatments and paw thickness was measured using vernier calipers after 1, 2, 3, 4, 6 and 24 h of dextran injection.

7.2.2. Antinociceptive studies.

Animals were divided into 10 groups of 5 each. 20 µL of capsaicin was injected into the plantar surface of the right hind paw. Animals were observed individually for 10 min after capsaicin administration and the number of paw lickings and twitchings was recorded as an indicator of hyperalgesia. All treatments were administered intraperitoneally 30 min before

capsaicin injection. Group I was control in which the animals were injected vehicle, in group II animals were injected diclofenac at a dose 10 mg Kg^{-1}. Group III and IV animals were injected compound **7i** at doses 5 and 10 mg Kg^{-1}, respectively; group V and VI animals were injected compound **7d** at doses 5 and 10 mg Kg^{-1}, respectively; group VII and VIII animals were given compound **7b** at doses 5 and 10 mg Kg^{-1}, respectively and group IX and X animals were injected compound **7h** at same two doses as for other compounds.

7.2.3. Studies for checking toxicity.

Mice were divided into 3 groups comprising of three animals in each group. Oral doses of the compound **7b** were administered at 5 mg, 50 mg and 300 mg and animals were observed continuously for the first 4 hours for any signs of toxicity. Thereafter, the animals were observed at regular intervals for the first 24h followed by once daily for the next 14 days. After 14 days, the animals were sacrificed and histological studies were conducted on the liver, kidney and heart.

7.2.4. Lipoxygenase inhibitory activities

For 5-LOX inhibition studies, solutions of compounds at 0.01 μM, 0.1 μM, 1 μM, 10 μM and 100 μM concentrations were prepared in DMSO. 10 μL of each compound from the above concentrations was added to 90 μL solution (in assay buffer) of 5- LOX enzyme (Soyabean lipoxygenase) taken in the wells of a 96-well plate. Each compound was tested in duplicate and the average of two values with deviation <5% was taken for calculation. Two wells were taken as blanks (assay buffer + AA) and four wells were taken as positive controls (enzyme in assay buffer + AA). The reaction was initiated by the addition of 10 μL of the substrate (AA). After shaking the 96-well plate on a shaker for 5 min, 100 μL of the chromogen (developing reagent) was added to each well. The plate was again shaken for 5 min and read at 490 nm in a

microplate scanning spectrophotometer. Percent 5-LOX inhibitory activity was determined using the mean of the two values for each sample

[A500/min/9.47 mM $^{-1}$] x [0.21 ml/0.09 ml] x sample dilution

Where :

A500/min = A500 (sample)/min - A500 (blank)/5 min,

9.47 mM $^{-1}$ = -Extinction coefficient of chromogen,

0.21 ml = Total volume of the solution in each well and

0.09 ml = Volume of the enzyme solution used.

Percent 5-LOX inhibition = [{L.A. (P.C.) - L.A. (I.)}/L.A.(P.C.)] x 100

L.A. (P.C.) = Lipoxygenase Activity of positive control, L.A. (I.) = Lipoxygenase Activity of inhibitor.IC_{50} values were determined from the graph between Percent Inhibition versus concn of inhibitor using KaleidaGraph 3.5.

7.2.5. COX-1/COX-2 inhibitory activities

In vitro COX-1 and COX-2 inhibitory activities were evaluated using "COX inhibitor screening assay" kits with 96-well plates (catalog no. 560101, Cayman Chemical, Ann Arbor, MI) according to the manufacturer's instructions. As per the kit specifications, the enzymes were ovine COX-1 and human recombinant COX-2. This screening assay directly measures PGF2a produced by $SnCl_2$ reduction of COX-derived PGH2. COX-1 and COX-2 initial activity tubes were prepared taking 950 µL of reaction buffer (0.1M Tris-HCl, pH 8.0, containing 5 mM EDTA and 2 mM phenol), 10 µL of heme, 10 µL of COX-1 and COX-2 enzymes into respective tubes. Similarly, COX-1 and COX-2 inhibitor tubes were prepared by adding 20 µL of inhibitor (compound under test with final concentrations of 100, 10, 1, 0.1, 0.01, and 0.001 µM) in each tube in addition to the above ingredients, making a final volume of 1 mL. The background tubes

correspond to inactivated COX-1 and COX-2 enzymes obtained after keeping the tubes containing enzymes in boiling water for 3 min. After incubation of the tubes at 37 ^{o}C for 20 min, reactions were initiated by adding 10 µL of arachidonic acid in each tube and again incubating at 37 ^{o}C for 2 min. The reaction was quenched with 50 µL of 1 M HCl. PGH2 thus formed was reduced to PGF2a by adding 100 µL of $SnCl_2$. The prostaglandin produced in each well was quantified using broadly specific prostaglandin antiserum. The PGs and PGacetylcholinesterase (AChe) conjugate (PG tracer) have a competition for a limited amount of PG antiserum. Because the concentration of the PG tracer is held constant while the concentration of PG varies, the amount of PG tracer that is able to bind to the PG antiserum will be inversely proportional to the concentration of PG in the well. This rabbit antiserum-P (either free or tracer) complex binds to a mouse monoclonal antirabbit antibody that has been previously attached to the well. The plate is washed to remove any unbound reagents, and then Ellman's reagent (which contains the substrate to AChe) is added to the well. The product of this enzymatic reaction has a distinct yellow color and absorbs strongly at 420 nm. The intensity of this color, determined spectrophotometrically, is proportional to the amount of PG tracer bound to the well, which is inversely proportional to the amount of free PG present in the well during the incubation. The wells of the 96-well plate showing low absorbance at 420 nm indicate the higher level of prostaglandins in these wells and hence less inhibition of the enzyme. Therefore, the COX inhibitory activities of the compounds could be quantified from the absorbance values of different wells of the 96-well plates. The concentrations of the test compound causing 50% inhibition (IC_{50}) were determined using a dose-response inhibition curve (duplicate determinations) with GraphPad PRISM.

7.2.6. Kinetic Studies

7.2.6.1. K_a and K_i values

UV-vis spectral studies were performed on BioTek Synergy H1 hybrid reader. 10^{-3} M stock solutions of the compounds were prepared in ethanol-HEPES buffer (1:1), pH 7.2. The enzyme stock solution was prepared by diluting 20 µL of 5-LOX and COX-2 to 1 mL in ethanol-HEPES buffer (1:1), pH 7.2. The spectra were recorded on incremental addition of 10 µL of enzyme stock solution to 10^{-4} M (prepared by diluting stock solution) compound solution. The change in the spectral reading at the maxima were used in the Benesi Hildebrand equation to find the K_a values.

BENESI HILDEBRAND EQUATION:

$1/(A_f - A_{obs}) = 1/(A_f - A_{fc}) = 1/K_a(A_f - A_{fc})$ [L]

Where:

A_f = absorbance of free host

A_{obs} = absorbance observed

A_{fc} = absorbance at saturation

K_i (inhibition constant) was calculated as:

$K_i = IC_{50}/(1+[L]/K_d)$

Where:

K_d = dissociation constant $= Ka^{-1}$

7.2.6.2. Isothermal calorimetric experiments. The compound solution was titrated into the sample cell (containing the enzyme) using a 250 µL rotating stirrer syringe set at 500 rpm. The reference cell contained HEPES buffer. Each experiment consisted of 19 consecutive injections of 2 µL of 10 µM of the compound to the enzyme contained in the sample cell after regular time intervals of 120 s to guarantee the equilibrium in each titration point. Control experiments were

performed for comparison. The total heat Q produced or absorbed in the active cell volume V_0 determined at fractional saturation Θ after the i^{th} injection is given by equation 1

$$Q = n \Theta M_t \Delta H V_0 \quad (1)$$

Where, M_t is the total concentration of the macromolecule

n is the total number of binding sites in the macromolecule and

ΔH is the molar heat of ligand binding

The enthalpy change for the i^{th} injection ΔH(i) for an injection volume dVi is then given by the following equation 2. $\Delta H(i) = Q(i) + dV_i/V_0 [Q(i) – Q(i-1)/2] – Q(i-1)$ (2)

The control titrations consisting in identical titrant solution with the same cell filled just with the buffer solution and also the successive buffer additions to the enzyme solution were carried out to determine the background heat which was to be subtracted from the main experiment. The origin 7.0 software provided by Microcal was used to determine the titration heat profiles for determining the binding parameters. The data fitted well to the single binding site model.

7.2.6.3. Double reciprocal Plots.

To construct the double reciprocal plots, 50 µl of arachidonic acid (substrate) was supplied to another vial and a 450 µl solution of HEPES:DMSO (1:1) was added to it to give a final concentration of 2 mM. The 5 µl aliquot of this solution gives a final concentration of 50 µM in the reaction.[23] The change in absorbance of substrate at maxima on the incremental addition of 5 µl to a fixed concentration of the enzyme (5-LOX/COX-2) indicates the progress of the enzyme catalysed reaction which was plotted in the form of double reciprocal plot. Same procedure was repeated in presence of a fixed concentration of the inhibitors (compounds) for two different concentrations 10 µM and 20 µM, respectively. All readings were taken on BioTek Synergy H1 hybrid reader.

7.2.6.4. Mechanistic investigations with misoprostol and substance P

Animal were divided into 7 groups of 5 animals each. All treatments were administered intraperitoneally 30 min before capsaicin injection. Group I was control wherein the animals were injected normal saline. In group II and III animals were injected compound **7b** and **7h**, respectively at a dose of 5 mg Kg^{-1}; in group IV and V, animals were injected with misoprostol (200 µg) 30 min before compound **7b** and **7h**, respectively (5 mg Kg^{-1}) followed by capsaicin after 30 min. In group VI and VII, animals were injected with substance-P (10 µg) 30 min before compound **7b** and **7h**, respectively (5 mg Kg^{-1}) followed by capsaicin after 30 min.

7.2.7. Mass spectra and LC-MS

Mass spectra were recorded on Bruker MicroTOF QII mass spectrometer (Bruker Daltonik, Bremen, Germany). Machine was calibrated with sodium formate. Using KdScientific automated pump with flow rate 180 µL/h, 50 µM solution in acetonitrile-water-formic acid (7:2.9:0.1) was injected to electrospray ionization source. Desolvation was performed with dry N_2 gas heated at 180 ^oC. Various parameters of the mass spectrometer were optimized for maximum ion abundance. Typically, the capillary voltage was 4500 V and vacuum was maintained at 3-4x10^{-7} mbar.

For LC-MS, Dionex Ultimate 3000 system was linked to mass spectrometer. Chirobiotic® T 10 µm chiral HPLC column (25 cm x 4.6 mm) was used. Acetonitrile-water (1:1) was used as eluent. 2 µL of sample (injection volume) was loaded to the column, flow rate was kept 0.2 ml and absorbance was set at 200, 220 and 254 nm. Sodium formate was used as internal calibrant.

7.2.8. Molecular Docking studies

The compounds were build using the builder toolkit of the software package ArgusLab4.0.1 and energy minimized using semi-empirical quantum mechanical method PM3 [37]. The crystal

coordinates of human 15- LOX (pdb ID 3V99) (have 78 % similarity to Soyabean cyclooxygenase) were downloaded from the protein data bank. Structure of this protein is a monomer and carries 3-(2-oct-1-ynylphenyl)-acrylic acid as a ligand in its binding site. In the molecular tree view the active site of the enzyme is defined as 15 Å around the ligand. The molecule to be docked in the active site of the protein was pasted in the work space carrying the structure of the enzyme. The docking program implements an efficient grid based docking algorithm which approximates an exhaustive search within the free volume of the binding site cavity. The conformational space was explored by the geometry optimization of the flexible ligand (rings were treated as rigid) in combination with the incremental construction of the ligand torsions. Thus docking occurs between the flexible ligand parts of the compound and the enzyme. The ligand orientation was determined by a shape scoring function based on Ascore and the final positions were ranked by lowest interaction energy values. H-bonding and hydrophobic interactions between the compound and enzyme were explored.

The crystal coordinates of COX-2 (murine) (highly similar to human COX-2) were downloaded from the Protein Data Bank with PDB code 3MQE. Compounds were built using the builder Toolkit of the software package Argus- Lab, version 4.0.1 and SYBYL, version 7.1 and energy minimized using semi-empirical quantum mechanical method PM3. In the molecule tree view, the monomeric structure of the enzyme was selected and the active site was defined as 15 Å around the ligand. The molecule to be docked in the active site of the enzyme was pasted in the work space carrying the structure of the enzyme. The docking program implements an efficient grid based docking algorithm that approximates an exhaustive search within the free volume of the binding site cavity. The conformational space was explored by the geometry optimization of the flexible ligand (rings are treated as rigid) in combination with the incremental

construction of the ligand torsions. Thus, docking occurred between the flexible ligand parts of the compound and enzyme. The ligand orientation was determined by a shape scoring function based on Ascore, and the final positions were ranked by lowest interaction energy values. The $E_{interaction}$ is the sum of the energies involved in H-bond interactions, hydrophobic interactions, and van der Waal's interactions. H-Bond and hydrophobic interactions between the compound and enzyme were explored by measuring the distances between the various groups of the ligand and the amino acid residues.

SUPPORTING INFORMATION

Supplementary information includes ^{1}H, ^{13}C and DEPT-135 NMR, HRMS, docking images, and Docking score.

AUTHOUR INFORMATION

[a]Department of Chemistry, Guru Nanak Dev University, Amritsar-143005. [b]Department of Pharmaceutical Sciences, Guru Nanak Dev University, Amritsar-143005.

ACKNOWLEDGEMENTS

Financial assistance from Department of Science & Technnology, New Delhi is gratefully acknowledged. PP thanks Council of Scientific and Industrial Research, New Delhi for Senior Research Fellowship. University Grants Commission, New Delhi is gratefully acknowledged for creating state of the art research facility under the University with Potential for Excellence Programme.

ABBREVIATIONS

ACN, acetonitrile; COX, cyclooxygenase; LOX, lipoxygenase; SAID, steroidal anti-inflammatory drugs; NSAID, non-steroidal anti-inflammatory drugs; COXIBS, selective

cyclooxygenase-2 inhibitors; DCM, dichloromethane; OECD, Organization for Economic Cooperation and Development; TPSA, total polar surface area.

References and notes

[1] B. Samuelsson, Drugs 33 (1987) 2-9.

[2] P. Davies, P.J. Bailey, M.M. Goldenberg, A-W Hutchinson, Ann. Rev. Immonol. 2 (1984) 335-357.

[3] W. Minor, J. Steczko, B. Stec, Z. Otwinowski, J.T. Bolin, R. Walter, B. Axelrod, Biochemistry 35 (1996) 10687-10701.

[4] J.R. Vane, Y.S. Bakhle, R.M. Bottling, Annu. Rev. Pharmacol. Toxicol. 38 (1998) 97-120.

[5] J.Z. Haeggstrom, C.D. Funk, Chem. Rev. 111 (2011) 5866-5898.

[6] C.A. Rouzer, L.J. Marnett, Chem. Rev. 103 (2003) 2239-2304.

[7] S.E. Wenzel, Prostaglandins, leukotrienes and essential Fatty acids 69 (2003) 145–155.

[8] A.J. Merched, K. Ko, K. H. Gotlinger, C. N. Serhan, L. Chan, The FASEB J. 22 (2008) 3595-3606.

[9] F. Stanke-Labesque, J. Pofelski, A. Moreau-Gaudry, G. Bessard, B. Bonaz, Inflamm. Bowel Dis. 14 (2008) 769-774.

[10] K. R. Gheorghe, M. Korotkova, A. I. Catrina, L. Backman, E. A. Klint, H. E. Claesson, O. Radmark, P. J. Jacobsson, Arthritis Res. Ther. 11 (2009) 1-11.

[11] S. Izraely, I. P. Witz, P. Larghi, C. Porta, E. Riboldi, P. Allavena, A. Mantovani, A. Sica, L. Bertazza, S. Mocellin, M. DeWitte, E. Voronov, R. N. Apte, E. C. Keeley, B. Mehrad, R. M. Strieter, Y. Li, A. Fulton, A. Ben-Baruch, A. Burkhardt, A. Zlotnik, D. Luger, L. M. Wakefield, A. Peled, Bentham Science Publishers (2012).

[12] P. Carlo, C. Baigent, Molecular Interventions **2009**, 9, 31-39.

[13] B. Everts, P. Wahrborg, T. Hedner, Clin. Rheumatol. 19 (2000) 331-343.

[14] A. Rossi, C. Pergola, A. Koeberle, M. Hoffmann, F. Dehm, P. Bramanti, S. Cuzzocrea, O. Werz, L. Sautebin, Brit. J. Pharmacol. 161 (2010) 555-570.

[15] A. P. Sampson, Curr. Opin. Investig. Drugs 11 (2009) 1163-1172.

[16] J. M. Dogne, C. T. Supuran, D. Pratico, J. Med. Chem. 48 (2005) 2251-2257.

[17] Food and Drug Administration, News Release, September 30, 2004 and April 7, **2005**.

[18] P. Prasher, Pooja, P. Singh, Bioorg. Med. Chem. 22 (2014) 1642-1648.

[19] P. Singh, Pooja, Bioorg. Med. Chem. Lett. 23 (2013) 1433-1437.

[20] G. M. Cragg, P. G. Grothaus, D. J. Newman, J. Nat. Prod. 77 (2014) 703-723.

[21] G. Rastelli, J. Bajorath, A. Anighoro, J. Med. Chem. 57 (2014) 7874-7887.

[22] www.molinspiration.com.

[23] T. K. Maity, S. C. Mandal, P. K. Mukherjee, Phytother. Res. 12 (1998) 221-224.

[24] T. Sakurada, T. Matsumura, T. Moriyama, C. Sakurada, S. Ueno, S. Sakurada, Pharmacol. Biochem. Behaviour 75 (2003) 115-121.

[25] Organization for Economic Cooperation and Development (OECD), 2001. Guideline 423. Acute Oral Toxicity – Acute Toxic Class Method. 470 Adopted by the Council on 17th, December 2001.

[26] 5-LOX inhibitor screening assay kit, Item No. 760700. Cayman Chemical Co.

[27] Cayman Chemical Co., Cat. No. 560131 (COX-1/2).

[28] Y. S. Chi, B. S. Cheon, H. P. Kim, Biochem. Pharmacol. 61 (2001) 1195-1203.

[29] E. A. Meade, W. L. Smith, D. L. DeWitt, J. Biol. Chem. 268 (1993) 6610-6614.

[30] P. E. Lipsky, P. C. Isakson, J. Rheumatol. 24 (1997) 9-14.

[31] F. J. Blanco, R. Guitian, J. Moreno, F. J. De Toro, F. Galdo, J. Rheumatol. 26 (1999) 1366-1373.

[32] J. H. Hildebrand, H. A. Benesi, J. Am. Chem. Soc. 71 (1949) 2703-2707.

[33] M. L. Castellani, P. Conti, M. Felaco, J. Vecchiet, C. Ciampoli, G. Cerulli, P. Boscolo, T. C. Theoharides, Neurotoxicity Res. 15 (2009) 49-56.

[34] H. W. Koon, D. Zhao, Y. Zhan, S. H. Rhee, M. P. Moyer, C. Pothoulakis, J. Immunol. 176 (2006) 5050-5059.

[35] J. L. Wang, D. Limburg, M. J. Graneto, J. Springer, J. R. Hamper, S. Liao, J. L. Pawlitz, R. G. Kurumbail, T. Mariasz, J. J. Talley, J. R. Keifer, J. Carter, Bioorg. Med. Chem. Lett. 20 (2010) 7159-7163.

[36] N. C. Gilbert, Z. Rui, D. B. Neau, M. T. Waight, S. G. Bartlett, W. E. Boeglin, A. R. Brash, FASEB J. 26 (2012) 3222-3229.

[37] ArgusLab 4.0.1, M. A. Thompson, Planaria Software LLC, Seattle, WA 98155.

Captions:

Chart 1. Some commercially known 5-LOX inhibitors (**1** – **3**), previously reported compounds (**4** – **5**) and new design of the molecules (**6**, **7**).

Chart 2. Structures of new designed molecules.

Table 1. Concentration of the compounds **6** and **7** causing 50% inhibition in the 5-LOX, COX-1/2 activity (IC_{50}). Compounds **16** – **18** were taken for comparison [18].

Table 2. K_a, K_i and ΔG values of compounds **6** and **7** for 5-LOX and COX-2 enzymes.

Table 3. Isothermal calorimetric data of compounds **7** for 5-LOX enzyme.

Table 4 . Isothermal calorimetric data of compounds **7** for COX-2 enzyme.

Figure 1. Effect of various compounds on paw thickness after dextran injection. All results are expressed as mean ± SEM. **[a]** $p < 0.05$ vs control group at respective time interval.

Figure 2. Effect of various compounds on capsaicin induced pain in mice. All values are expressed as mean ± SEM. Statistical significance has been calculated using one way ANOVA followed by Tukey's multiple comparison test. ** $p < 0.01$ vs control group.

Figure 3. Isothermal calorimetric data of compounds 7 for 5-LOX. A_1, B_1: compound **7b**, A_2, B_2: compound **7d**, A_3, B_3: compound **7h** and A_4, B_4: compound **7i**. A. ITC raw data 19 x 2 µL injections, B. Integrated heat pulse data.

Figure 4. Plots showing competitive inhibition of 5-LOX by: (a) compound **7b**, (b) compound **7d**, (c) compound **7h**, (d) compound **7i;** Competitive inhibition of COX-2 by: (e) compound **7b**, (f) compound **7d**, (g) compound **7h** and (h) compound **7i**. Arrow indicates increase in inhibitor concentration.

Figure 5. Effect of misoprotol and substance P pretreatment on antihyperalgesic effect of compound **7b** and **7h** in capaicin induced hyperalgesia in mice. All values are expressed as mean

± SEM. ** p< 0.01 vs control group; # p< 0.01 vs compound **7b** group, $ p< 0.01 vs compound **7h** group.

Figure 6. A) Crystal coordinates of COX-2 (pdb ID 3MQE) [35] in association with compound 7**b** (green) (generated in Pymol). Dotted lines indicate H-bond interactions between the compound and amino acids. B) CPK model showing the placement of compound **7b** (blue) in the active site pocket of COX-2 enzyme.

Figure 7. A) Crystal coordinates of 5-LOX (pdb ID 3V99) [36] in association with compound **7b** (blue) (generated in Pymol). Dotted lines indicate H-bond interactions between the compound and amino acids. B) CPK model showing the placement of compound **7b** (green) in the active site pocket of 5-LOX enzyme.

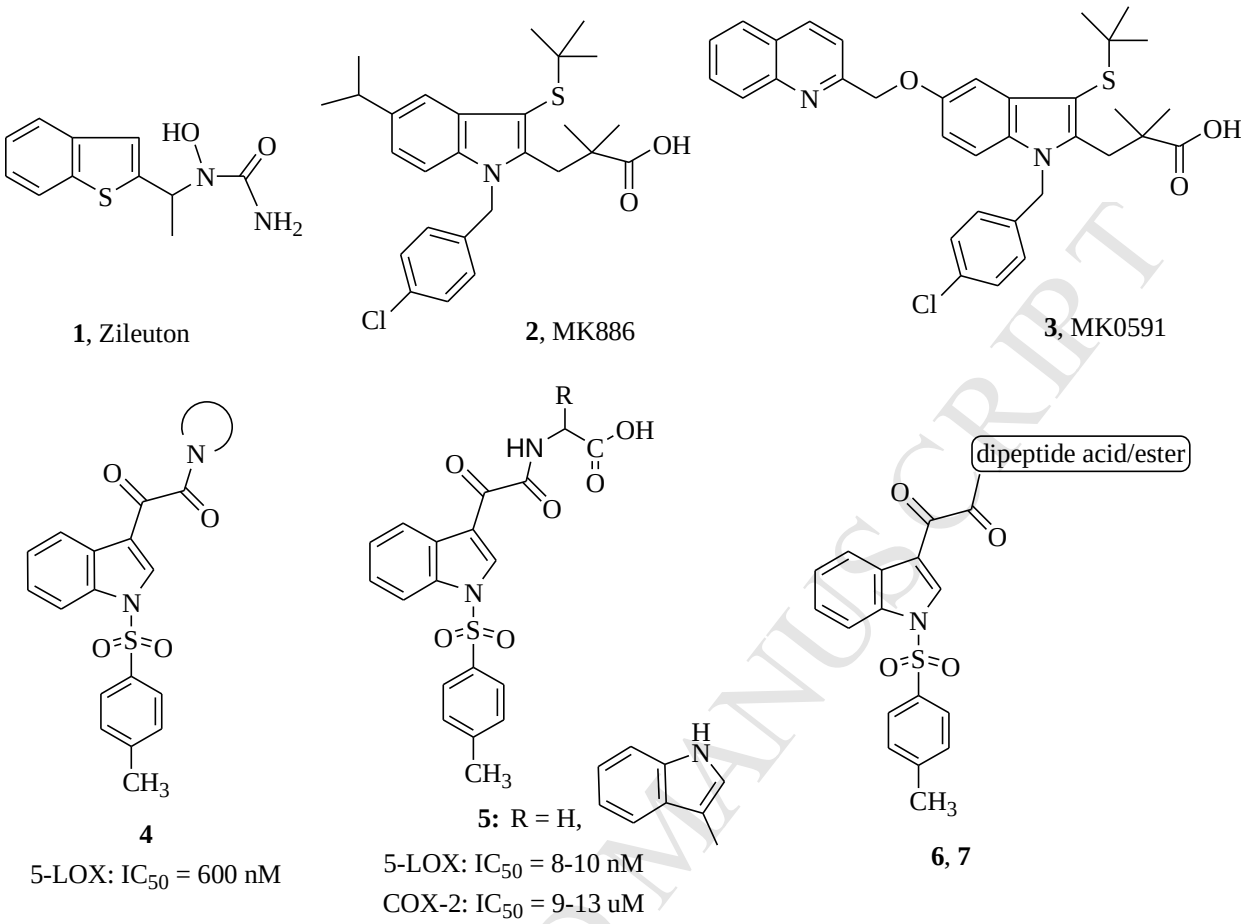

Chart 1. Clinically used 5-LOX inhibitors (**1** – **3**), previously reported compounds (**4** – **5**) and new design of the molecules (**6**, **7**).

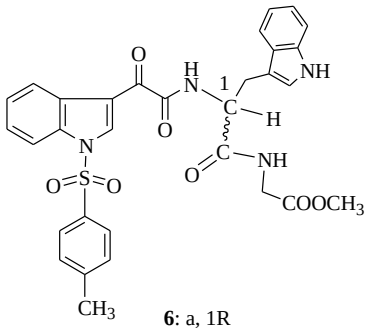

6: a, 1R
b, 1S

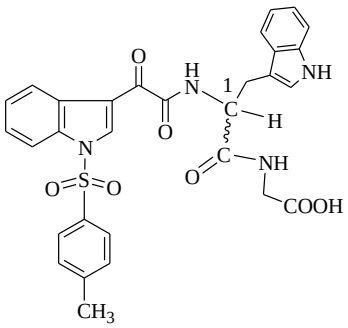

7: a, 1R
b, 1S

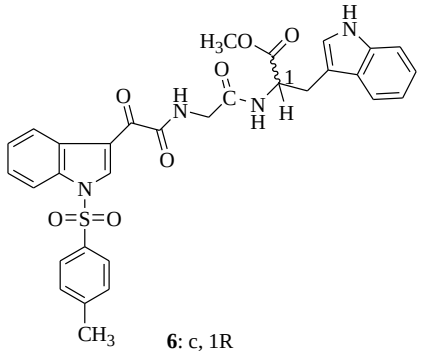

6: c, 1R
d, 1S

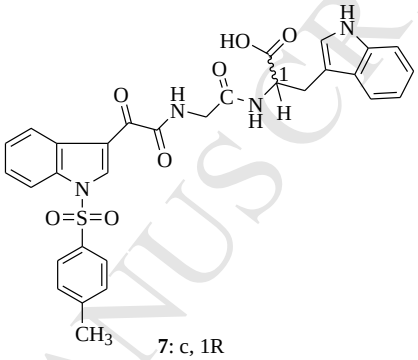

7: c, 1R
d, 1S

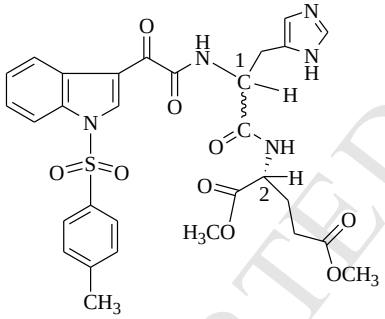

6: e, 1R, 2R
f, 1R, 2S
g, 1S, 2R
h, 1S, 2S

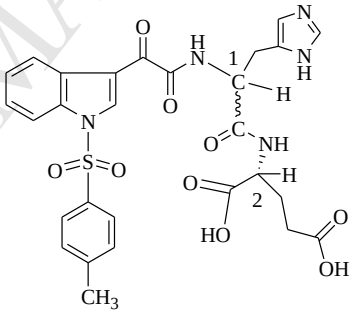

7: e, 1R, 2R
f, 1R, 2S
g, 1S, 2R
h, 1S, 2S

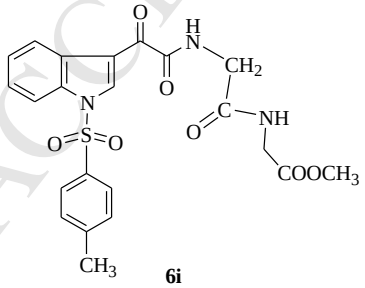

6i

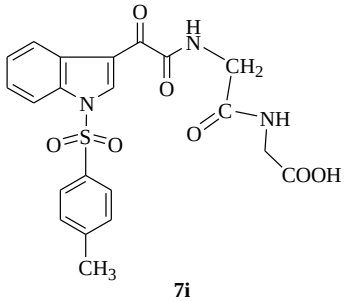

7i

Chart 2. Structures of new designed molecules.

Table 1. Concentration of the compounds **6** and **7** causing 50% inhibition in the 5-LOX, COX-1/2 activity (IC_{50}). Compounds **16** – **18** were taken for comparison [18].

Compound	IC_{50} (μM)			Selectivity for COX-2[a]
	5-LOX	COX-1	COX-2	
16	0.0086	90.11	9.11	9.89
17	0.010	87.22	13.5	6.46
18	2.80	>100	0.97	>100
6a	8.38	71.30	10.31	6.97
6b	0.8	9.89	0.047	210
6c	12.22	65.52	6.61	10.57
6d	1.0	90.90	8.89	10
6e	3.70	20.20	8.33	2.42
6h	0.6	76.45	3.63	21
6i	0.1	104.4	10.34	10
7a	5.61	>100	1.00	>100
7b	0.002	2.21	0.0063	351
7c	15.21	98.31	2.5	39.32
7d	0.004	43.5	0.099	440
7e	2.33	150.65	21.31	7.06
7h	0.08	12.87	0.54	24
7i	0.005	>100	0.89	>100
Wogonin	-	-	46	-
Indomethacin	-	0.08	0.96	0.08
Celecoxib	-	15	0.04	375
SC-558	-	13	0.05	>200
Zileuton	0.3	-	-	-
MK 0591	1.6		-	-
Diclofenac		0.61	0.63	~1

[a]Selectivity index = IC_{50}[COX-1]/IC_{50}[COX-2]

Table 2. K_a, K_i and ΔG values of compounds **6** and **7** for 5-LOX and COX-2 enzymes.

	5-LOX			COX-2		
Compd	**K_a**(M^{-1})	**K_i** (μM)	**ΔG** (KJ $mol^{-1}K^{-1}$)	**K_a**(M^{-1})	**K_i** (μM)	**ΔG** (KJ $mol^{-1}K^{-1}$)
6b	5.6×10^4	0.946	-27.20	7.91×10^3	2.900	-22.20
6d	7.7×10^4	0.753	-27.80	9.87×10^3	1.342	-22.70
6h	3.02×10^5	0.356	-31.26	4.43×10^4	0.983	-26.50
6i	2.08×10^5	0.097	-30.33	1.81×10^2	4.659	-12.87
7b	3.36×10^6	0.042	-37.20	3.29×10^5	0.109	-31.48
7d	2.06×10^6	0.064	-36.02	3.25×10^6	0.005	-37.15
7h	1.99×10^5	0.536	-32.22	7.76×10^5	0.012	-33.60
7i	2.99×10^5	0.232	-31.23	1.90×10^3	3.122	-18.70

Table 3. Isothermal calorimetric data of compounds **7** for 5-LOX enzyme.

Compd	**N**	**K_a (M^{-1})**	**ΔH (KJ/mol)**	**TΔS (KJ/mol)**	**ΔG (KJ/mol)**
7b	0.91±0.05	$(3.41 \pm 0.81) \times 10^6$	-26.15±0.6	11.04±0.8	-37.19±1.5
7d	1.09±0.1	$(1.99 \pm 0.79) \times 10^6$	-25.06±0.4	10.92±0.7	-35.98±1.1
7h	1.29±0.09	$(2.99 \pm 0.99) \times 10^5$	-20.21±0.78	9.11±0.65	-29.32±0.88
7i	1.39±0.11	$(5.43 \pm 1.09) \times 10^5$	-25.88±2.25	7.33±1.33	-25.88±2.22

Table 4 . Isothermal calorimetric data of compounds **7** for COX-2 enzyme.

Compd	N	$K_{asso.}$ (M^{-1})	ΔH (KJ/mol)	TΔS (KJ/mol)	ΔG (KJ/mol)
7b	1.31±0.07	(2.99±0.09) x 10^5	-22.81±0.1	8.42±0.08	-31.23±0.78
7d	0.99±0.15	(3.79±0.71) x 10^6	-30.61±0.4	6.92±0.55	-37.53±0.88
7h	1.11±0.62	(6.01±0.93) x 10^5	-20.88±1.01	12.08±1.25	-32.96±1.11
7i	0.86±0.95	(2.53±0.91) x 10^3	-12.01±1.25	7.30±1.33	-19.41±1.22

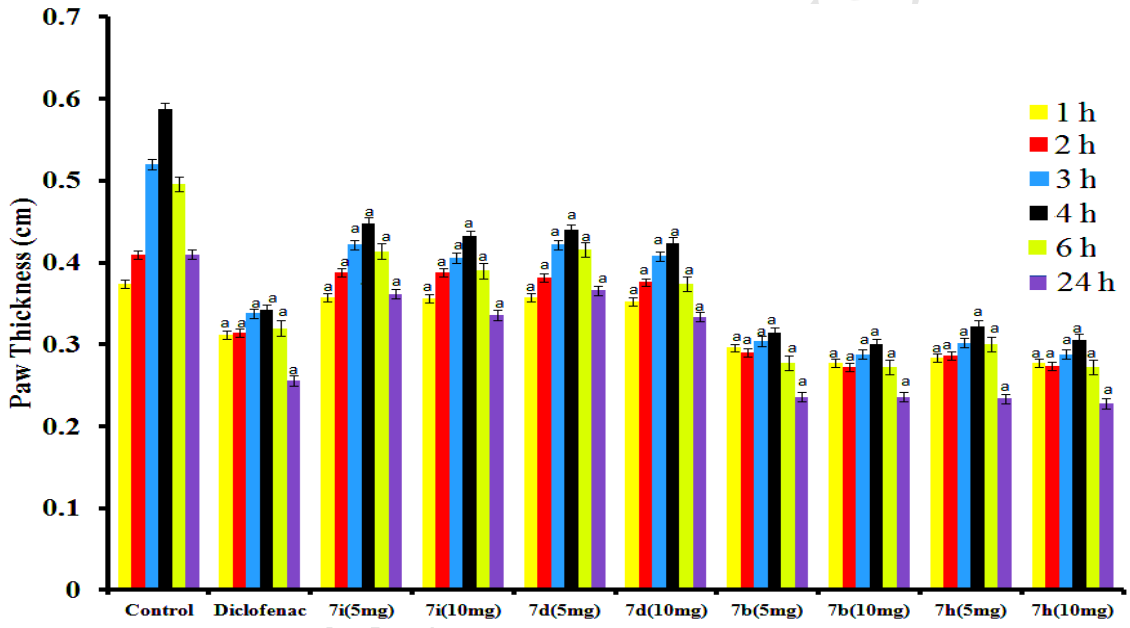

Fig. 1. Effect of various compounds on paw thickness after dextran injection. All results are expressed as mean ± SEM. [a] $p < 0.05$ vs control group at respective time interval.

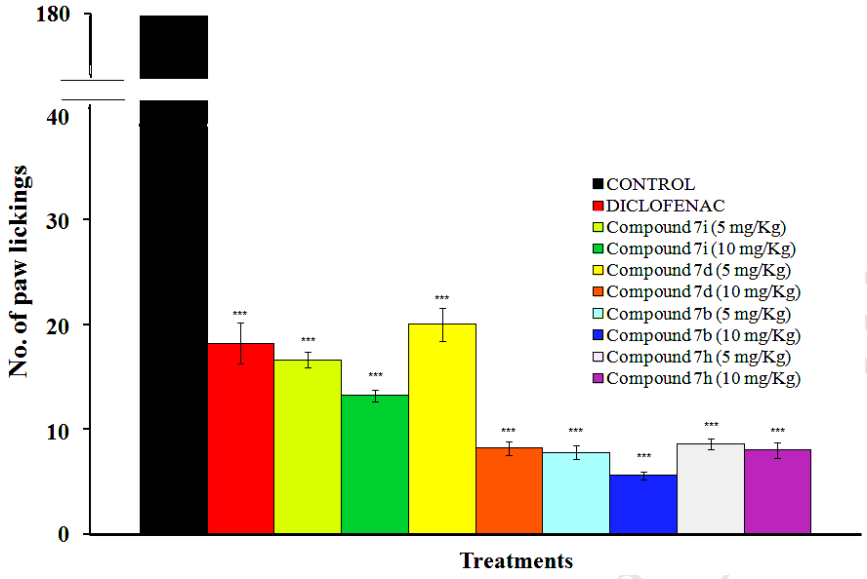

Fig. 2. Effect of various compounds on capsaicin induced pain in mice. All values are expressed as mean ± SEM. Statistical significance has been calculated using one way ANOVA followed by Tukey's multiple comparison test. ** $p < 0.01$ vs control group.

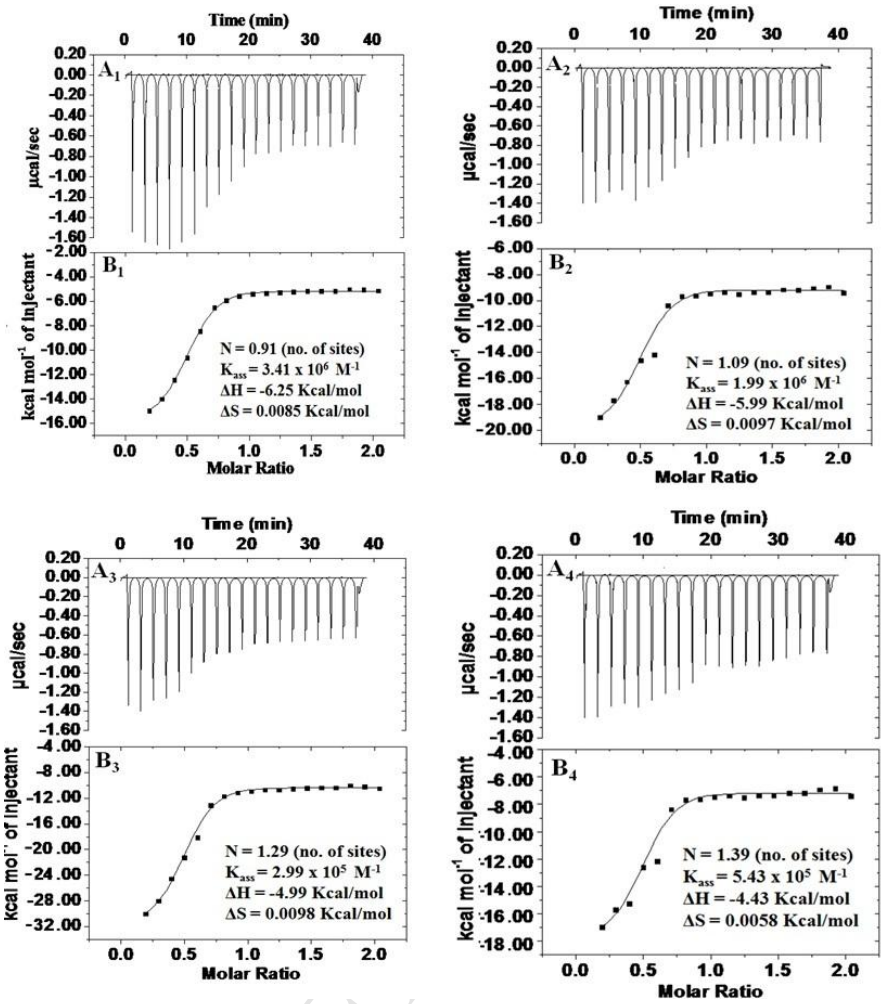

Fig. 3. Isothermal calorimetric data of compounds **7** for 5-LOX. A_1, B_1: compound **7b**, A_2, B_2: compound **7d**, A_3, B_3: compound **7h** and A_4, B_4: compound **7i**. A. ITC raw data 19 x 2 µL injections, B. Integrated heat pulse data.

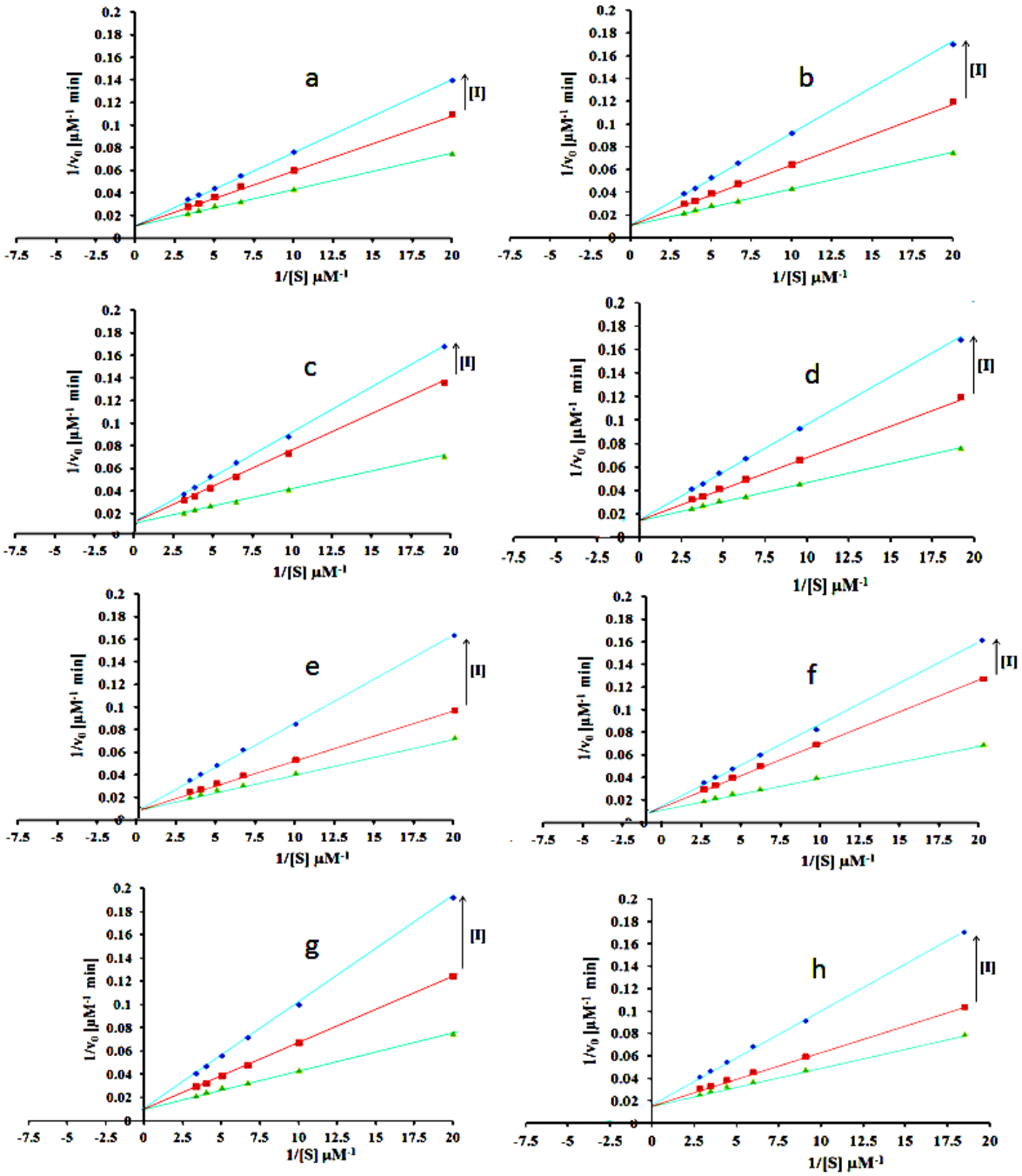

Fig. 4. Plots showing competitive inhibition of 5-LOX by: (a) compound **7b**, (b) compound **7d**, (c) compound **7h**, (d) compound **7i;** Competitive inhibition of COX-2 by: (e) compound **7b**, (f) compound **7d**, (g) compound **7h** and (h) compound **7i**. Arrow indicates increase in inhibitor concentration.

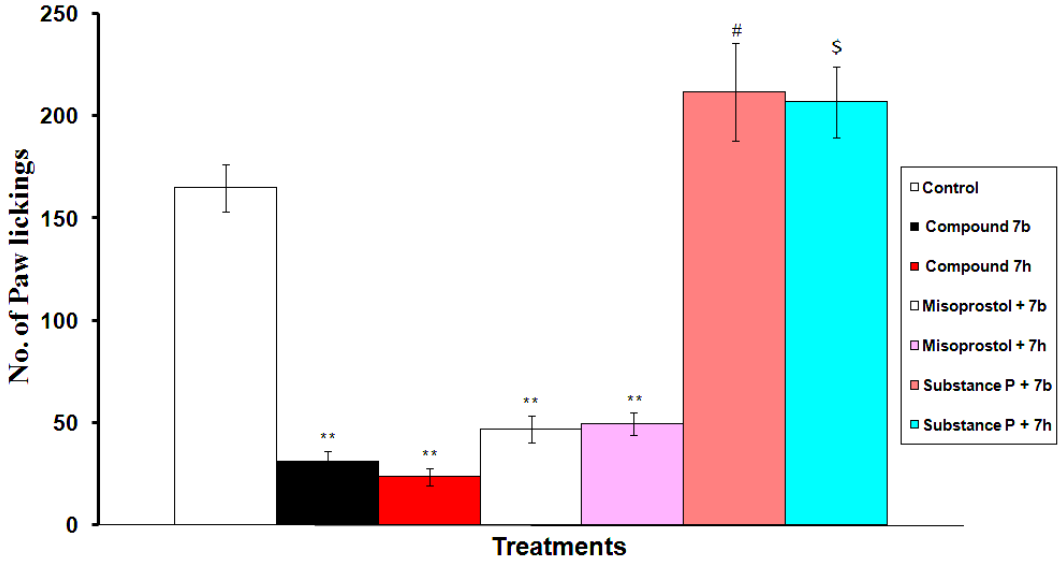

Fig. 5. Effect of misoprotol and substance P pretreatment on antihyperalgesic effect of compound **7b** and **7h** in capaicin induced hyperalgesia in mice. All values are expressed as mean ± SEM. ** $p < 0.01$ vs control group; # $p < 0.01$ vs compound **7b** group, $ $p < 0.01$ vs compound **7h** group.

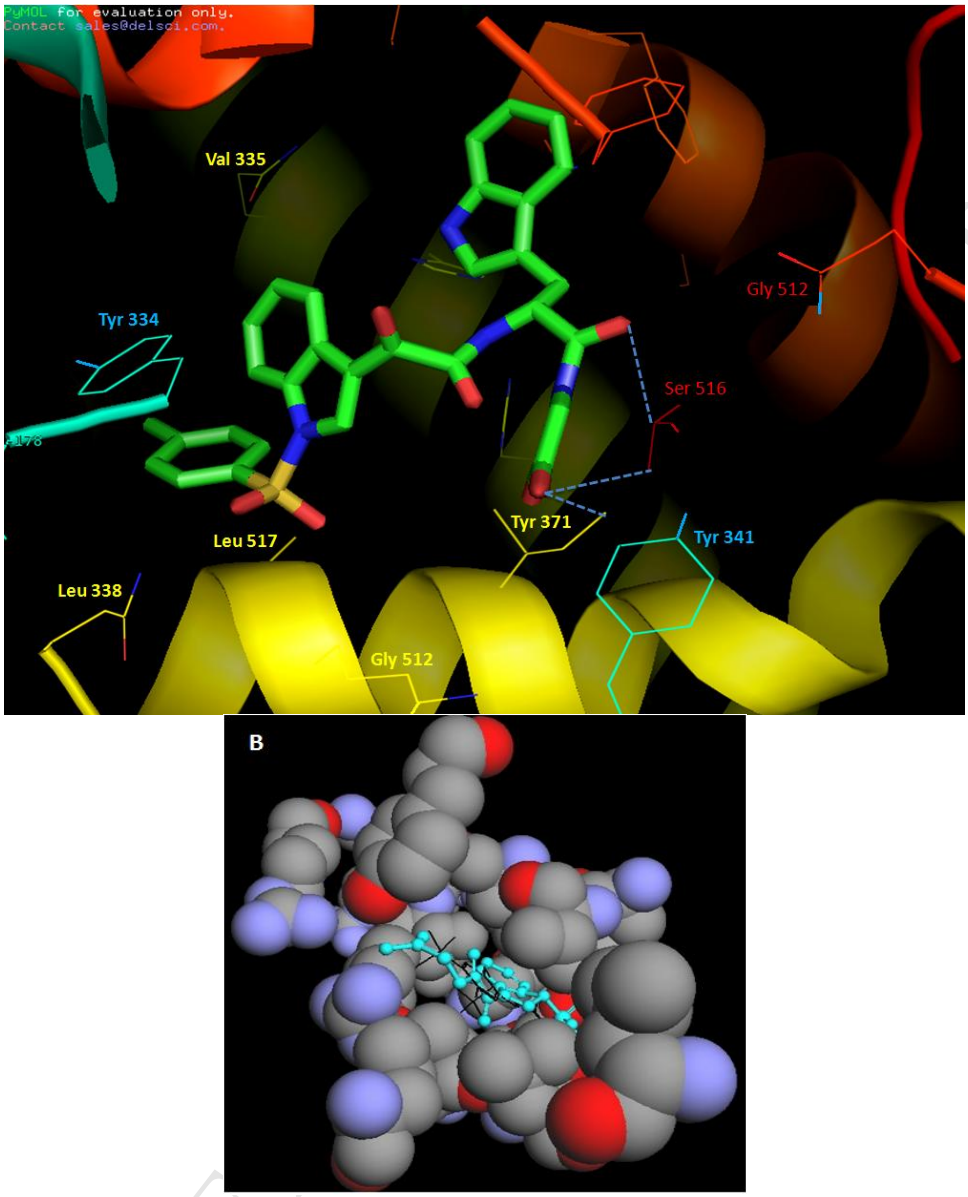

Fig. 6. A) Crystal coordinates of COX-2 (pdb ID 3MQE) [35] in association with compound 7**b** (green) (generated in Pymol). Dotted lines indicate H-bond interactions between the compound and amino acids. B) CPK model showing the placement of compound **7b** (blue) in the active site pocket of COX-2 enzyme.

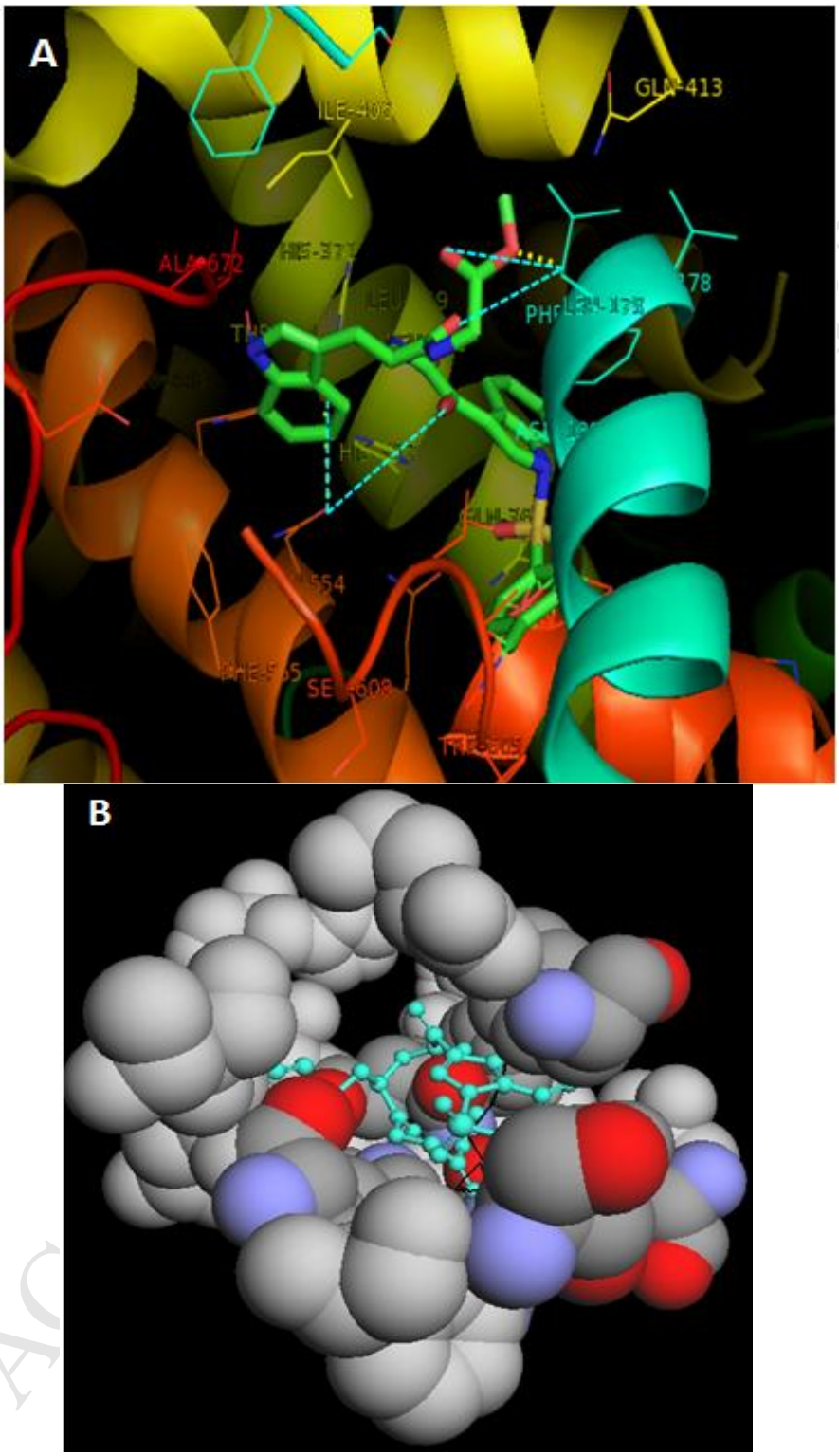

Fig. 7. A) Crystal coordinates of 5-LOX (pdb ID 3V99) [36] in association with compound **7b** (blue) (generated in Pymol). Dotted lines indicate H-bond interactions between the compound and amino acids. B) CPK model showing the placement of compound **7b** (green) in the active site pocket of 5-LOX enzyme.

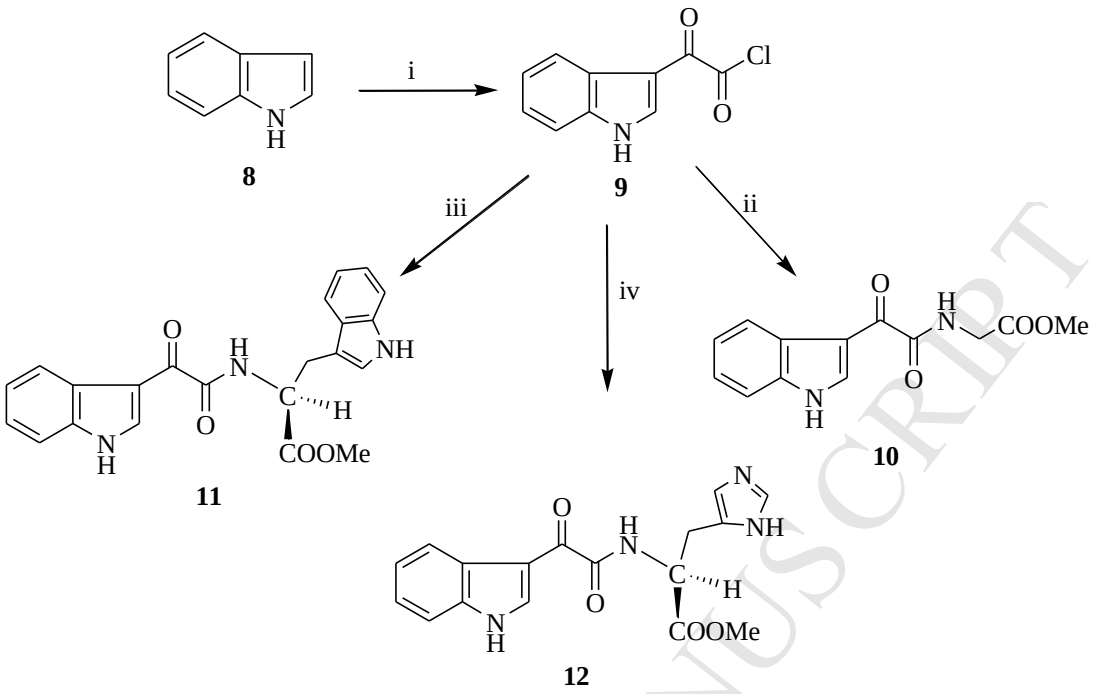

Reaction conditions:

i) $(COCl)_2$, dry ether, 0 ^oC

ii) Dry ACN, K_2CO_3, glycine methyl esterHCl, 0-5 ^oC

iii) Dry ACN, K_2CO_3, L-tryptophan methyl esterHCl, 0-5 ^oC

iv) Dry ACN, K_2CO_3, L-histidine methyl esterHCl, 0-5 ^oC

Scheme 1. Synthesis of compounds 10-12.

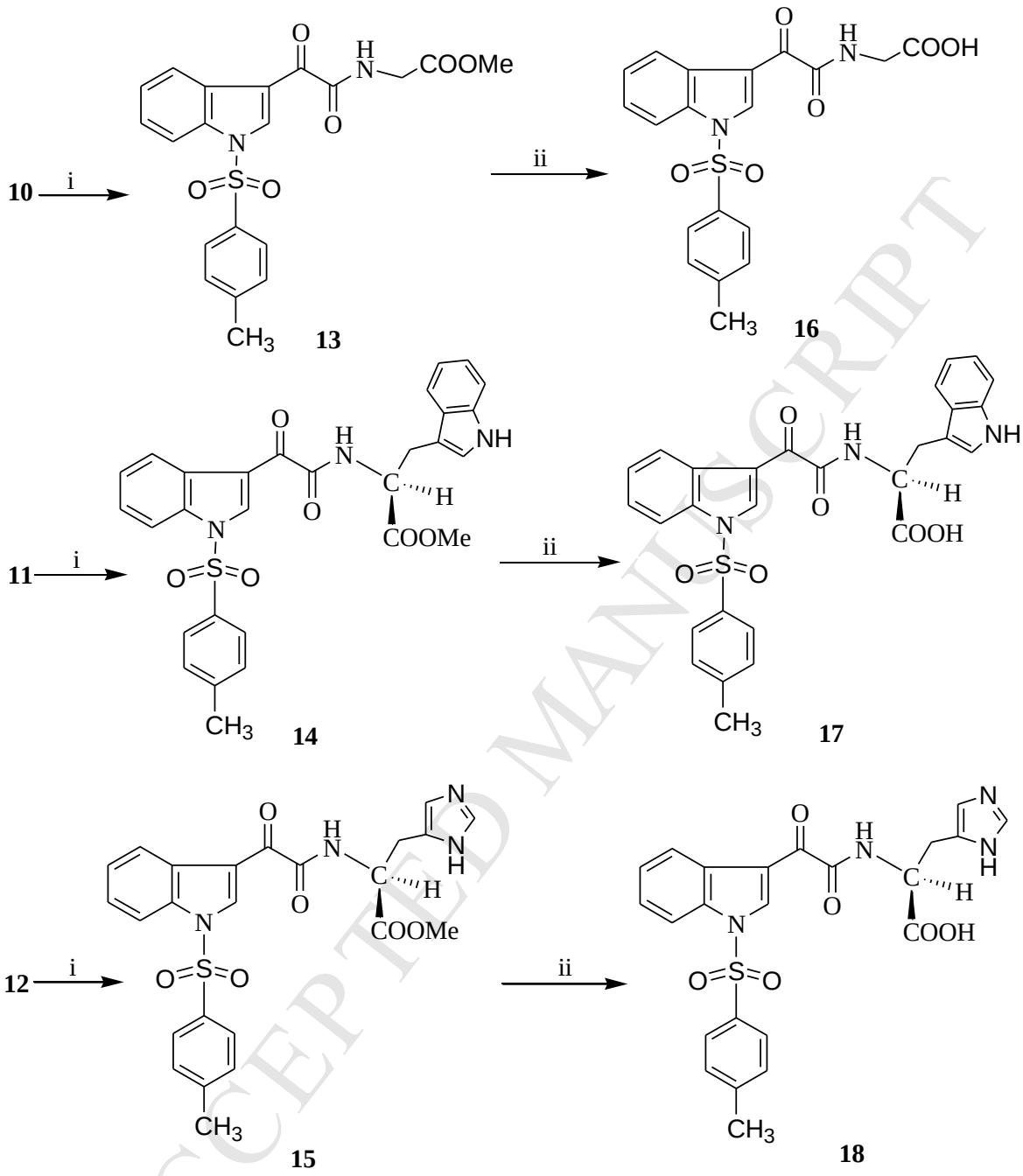

Reaction conditios: i) NaH, ACN, p-toluenesulphonyl chloride, 0 - 5 ^{o}C
ii) 1N NaOH, acetone - water, stir

Scheme 2. Synthesis of compounds 13 – 18.

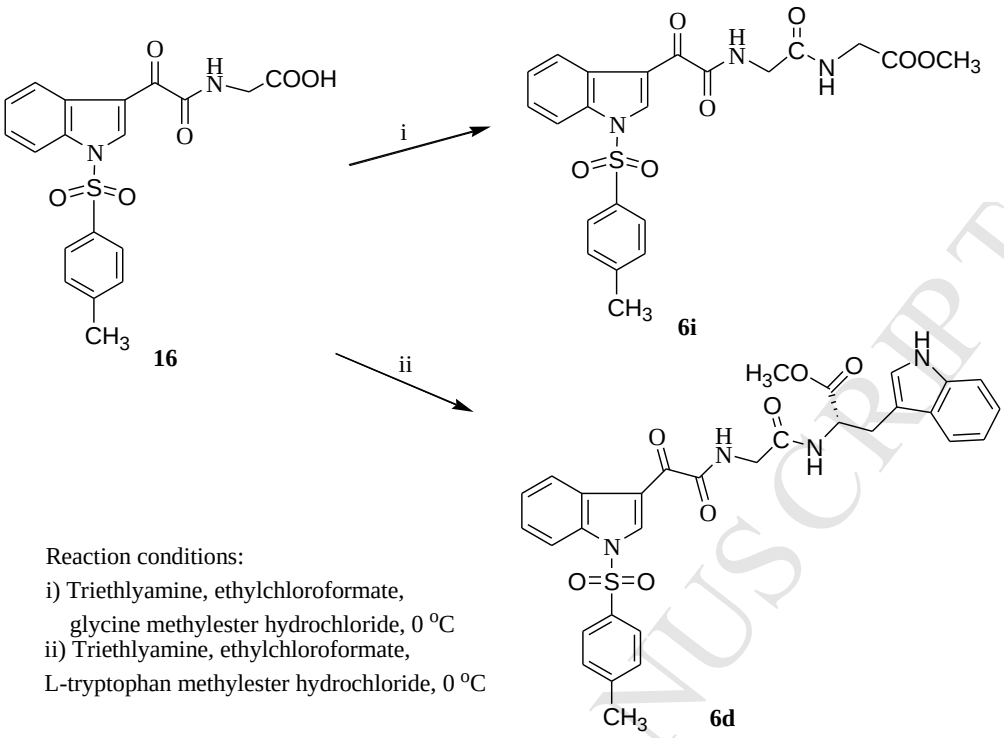

Reaction conditions:
i) Triethlyamine, ethylchloroformate,
glycine methylester hydrochloride, 0 ^{o}C
ii) Triethlyamine, ethylchloroformate,
L-tryptophan methylester hydrochloride, 0 ^{o}C

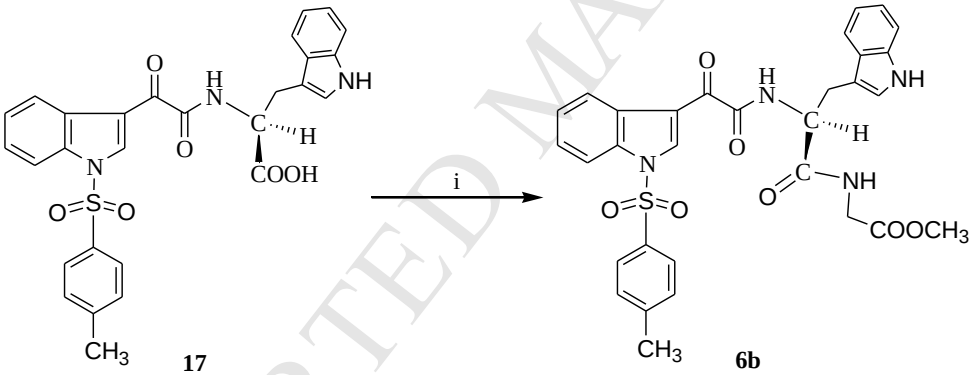

Reaction Conditions:
i) Ethylchloroformate, triethylamine, glycine methylester hydrochloride.

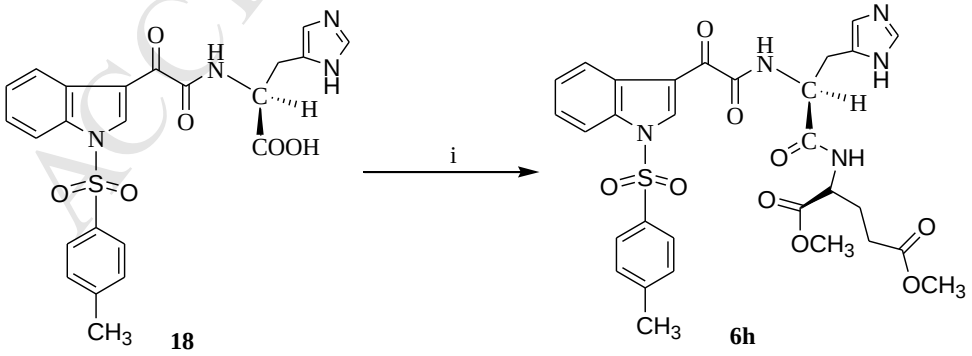

Reaction Conditions:
i) Ethylchloroformate, triethylamine, L-glutamic di methylester hydrochloride.

Scheme 3. Synthesis of compounds 6.

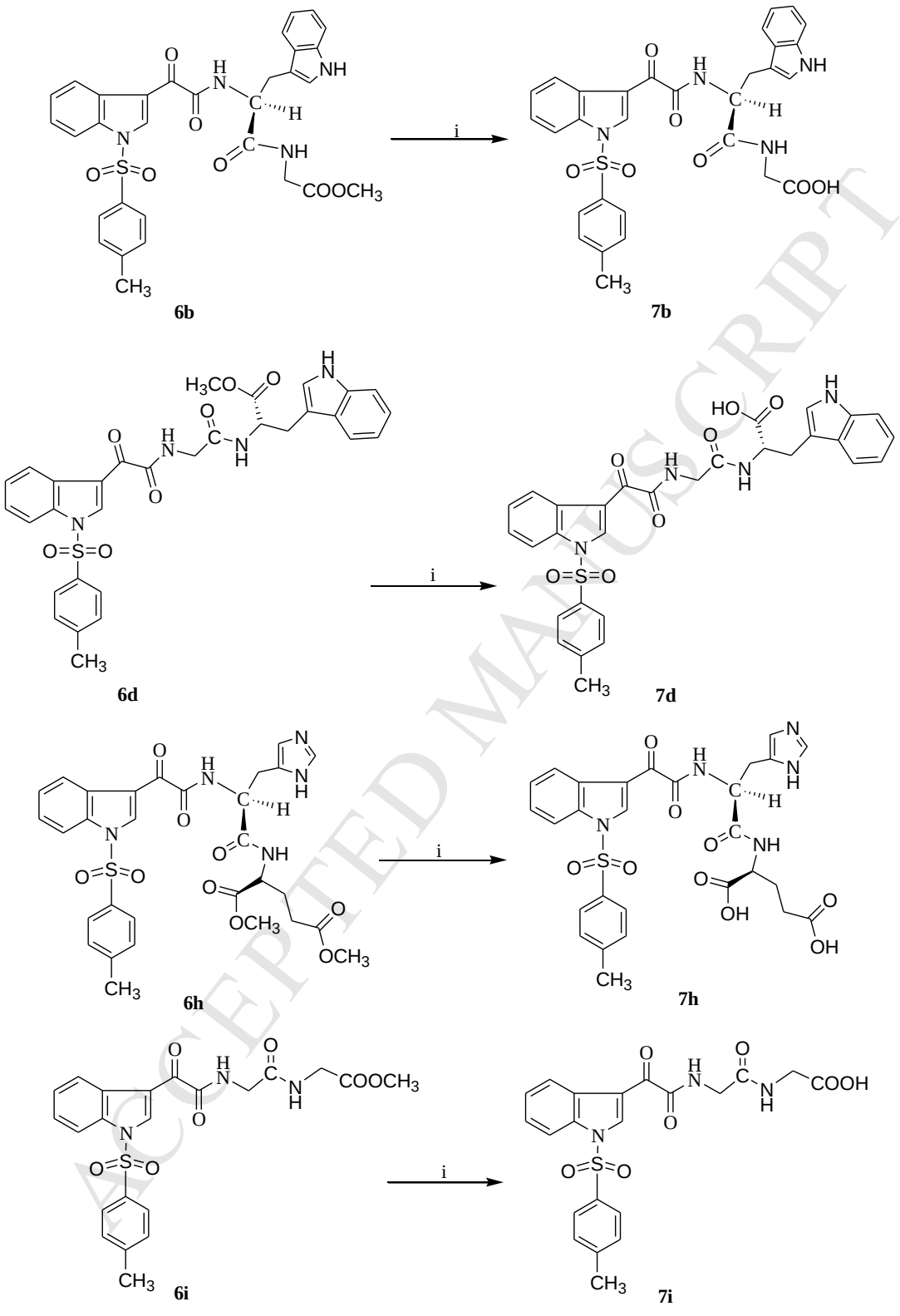

Reaction conditions:
i) 1N NaOH, acetone-water

Scheme 4. Synthesis of compounds 7.

Highlights

- ►Indoles bearing tosyl group at N-1 and dipeptide at C-3 were designed and synthesized.
- ►Some of these compounds exhibited appreciable anti-inflammatory and anti-hyperalgesic activities.
- ► Mechanistically, it was found that the compounds target both COX-2 and 5-LOX enzymes.

Indole Based Peptidomimetics as Anti-inflammatory and Anti-hyperalgesic Agents: Dual Inhibition of 5-LOX and COX-2 Enzymes

Palwinder Singh,[a] *Parteek Prasher,*[a] *Parvirti Dhillon,*[b] *Rajbir Bhatti*[b]

[a]Department of Chemistry, Guru Nanak Dev University, Amritsar – 143005, India

[b]Department of Pharmaceutical Sciences, Guru Nanak Dev University, Amritsar – 143005, India

Supplementary information

Table of contents

Molecular Docking studies

Table S1. Docking score of compounds 6 and 7 when docked in the active site of 5-LOX. and COX-2.

S. No	Compound	Docking score (Kcal/mol)	
		5-LOX	COX/2
1	**6i**	-18.57	17.79
2	**7i**	-20.43	21.88
3	**6b**	-18.57	11.11
4	**6a**	-11.57	9.81
5	**7b**	-28.43	23.96
6	**7a**	-13.43	11.90
7	**6h**	-18.88	18.98
8	**6f**	-11.31	14.84
9	**6g**	-12.22	11.73
10	**6e**	-12.48	12.01
11	**7e**	-17.56	15.87
12	**7f**	-18.21	12.34
13	**7g**	-20.95	12.20
14	**7h**	-22.06	22.28
15	**6d**	-18.88	11.21
16	**6c**	-10.04	9.99
17	**7d**	-26.56	26.19
18	**7c**	-14.58	16.76

Table S2. Docking score and H-bond interactions of compounds 6 and 7 in the active site of 5-LOX.

Compd	Docking Score (Kcal/mol)	H-bond interactions with amino acid residues				
6i	-18.57	H367 (2.81 Å), O=S=O	N554 (2.22 Å), COOMe	Q557 (2.42 Å), COOMe	-	-
7i	-20.43	H367 (2.23 Å), COOH	H372 (1.22 Å), COOH	L368 (2.77 Å), COOH	-	-
6b	-18.57	Q363 (1.11 Å), C=O	H372 (1.61 Å), O=S=O	-	-	-
6a	-11.57	H367 (2.22 Å), $CONH_2$	Q557 (2.88 Å), COOMe	-	-	-
7b	-28.43	F177 (2.61 Å), C=O	N554 (1.10 Å), C=O	F177 (3.57 Å), $CONH_2$		-
7a	-13.43	F177 (2.36 Å), O=S=O	H372 (1.22 Å), $CONH_2$	Q557 (2.91 Å), O=S=O	H367(2.72Å), $CONH_2$	-
6h	-18.88	H732 (2.99 Å), COOMe	H367 (1.59 Å), COOMe	S171 (1.99 Å), O=S=O	Q363 (3.69Å), C=O	-
6f	-11.31	L607 (1.99 Å), COOMe	L607 (2.44 Å), O=S=O	N554 (1.45 Å), C=O	-	-
6g	-12.22	Q557 (2.14 Å), COOMe	-	-	-	-
6e	-12.48	N554 (2.92 Å), COOMe	Q363 (1.72 Å), COOMe	Q363 (2.72 Å), COOMe	-	-
7e	-17.56	H367 (2.22 Å), $CONH_2$	H372 (1.99 Å), $CONH_2$	H367 (1.92 Å), COOH	Q557 (2.88 Å), COOH	F177 (1.39 Å), O=S=O
7f	-18.21	H367 (1.99 Å), COOH	F177 (2.44 Å), C=O	L607 (2.14 Å), $CONH_2$	-	-
7g	-20.95	H372 (2.54 Å), O=S=O	-	-	-	-
7h	-22.06	I406 (1.99 Å), C=O	I406 (3.40 Å), COOH	F177 (3.76 Å), $CONH_2$	Q363 (2.10 Å), O=S=O	-
6d	-18.88	H372 (2.93 Å), COOMe	-	-	-	-
6c	-10.04	H367 (1.11 Å), $COONH_2$	-	-	-	-
7d	-26.56	F177 (1.71 Å), COOH	L607 (2.21 Å), $CONH_2$	I406 (1.21 Å), $CONH_2$	-	-
7c	-14.58	L368 (2.99 Å), $CONH_2$	H367 (2.27 Å), COOH	-	-	-

Ziluton	-9.18	F177 (2.11 Å), C=O	S171 (2.81 Å), C=O	-	-	-
MK886	-9.96	H372 (2.72 Å), COOH	-	-	-	-
MK0591	-13.56	S171 (2.71 Å), N	H367 (2.06 Å), COOH	H367 (2.08 Å), COOH	H367 (2.41 Å), N	-

Table S3. Docking score and H-bond interactions of compounds 6 and 7 in the active site of COX-2.

Compd	**Docking Score (Kcal/mol)**	**H-bond interactions with amino acid residues**				
6i	17.79	R106 (2.73 Å), $CONH_2$	R106 (2.97 Å), $CONH_2$	R106 (2.89 Å), $CONH_2$	-	-
7i	21.88	Y371 (2.17 Å), O=S=O	Y371 (2.84 Å), N(indolic)	-	-	-
6b	11.11	R106 (2.73 Å), $CONH_2$	-	-	-	-
6a	9.81	R106 (2.84 Å), $CONH_2$	-	-	-	-
7b	23.96	S516 (2.20 Å), COOH	S516 (2.14 Å), $CONH_2$	Y371 (2.50 Å), COOH	-	-
7a	11.90	S516 (2.14 Å), $CONH_2$	-	-	-	-
6h	18.98	Y341 (2.72 Å), COOMe	R106 (1.95 Å), O=S=O	R106 (2.88 Å), O=S=O	R106 (2.28 Å), N(indolic)	R106 (2.89 Å), C=O
6f	14.84	Y341 (2.89 Å), COOMe	Y341 (2.34 Å), $CONH_2$	R106 (2.90 Å), $CONH_2$	-	-
6g	11.73	Y371 (2.89 Å), O=S=O	-	-	-	-
6e	12.01	Y371 (2.34 Å), C=O	Y371 (2.90 Å), O=S=O	Y334 (2.42 Å), C=O	Y334 (1.81 Å), COOMe	-
7e	15.87	L338 (2.86 Å), COOH	Y341 (2.25 Å), N(imidazolic)	-	-	-
7f	12.34	Y341 (2.87 Å), COOH	-	-	-	-
7g	12.20	Y341 (2.89 Å), C=O	R106 (2.42 Å), C=O	R106 (2.84 Å), C=O	-	-

7h	22.28	G512 (2.50 Å), O=S=O	R106 (2.81 Å), $CONH_2$	R106 (2.78 Å), $CONH_2$	-	-
6d	11.21	S516 (2.63 Å), $CONH_2$	-	-	-	-
6c	9.99	Y341 (2.84 Å), C=O	-	-	-	-
7d	26.19	R106 (2.87 Å), COOH	R106 (2.46 Å), COOH	S516 (2.39 Å), O=S=O	-	-
7c	16.76	Y371 (2.84 Å), $CONH_2$	A513 (2.72 Å), COOH	A513 (2.47 Å), COOH	-	-

Table S4. Physicochemical Indicators for compounds 6 and 7.

Compound	ClogP	TPSA	nATOMS	nON	nOHNH	nROTB
6i	2.22	140.648	33	10	2	9
7i	1.04	151.642	32	10	3	8
6b	2.11	156.439	44	11	3	12
7b	1.32	167.430	43	11	4	11
6d	2.40	150.321	44	11	3	12
7d	1.39	155.987	43	11	4	11
6h	2.80	160.700	48	14	5	13
7h	1.11	165.345	47	14	6	12

Synthesis of compounds 6a, 6c, 6e and 7a, 7c, 7e.

Oxalyl chloride was slowly added to the ice cooled solution of indole (**8**) in dry ether. The yellow colored solid (**9**) was filtered and dissolved in dry ACN followed by the addition of K_2CO_3. D-Amino acid ester hydrochloride was neutralized with triethylamine and added to the ACN solution of compound **9**. All additions to the reaction mixture were performed at 0 ^oC. C-3 Substituted indoles **19** and **20** (Scheme S1) were purified through column chromatography using ethyl acetate – hexane as the eluent.

Compounds **19** and **20** (1 mmol) and hexane washed NaH (1.2 mmol) were taken in dry ACN. Keeping this solution at 0 – 5 ^oC, p-toluene sulphonyl chloride (1.2 mmol) was added. The reaction mixture was stirred for 30 min and filtered. The filtrate was concentrated under vacuum and purified by column chromatography to procure compounds **21** and **22.** Compounds **21** and **22** were further treated with 1N NaOH in acetone – H_2O (1:1) to get compound **23** and **24.** Compound **23** and triethyl amine were taken in dry DCM. After stirring the contents for 2 – 3 min at 0 ^oC, ethylchloroformate was added to the reaction mass. Eventually, the neutralized solution of glycine methyl ester hydrochloride (neutralized with 1.5 equivalent solution of triethylamine) was added to the reaction mass. The coupling reaction was completed in 25 – 30 min and compound **6a** was procured**.** Similarly, compound **6e** was synthesized from compound **24** by coupling reaction with D-glutamic methyl diester hydrochloride salt (having ***'R'*** stereochemistry at the chiral carbon). Compounds **6(a,c,e)** were dissolved in acetone-water (2:1) containing 1N NaOH. The hydrolysis was completed in 15 – 20 min to yield compounds **7(a,c,e)** (Scheme S2)**.** The crude product was purified through column chromatography using ethyl acetate – hexane as eluent. NMR spectra of compounds **7a**, **7c** and **7e** was comparable to their corresponding enantiomer/diastereomer **7b**, **7d** and **7h** but optical rotation $[\alpha]_D$= –20, -18, -14 (c 1, MeOH) was different.

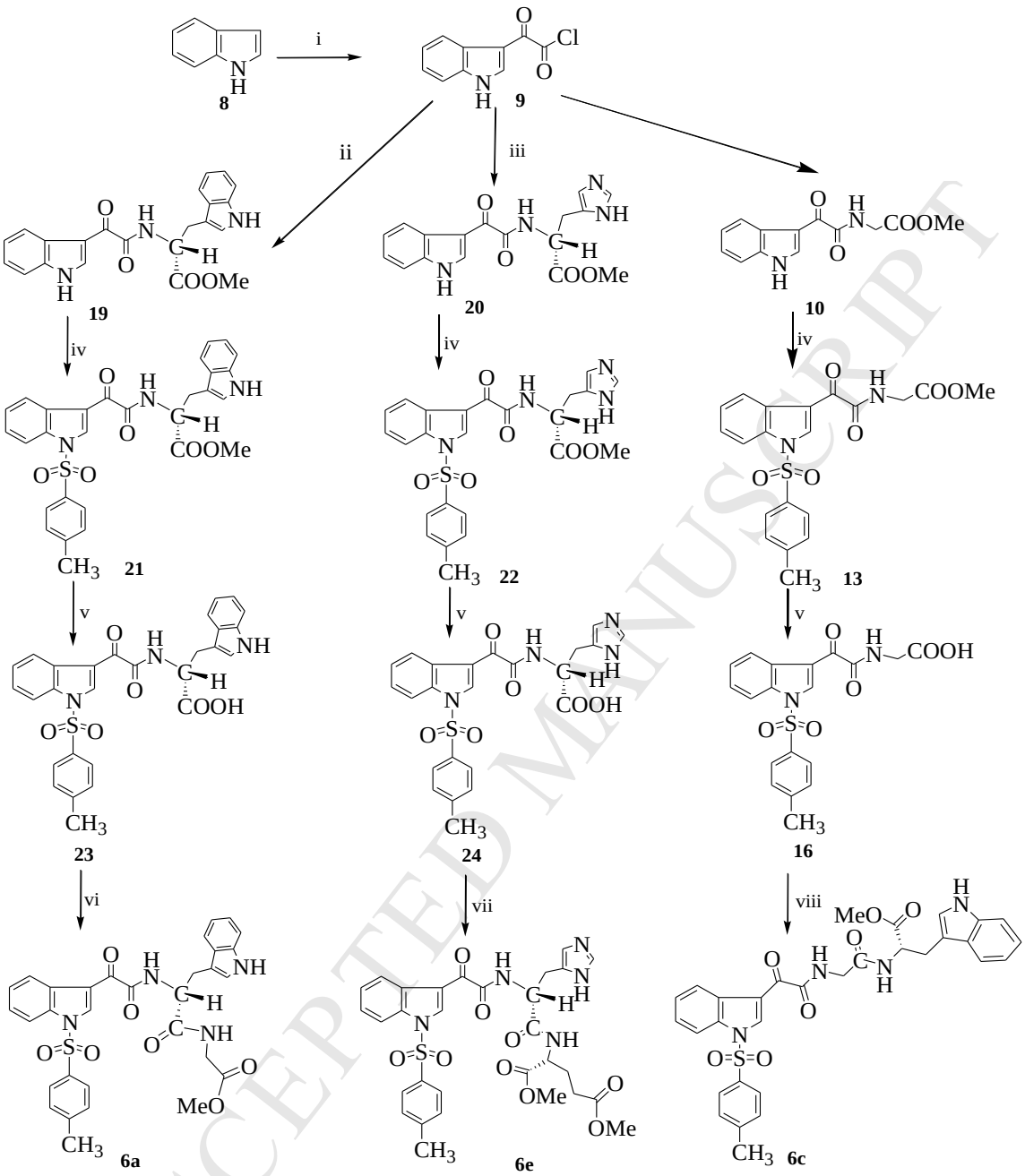

Reaction conditions:

i) $(COCl)_2$, dry ether, 0 ^oC

ii) Dry ACN, K_2CO_3, D-tryptophan methyl esterHCl, 0-5 ^oC

iii) Dry ACN, K_2CO_3, D-histidine methyl esterHCl, 0-5 ^oC

iv) NaH, ACN, p-toluenesulphonyl chloride, 0 - 5 ^oC

v) 1N NaOH, acetone - water, stir

vi) Ethylchloroformate, triethylamine, glycine methylester hydrochloride

vii) Ethylchloroformate, triethylamine, D-glutamic dimethyl ester hydrochloride

viii)Ethylchloroformate, triethylamine, D-trryptophan methyl ester hydrochloride

Scheme S1. Synthesis of compounds **6a**, **6c**, **6e**).

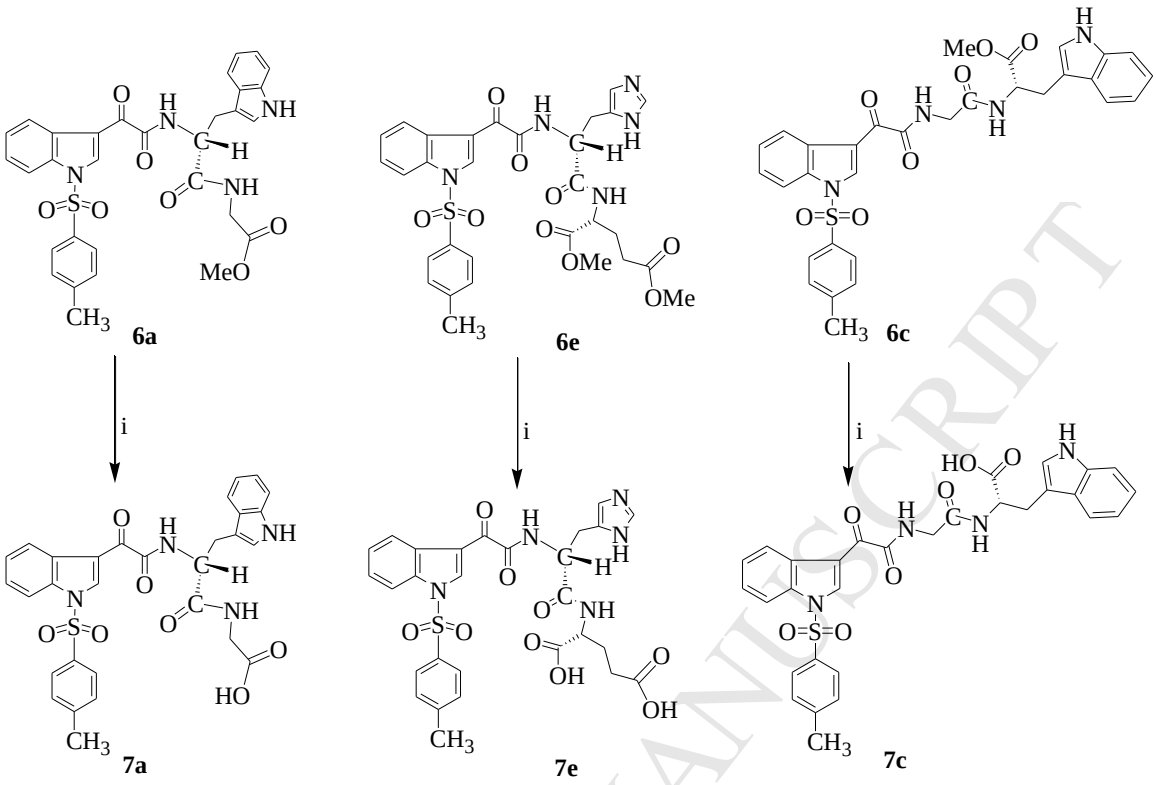

Reaction conditions:
i) 1N NaOH, acetone - water, stir

Scheme S2. Synthesis of compounds **7a, 7c, 7e.**

^{1}H NMR SPECTRA OF COMPOUNDS:

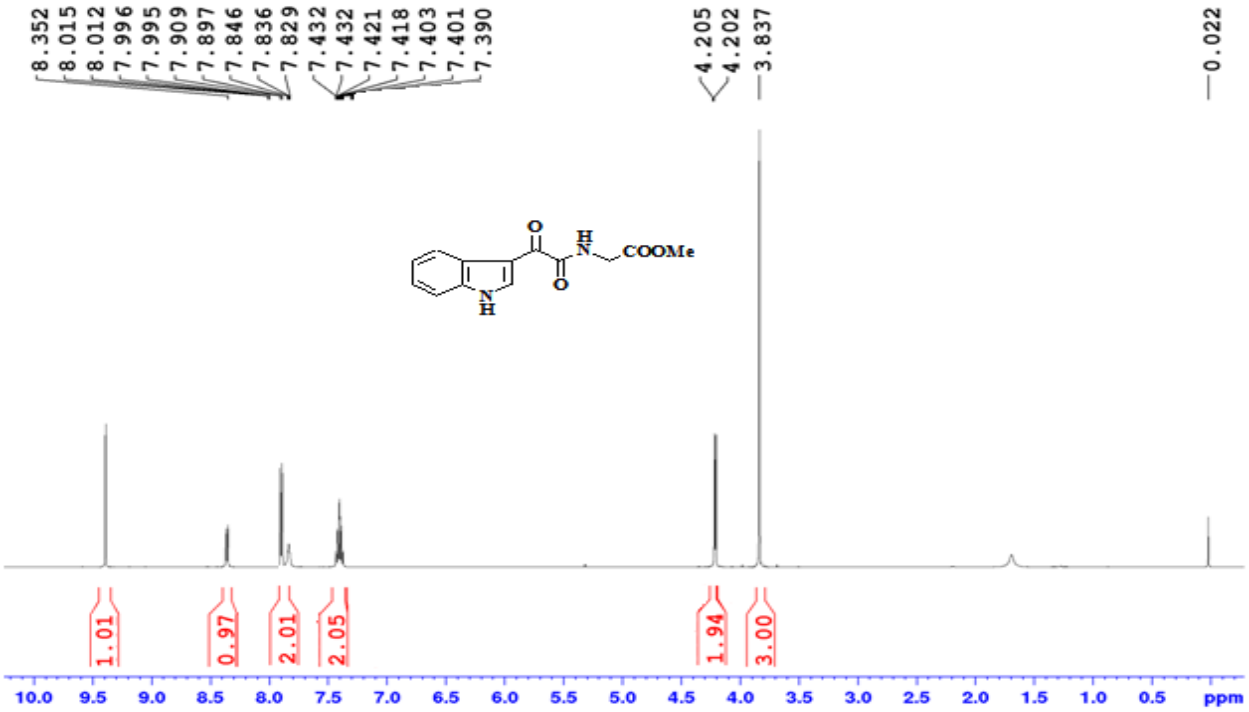

Figure S1. ^{1}H NMR spectrum of compound 10.

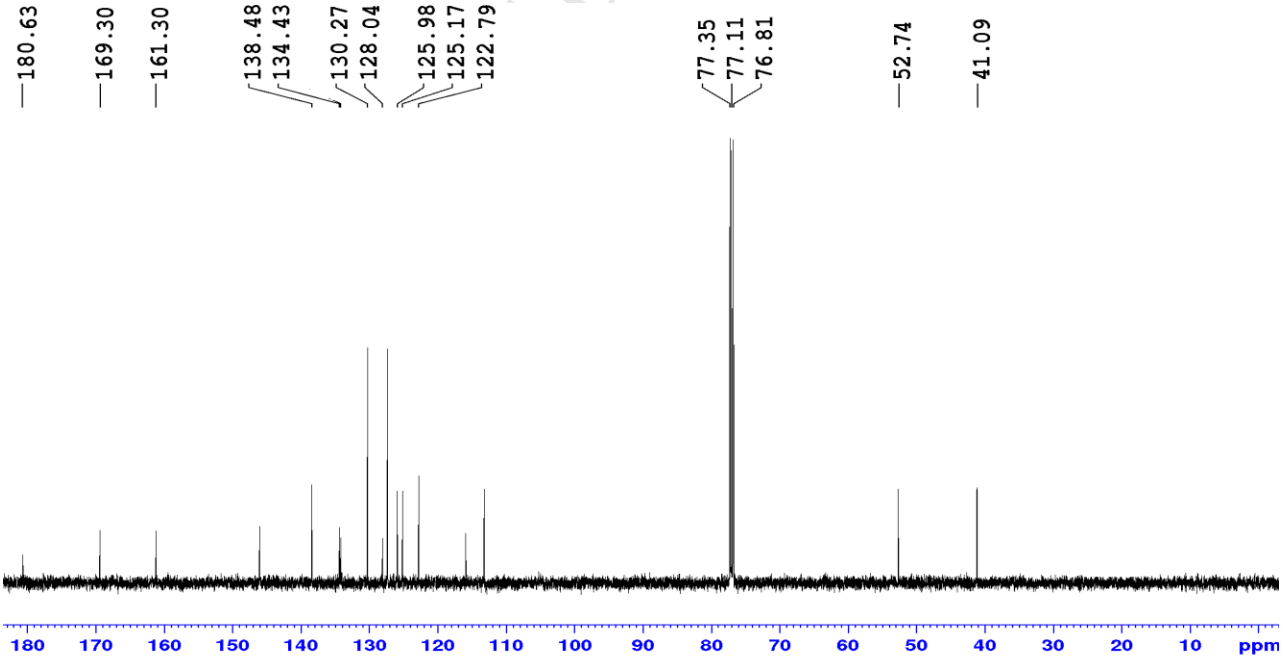

Figure S2. ^{13}C NMR spectrum of compound 10.

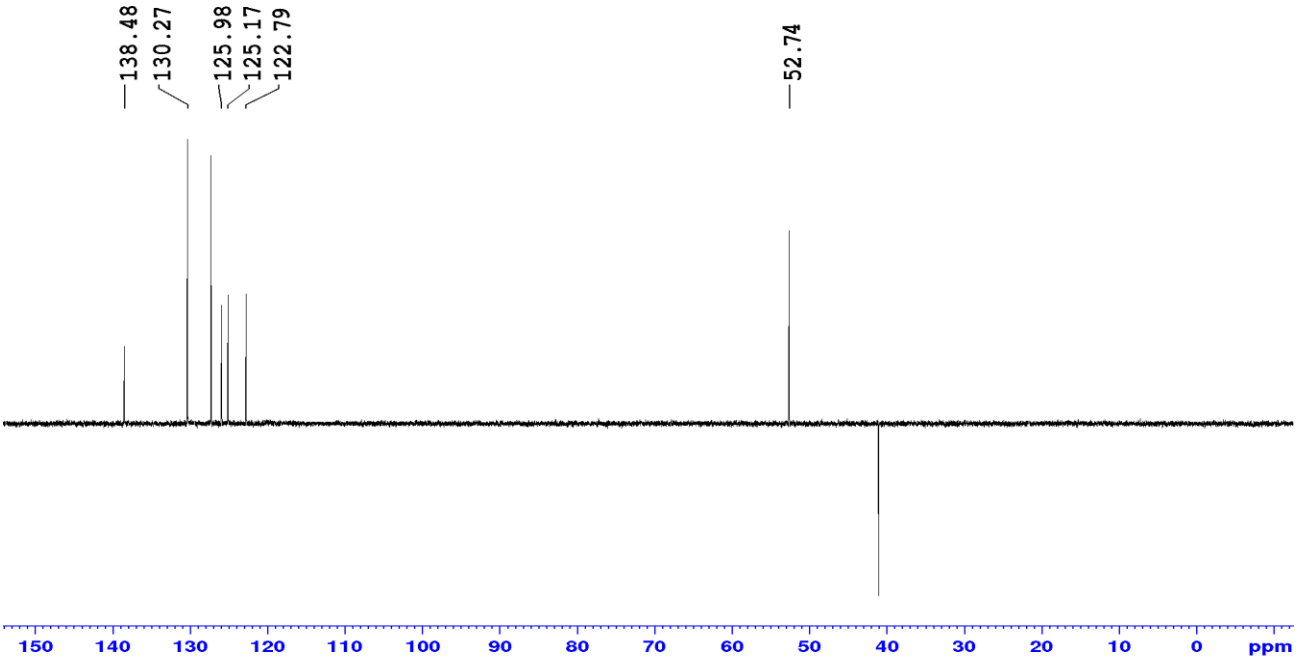

Figure S3. DEPT-135 NMR spectrum of compound 10.

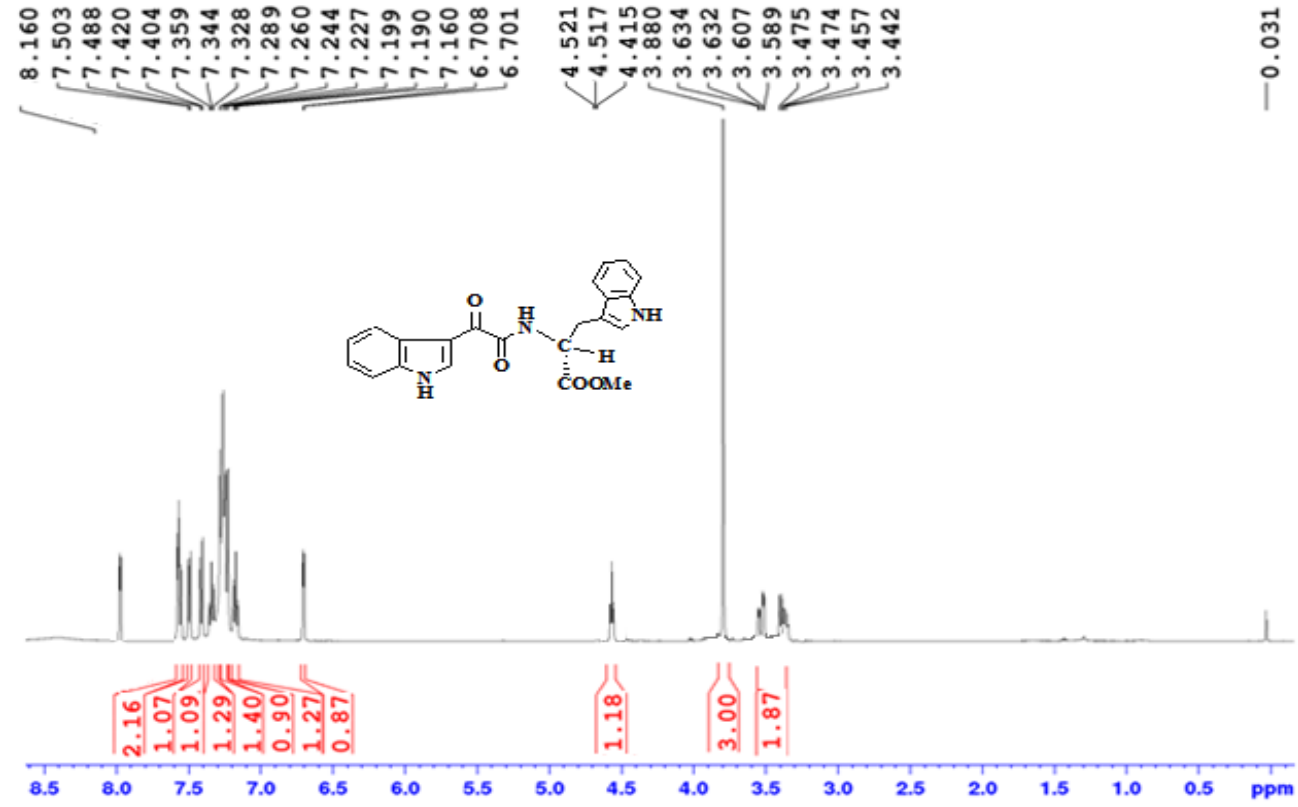

Figure S4. ^{1}H NMR spectrum of compound 11.

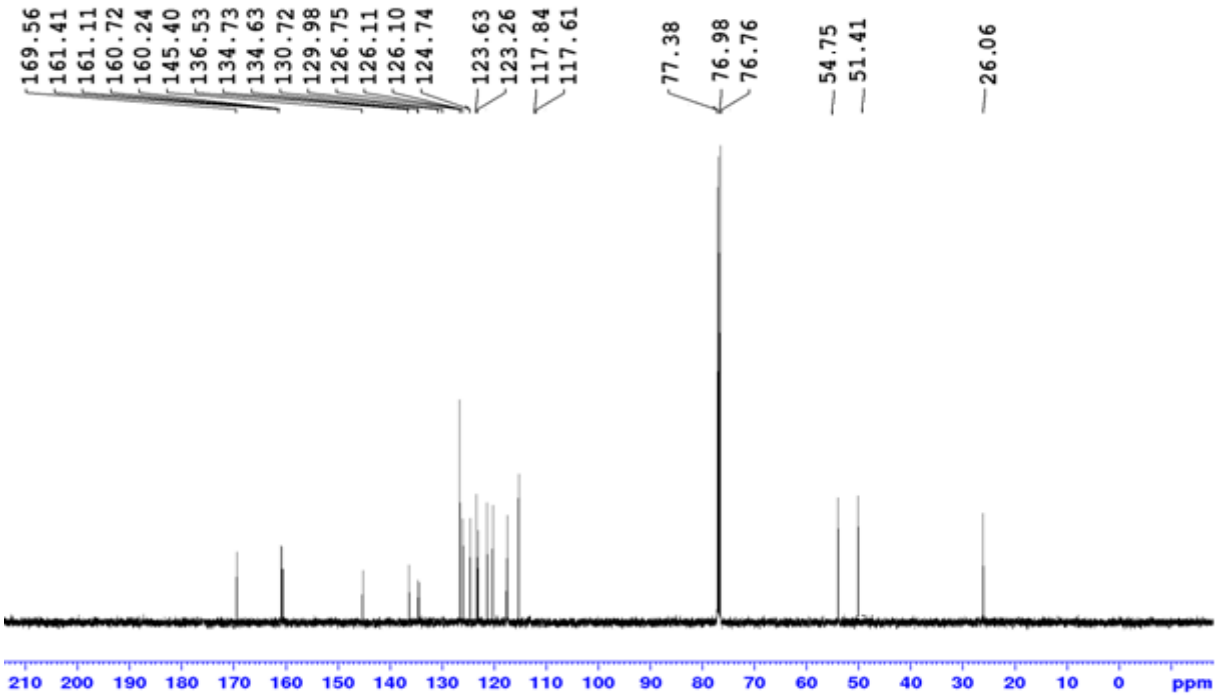

Figure S5. ^{13}C NMR spectrum of compound 11.

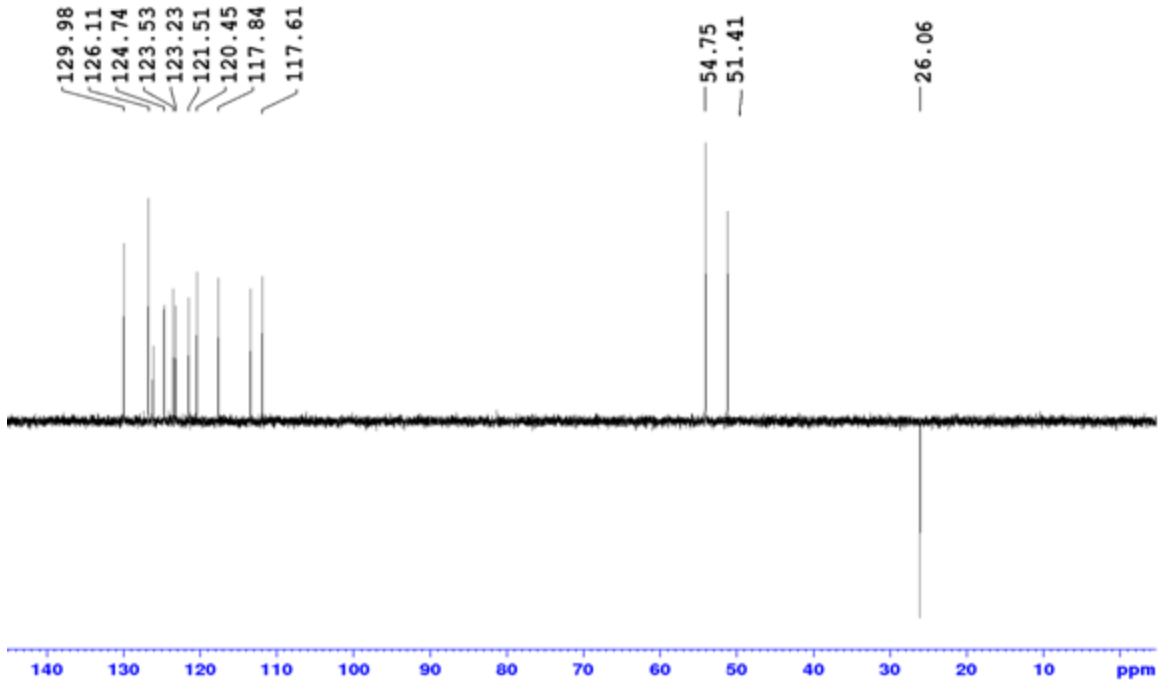

Figure S6. DEPT-135 NMR spectrum of compound 11.

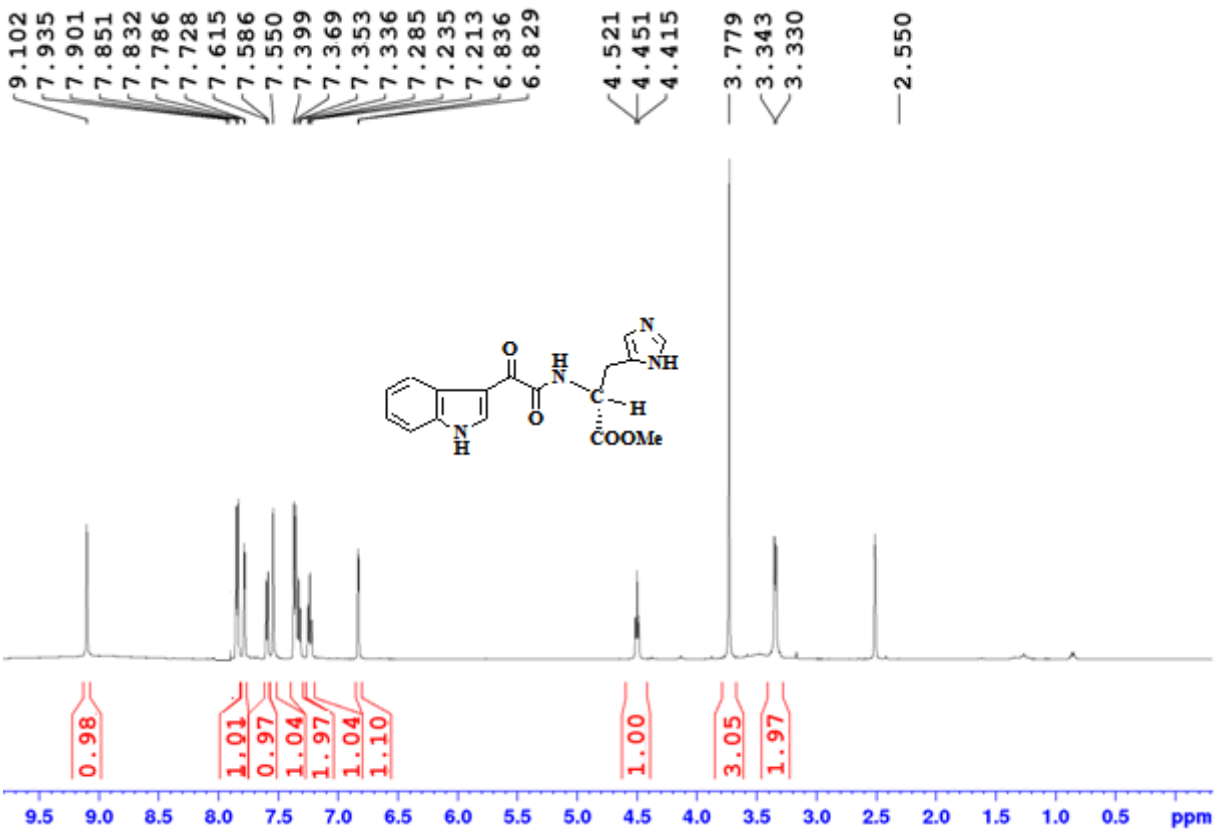

Figure S7. ^{1}H NMR spectrum of compound 12.

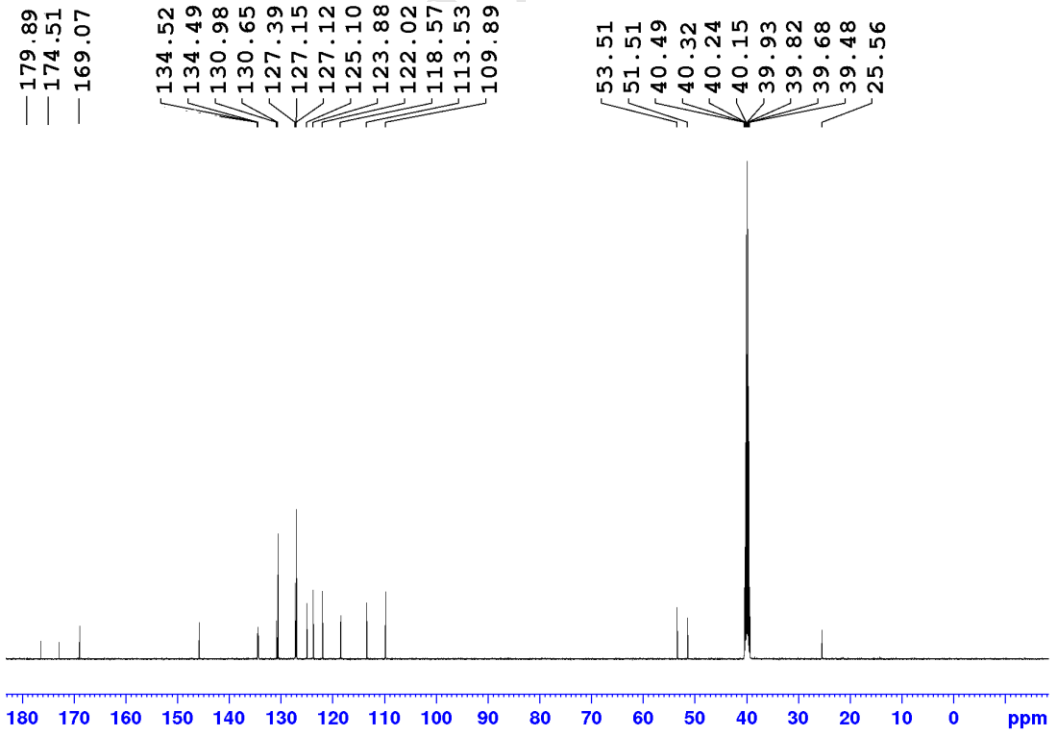

Figure S8. ^{13}C NMR spectrum of compound 12.

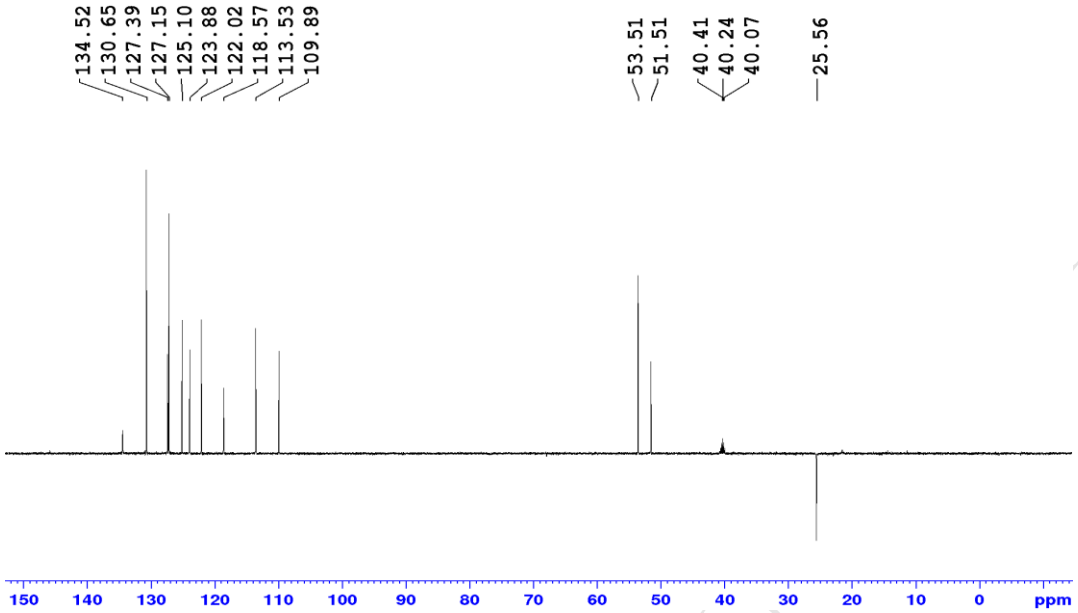

Figure S9. DEPT-135 NMR spectrum of compound 12.

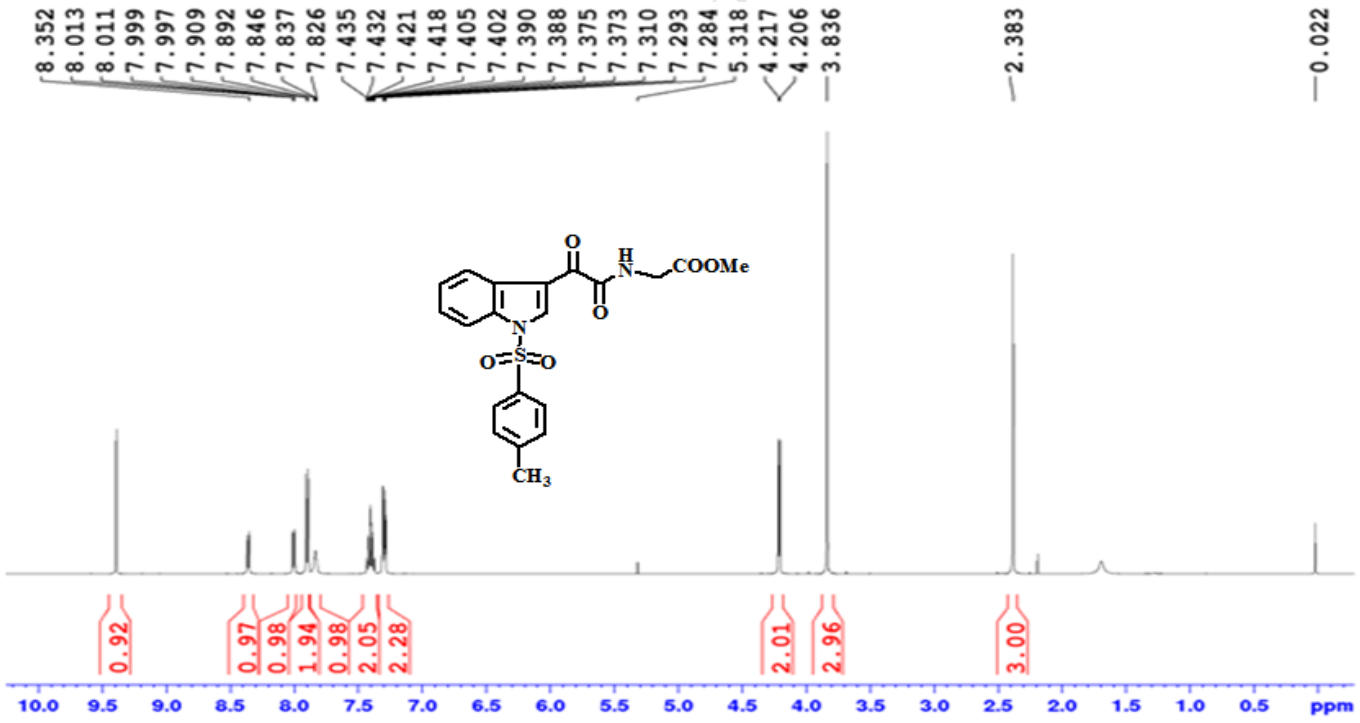

Figure S10. ^{1}H NMR spectrum of compound 13.

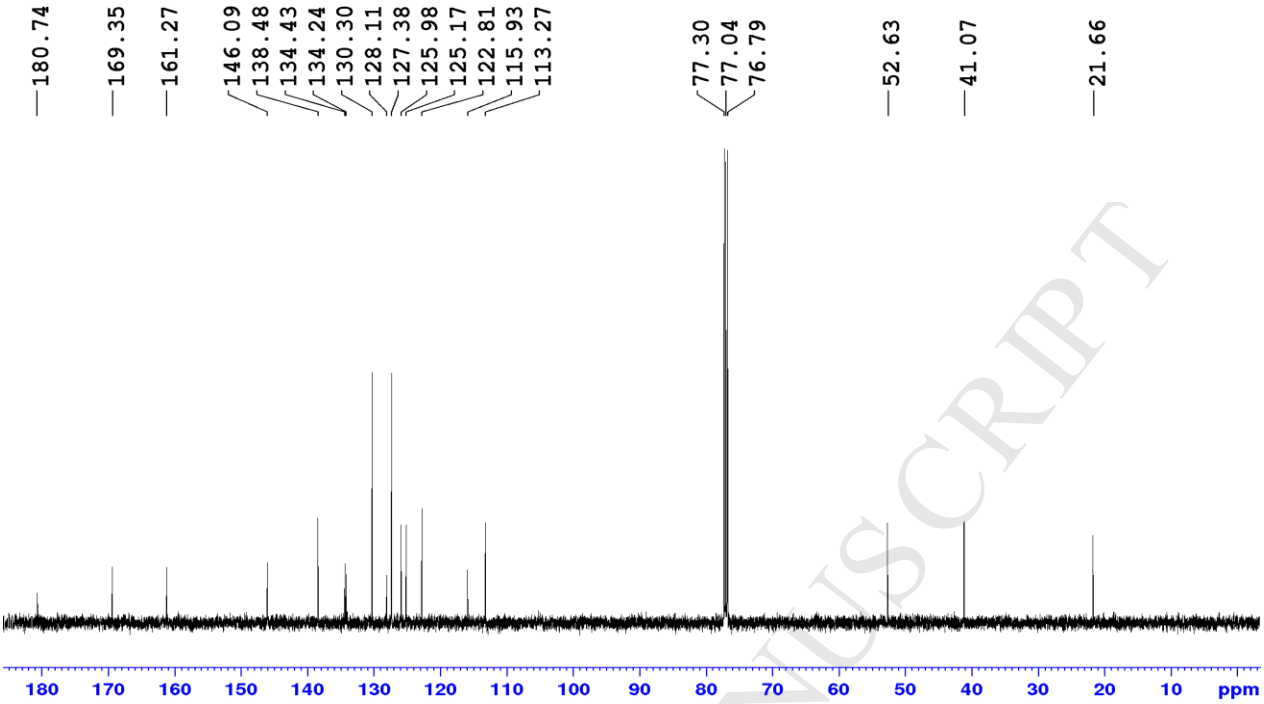

Figure S11. ^{13}C NMR spectrum of compound 13.

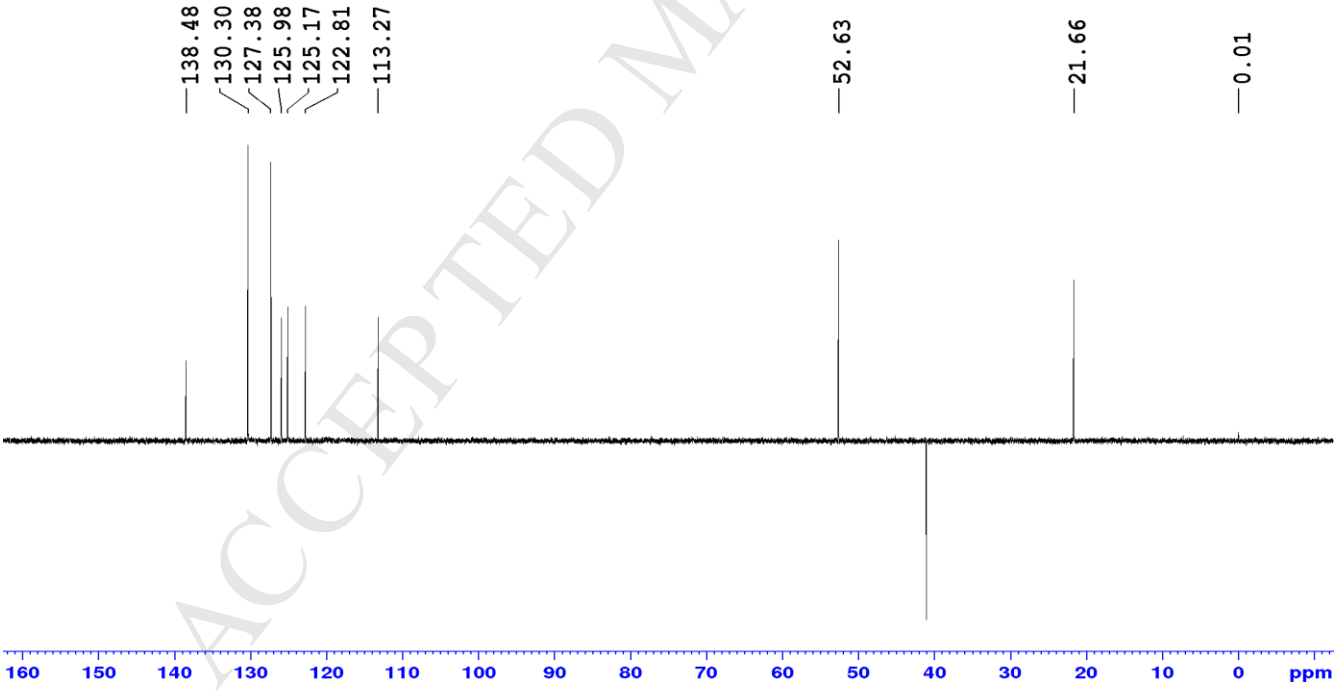

Figure S12. DEPT-135 NMR spectrum of compound 13.

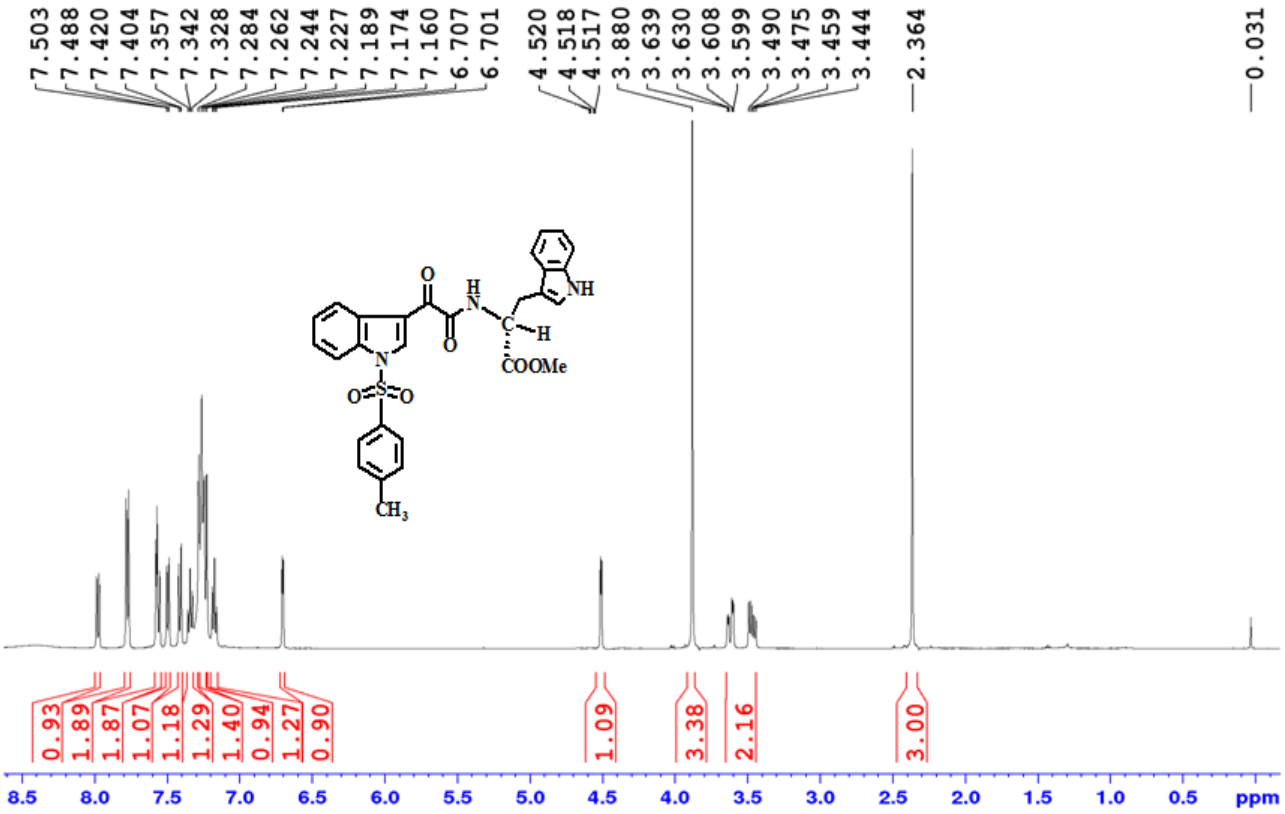

Figure S13. ^{1}H NMR spectrum of compound 14.

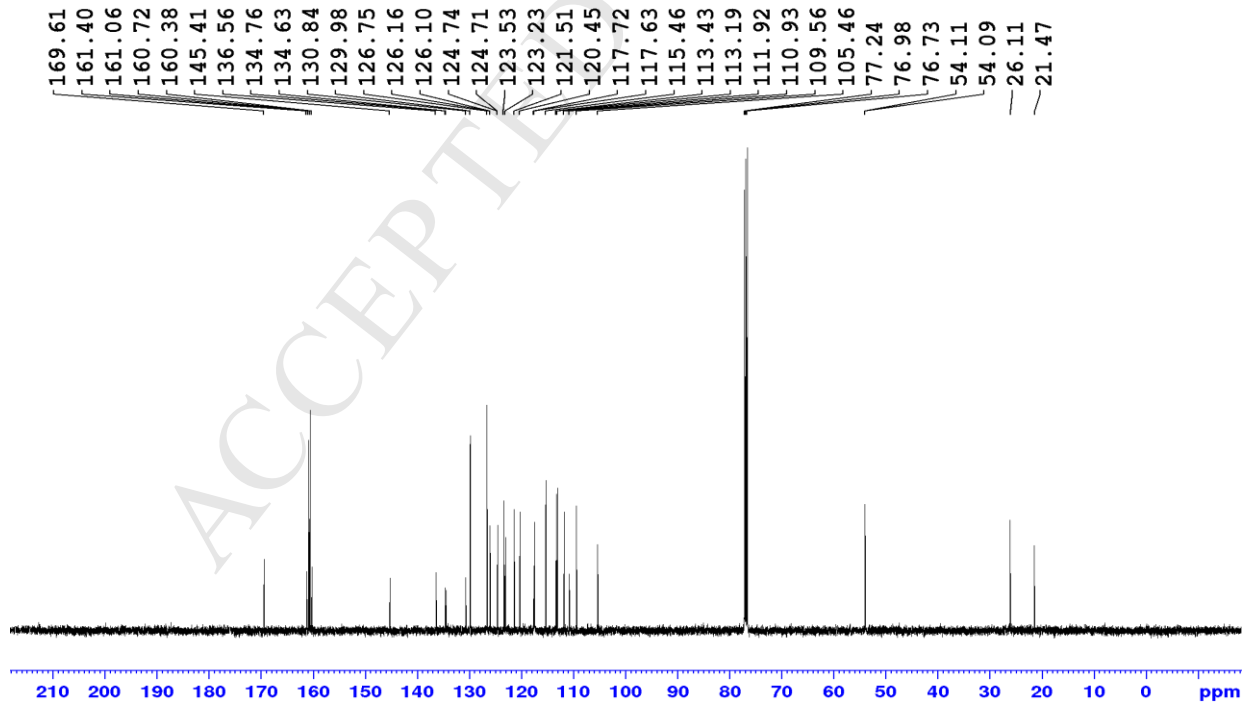

Figure S14. ^{13}C NMR spectrum of compound 14.

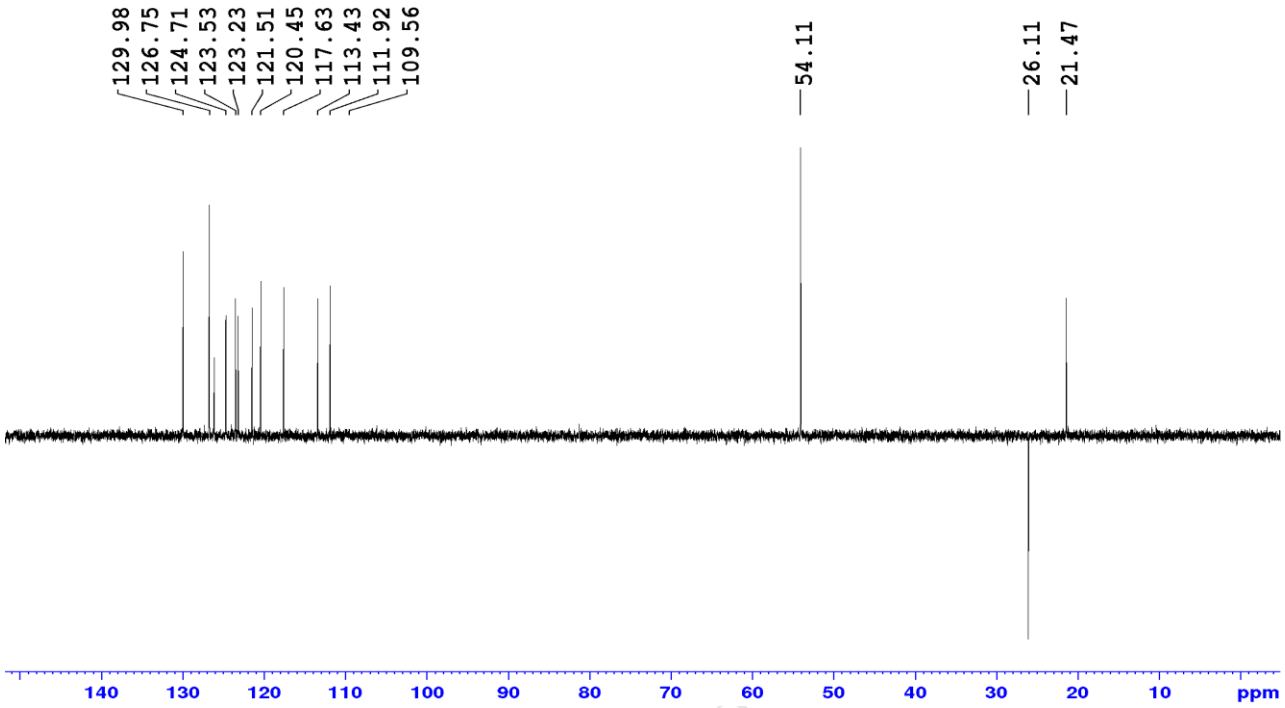

Figure S15. DEPT-135 NMR spectrum of compound 14.

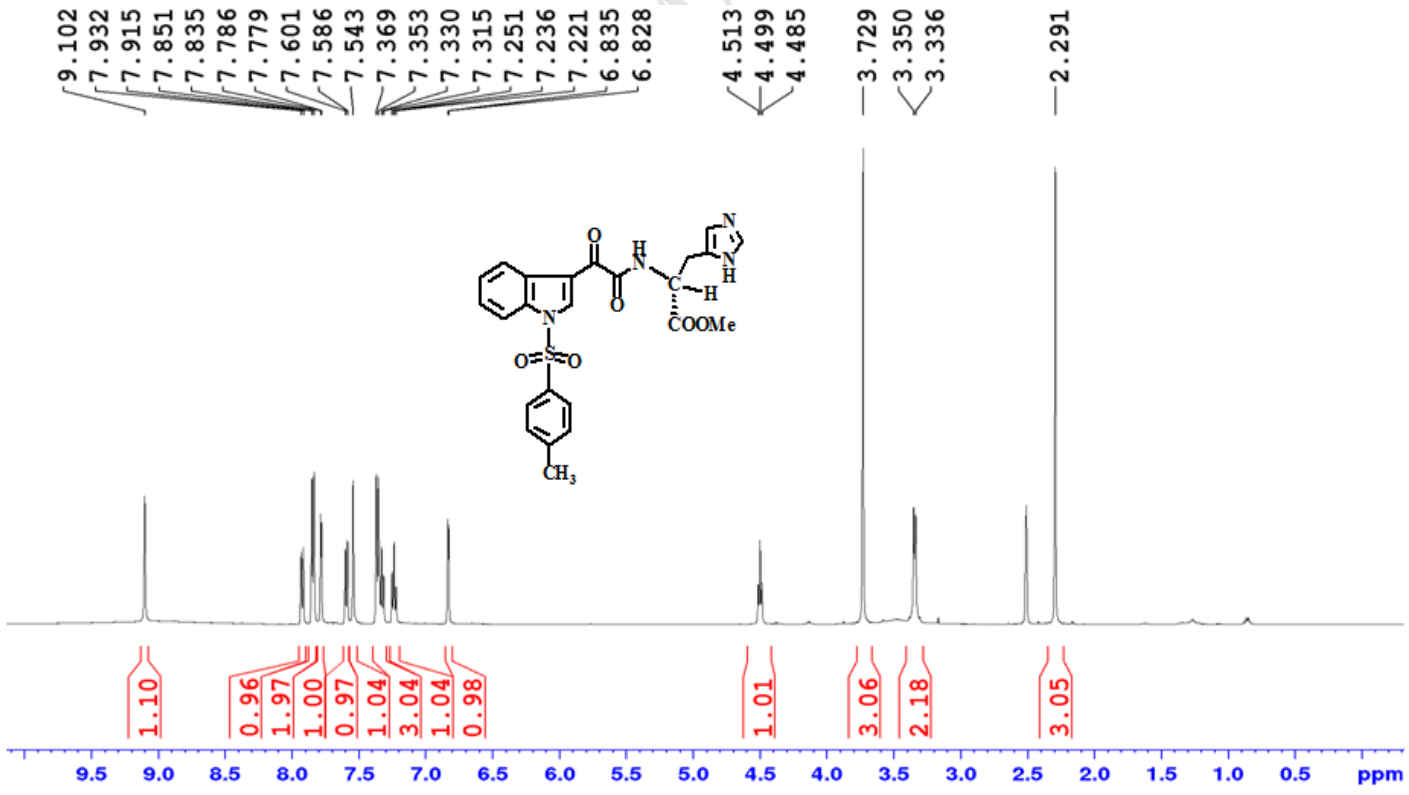

Figure S16. ^{1}H NMR spectrum of compound 15.

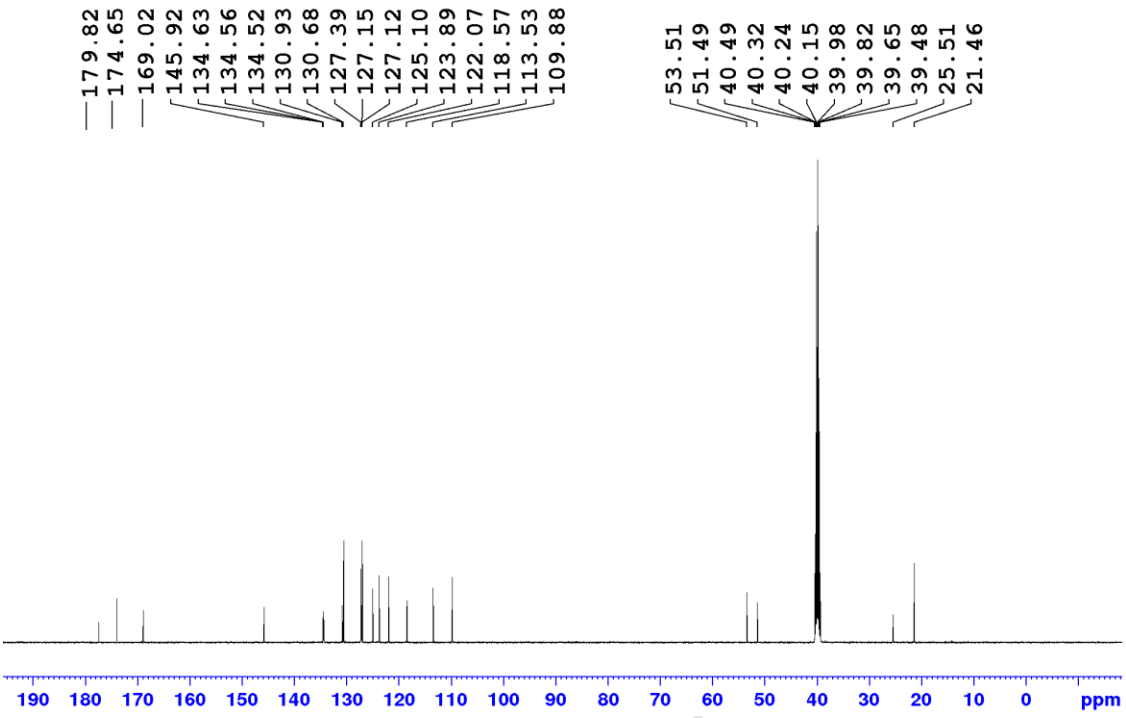

Figure S17. ^{13}C NMR spectrum of compound 15.

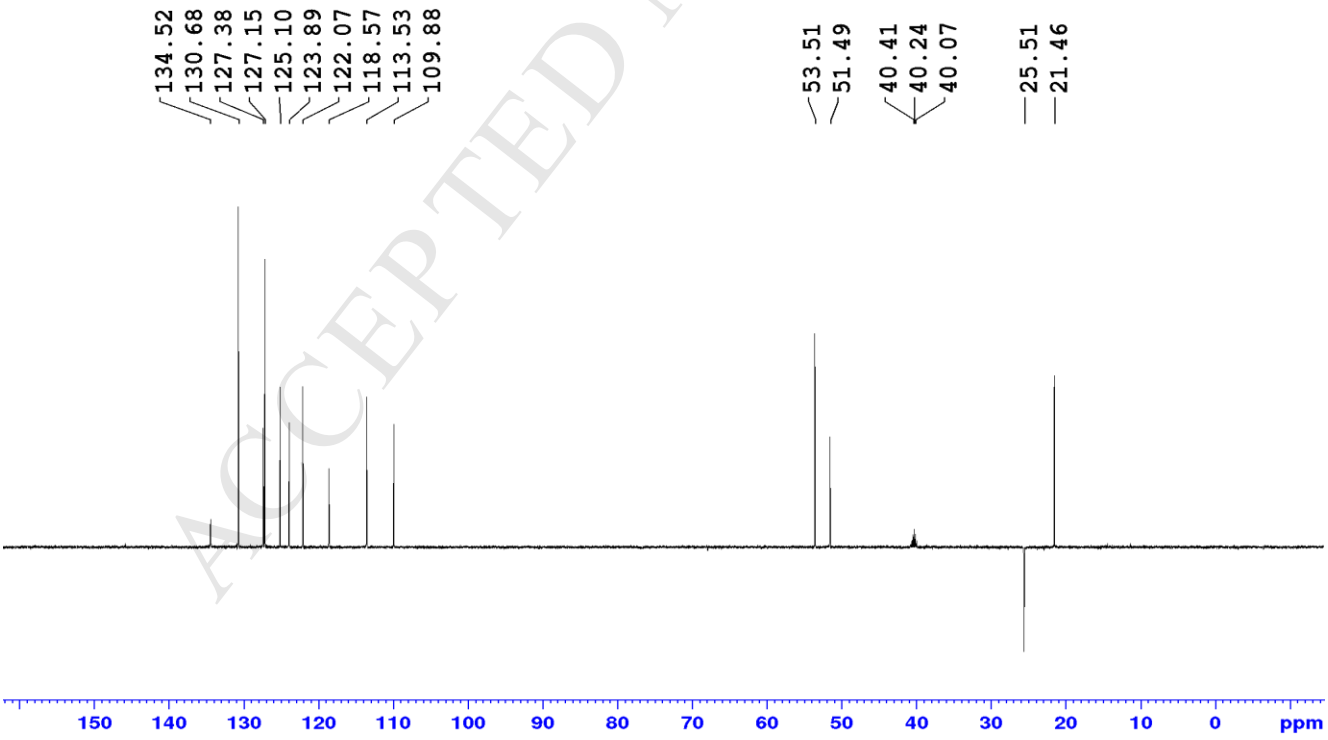

Figure S18. DEPT-135 NMR spectrum of compound 15.

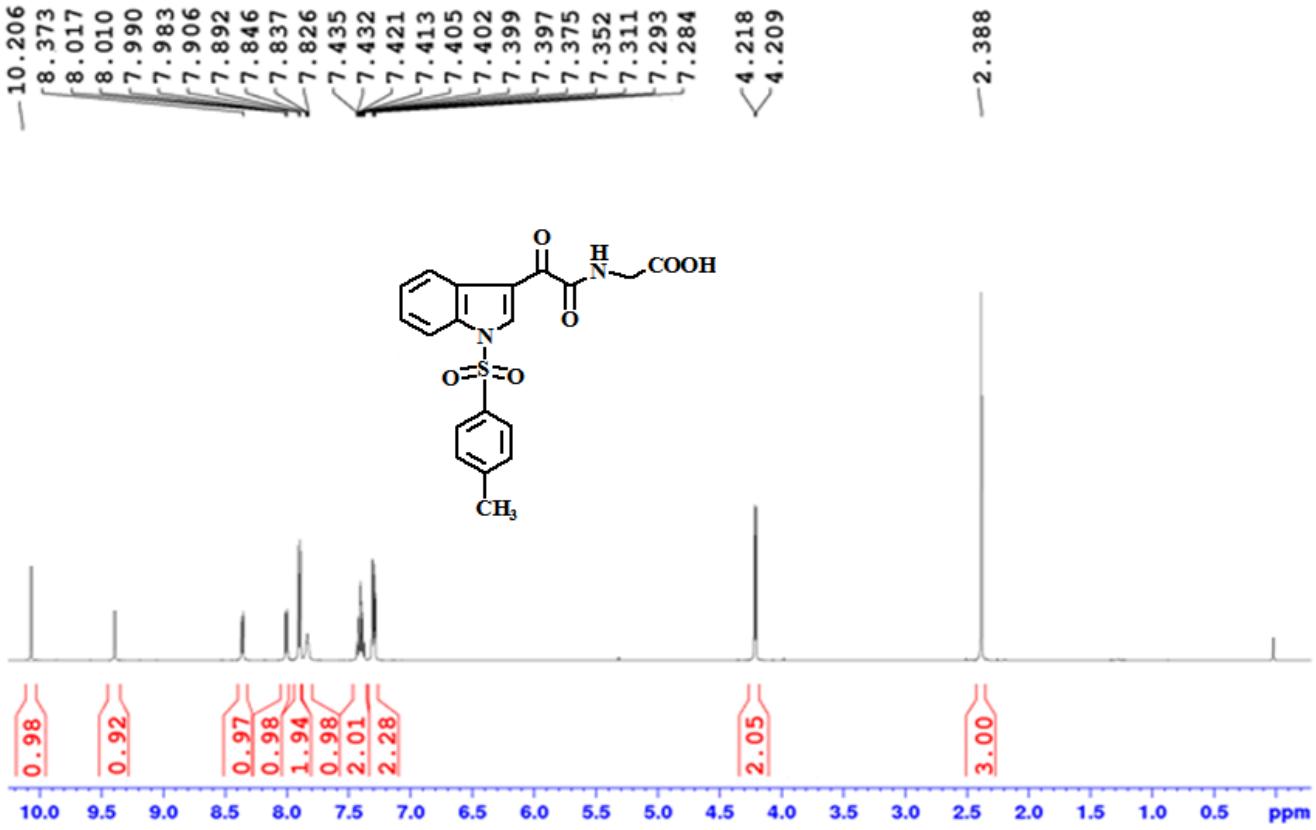

Figure S19. ^{1}H spectrum of compound 16

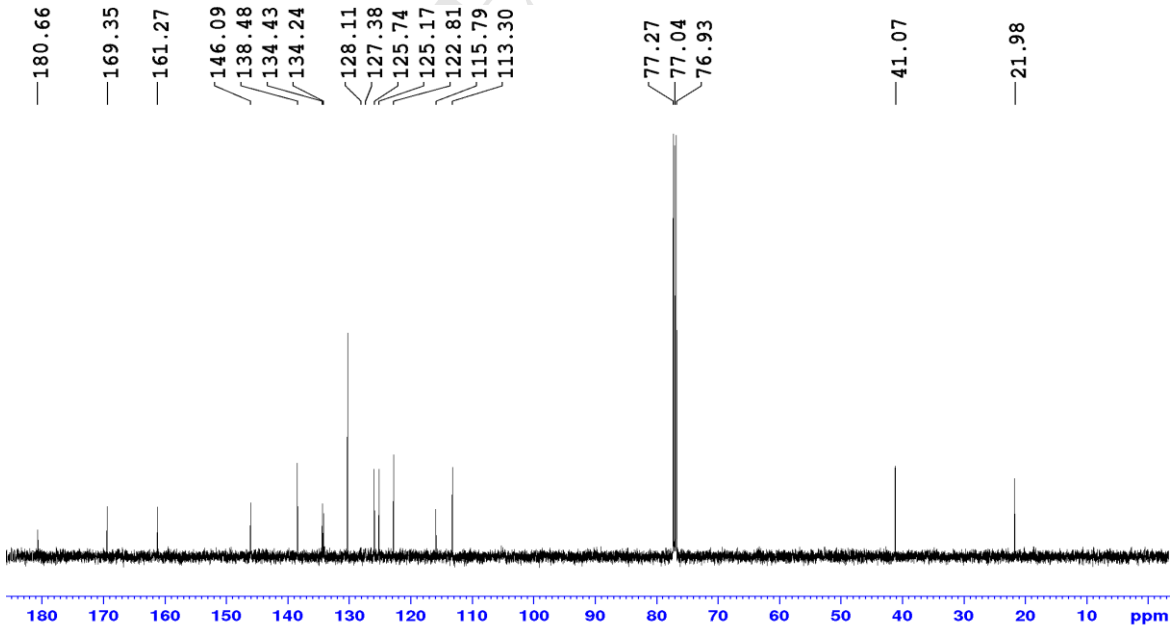

Figure S20. ^{13}C NMR spectrum of compound 16.

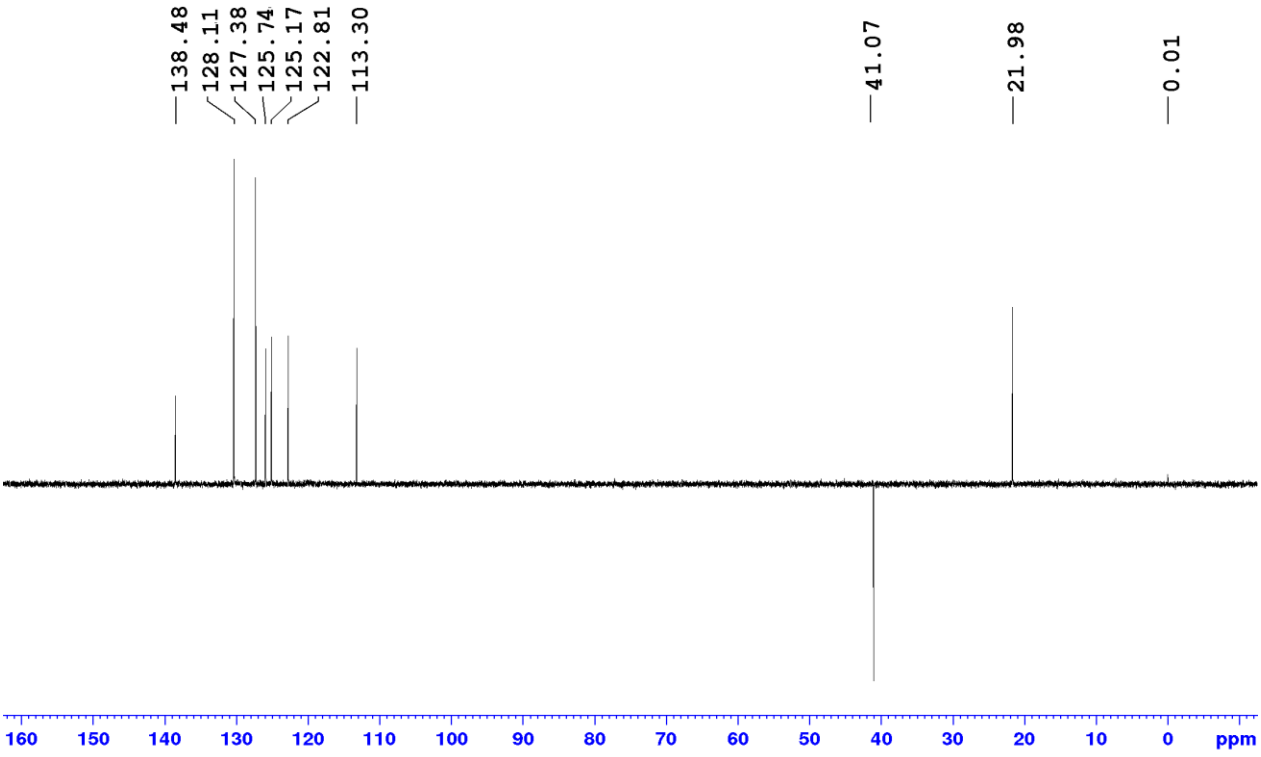

Figure S21. DEPT-135 NMR spectrum of compound 16.

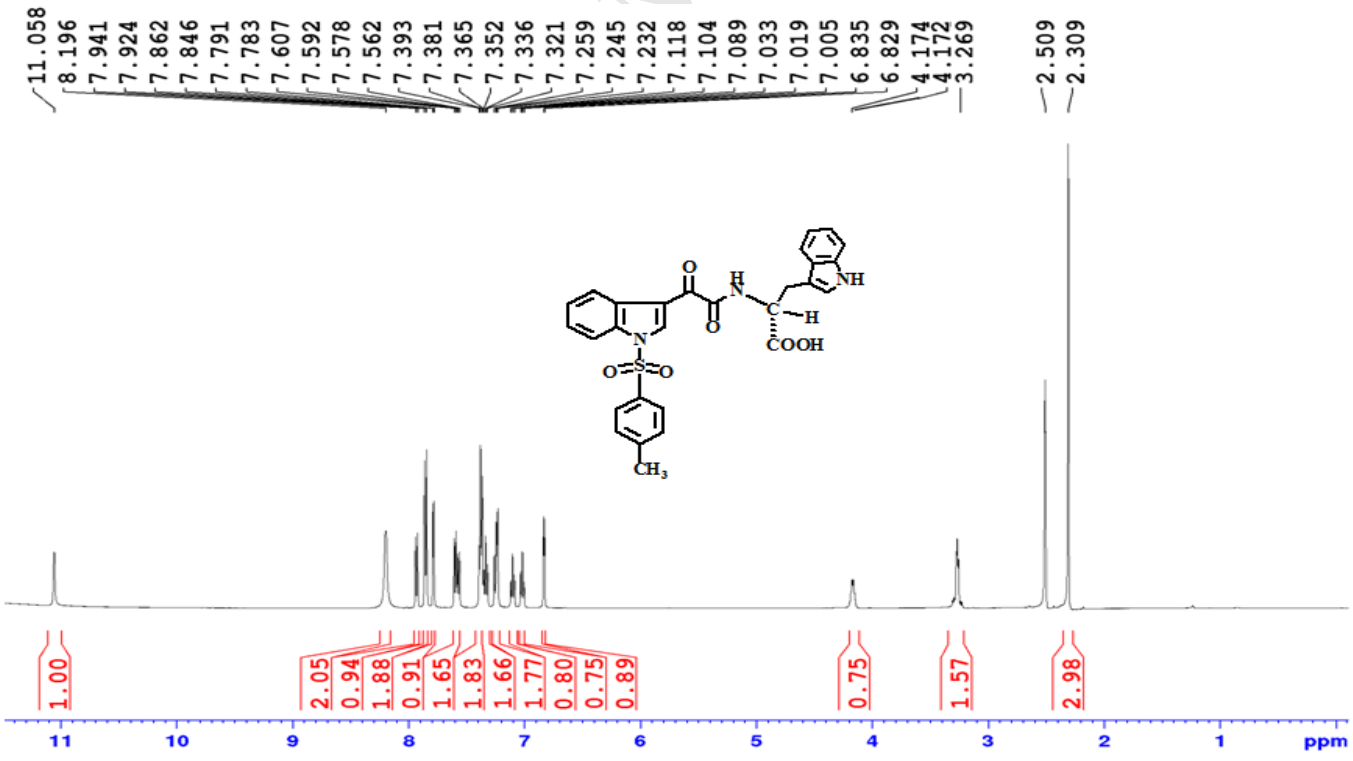

Figure S22. ^{1}H spectrum of compound 17.

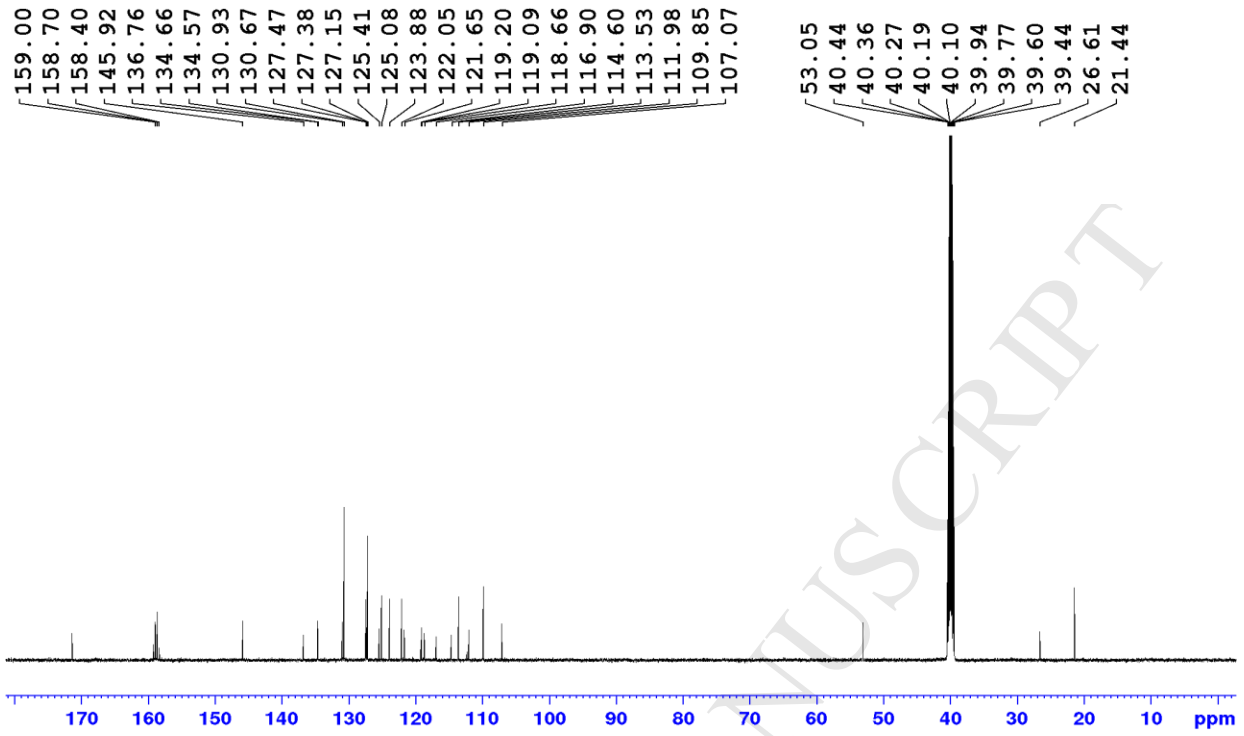

Figure S23. ^{13}C NMR spectrum of compound 17.

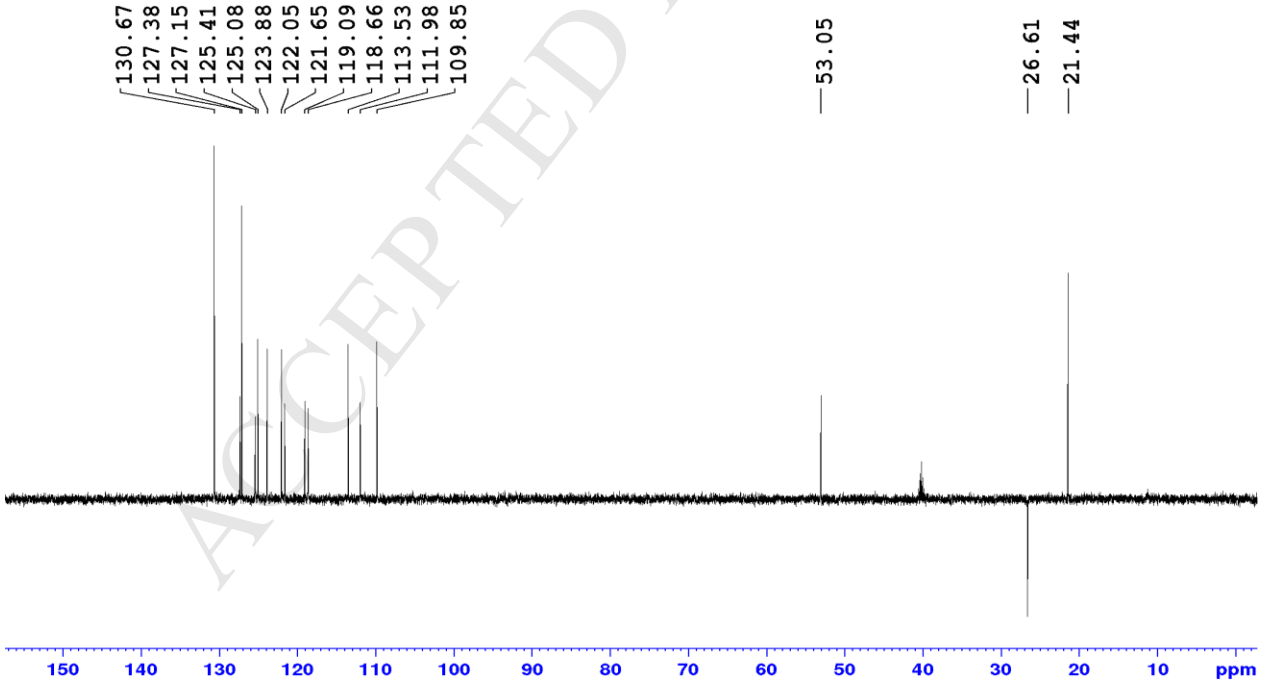

Figure S24. DEPT-135 NMR spectrum of compound 17.

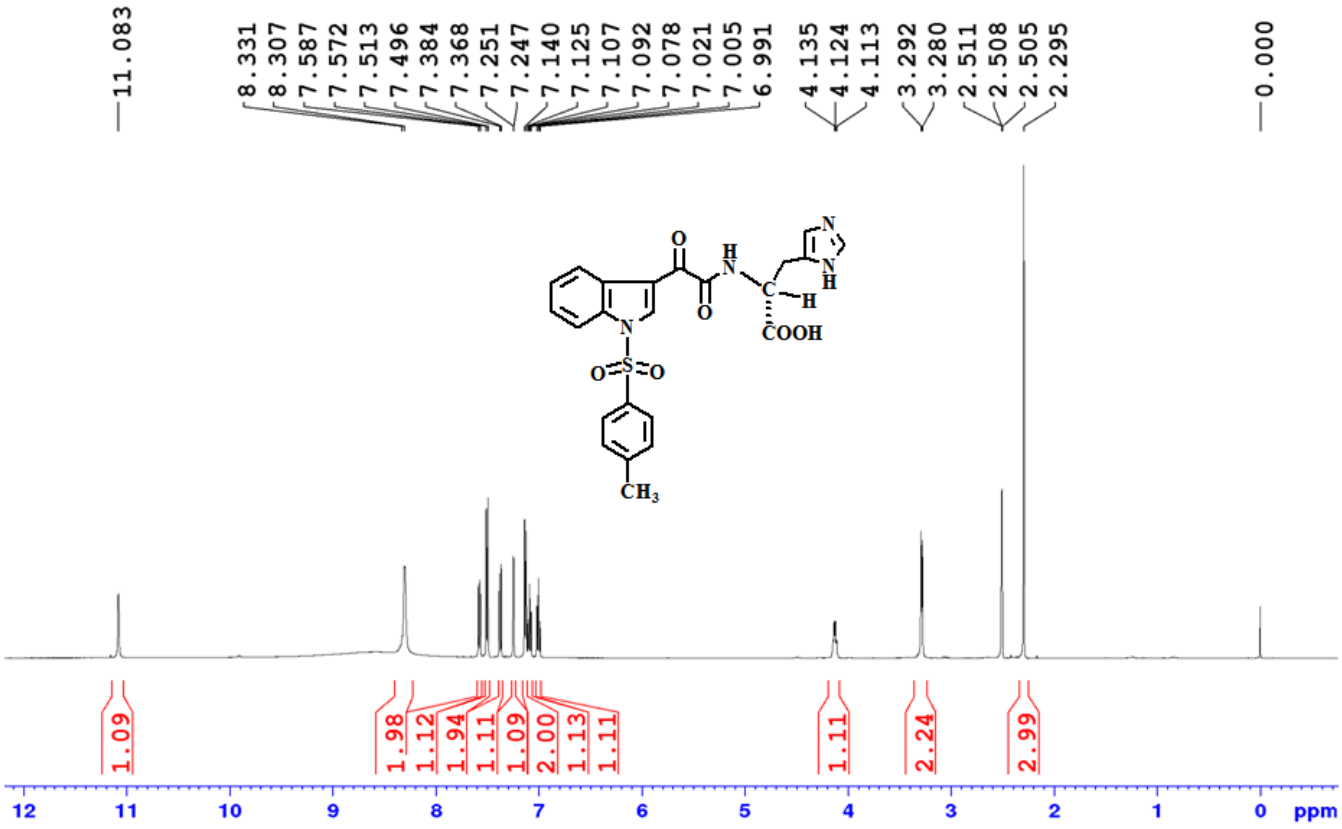

Figure S25. ^{1}H spectrum of compound 18.

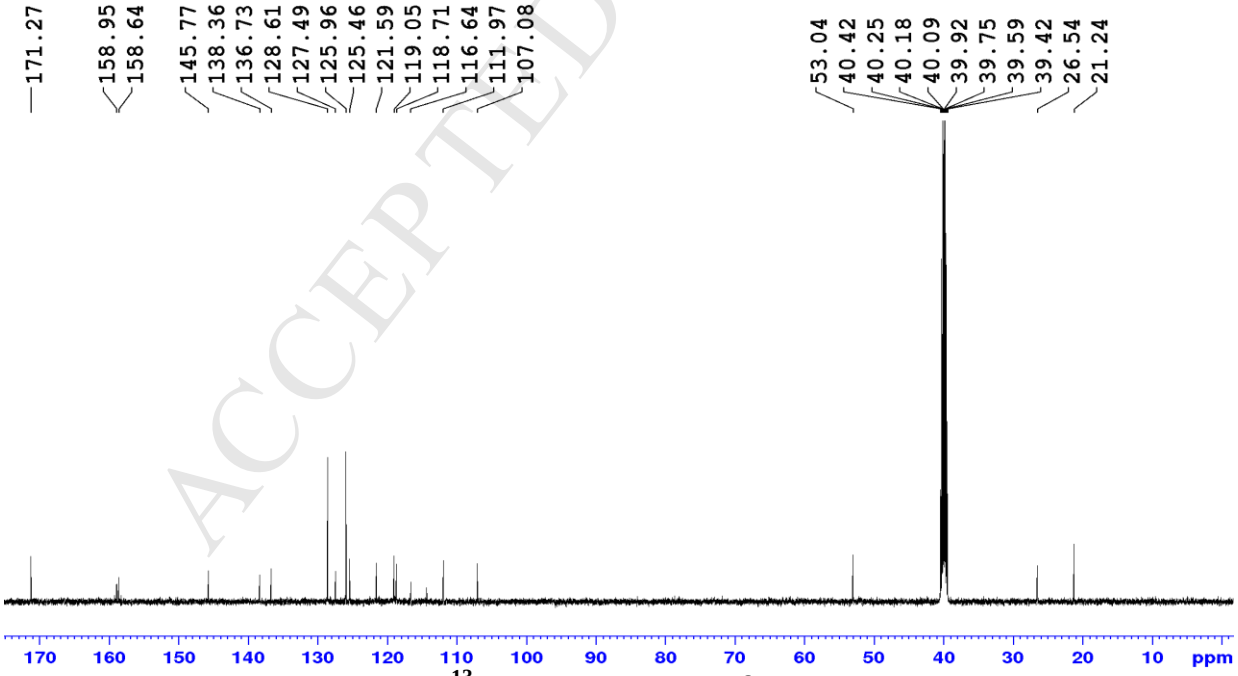

Figure S26. ^{13}C NMR spectrum of compound 18.

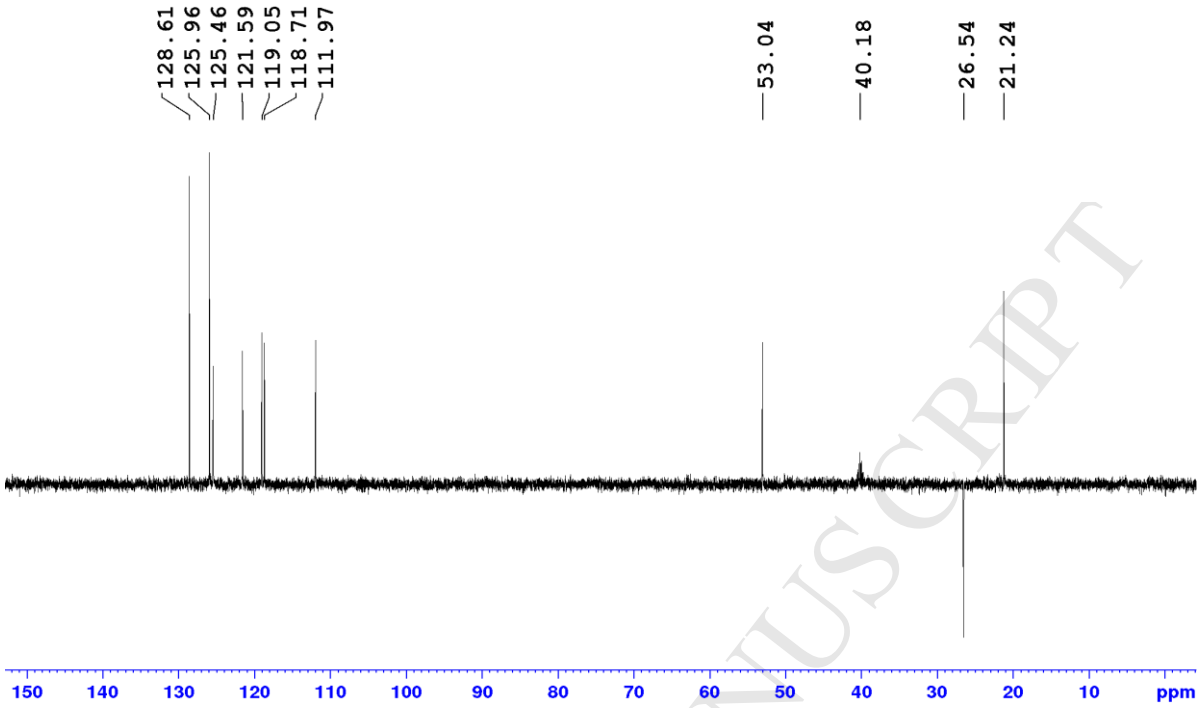

Figure S27. DEPT-135 NMR spectrum of compound 18.

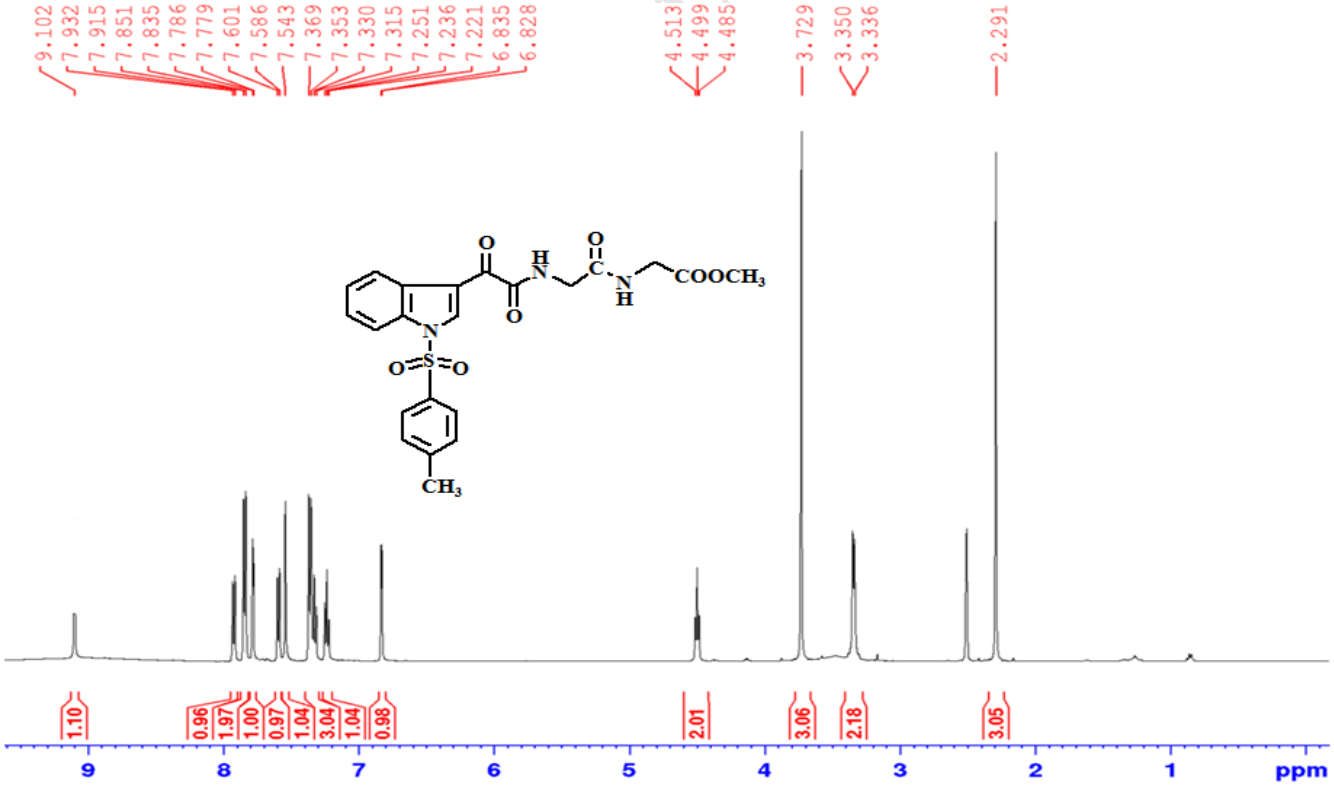

Figure S28. ^{1}H spectrum of compound 6i.

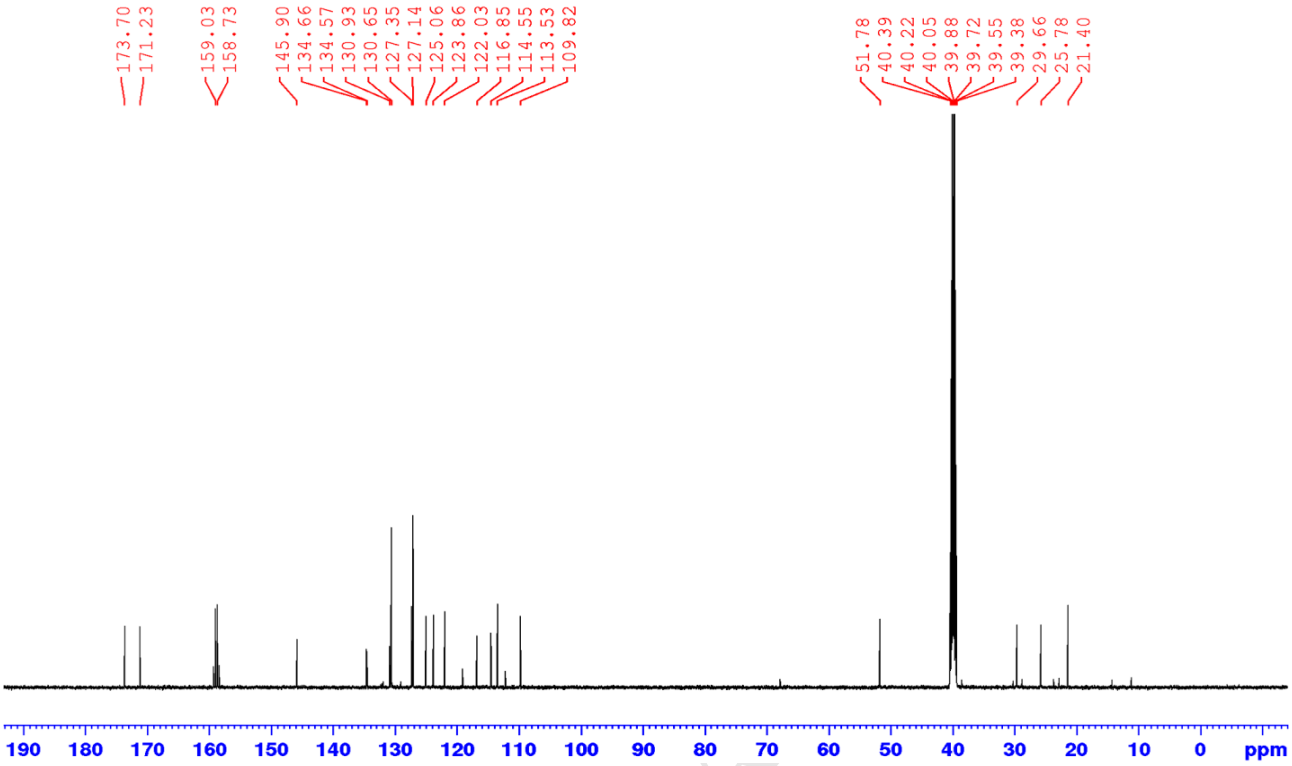

Figure S29. ^{13}C NMR spectrum of compound 6i.

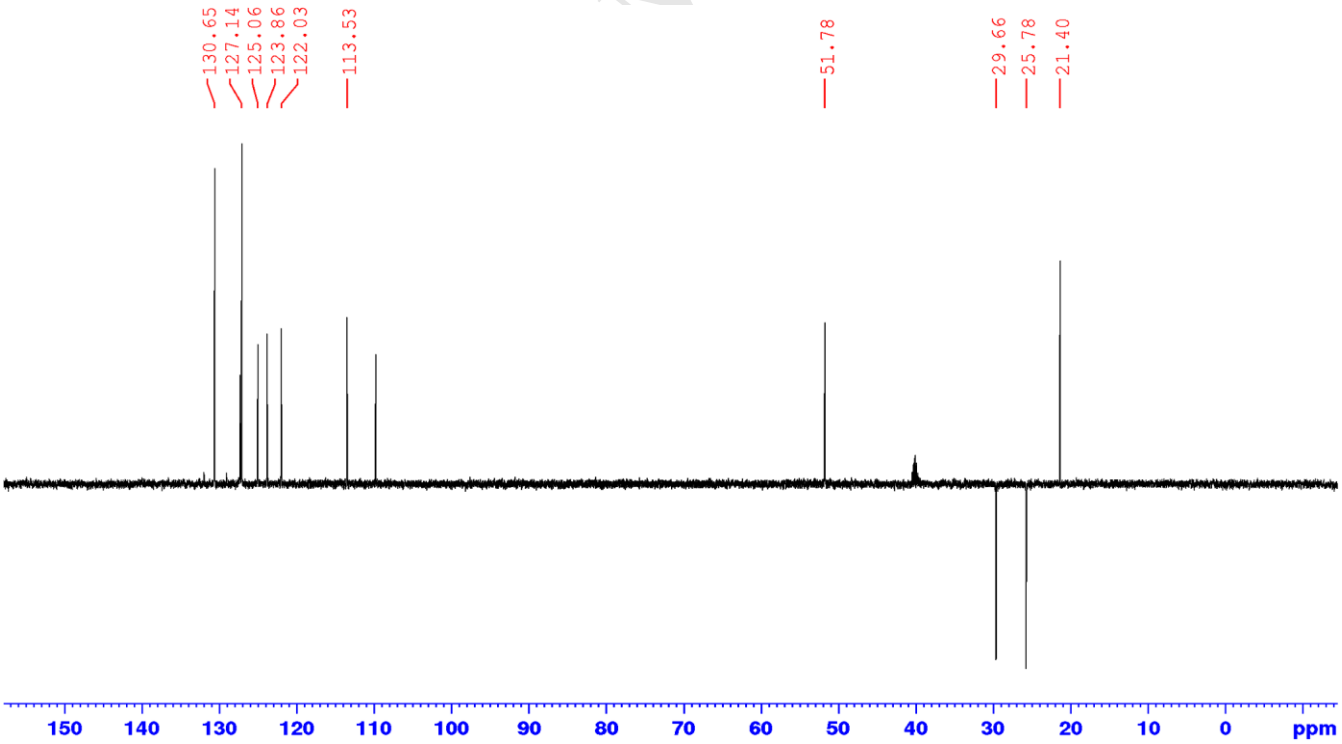

Figure S30. DEPT-135 NMR spectrum of compound 6i.

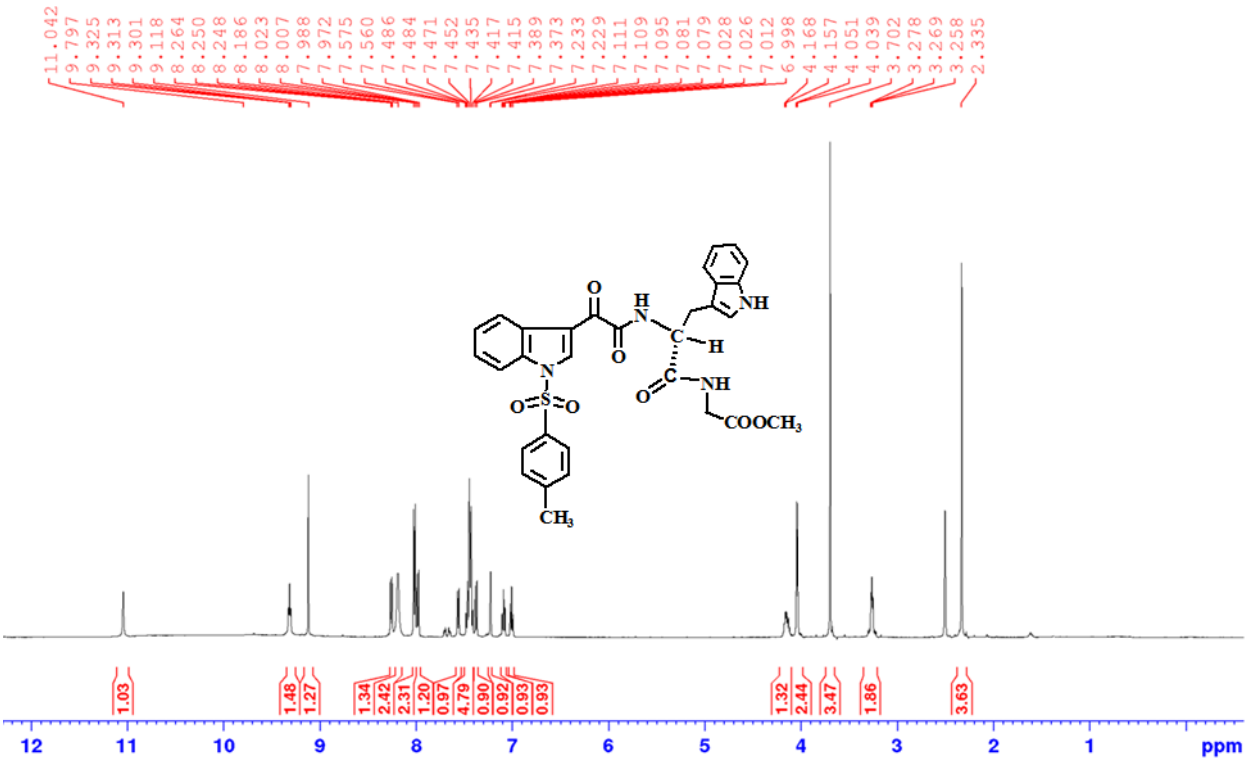

Figure S31. ^{1}H spectrum of compound 6b.

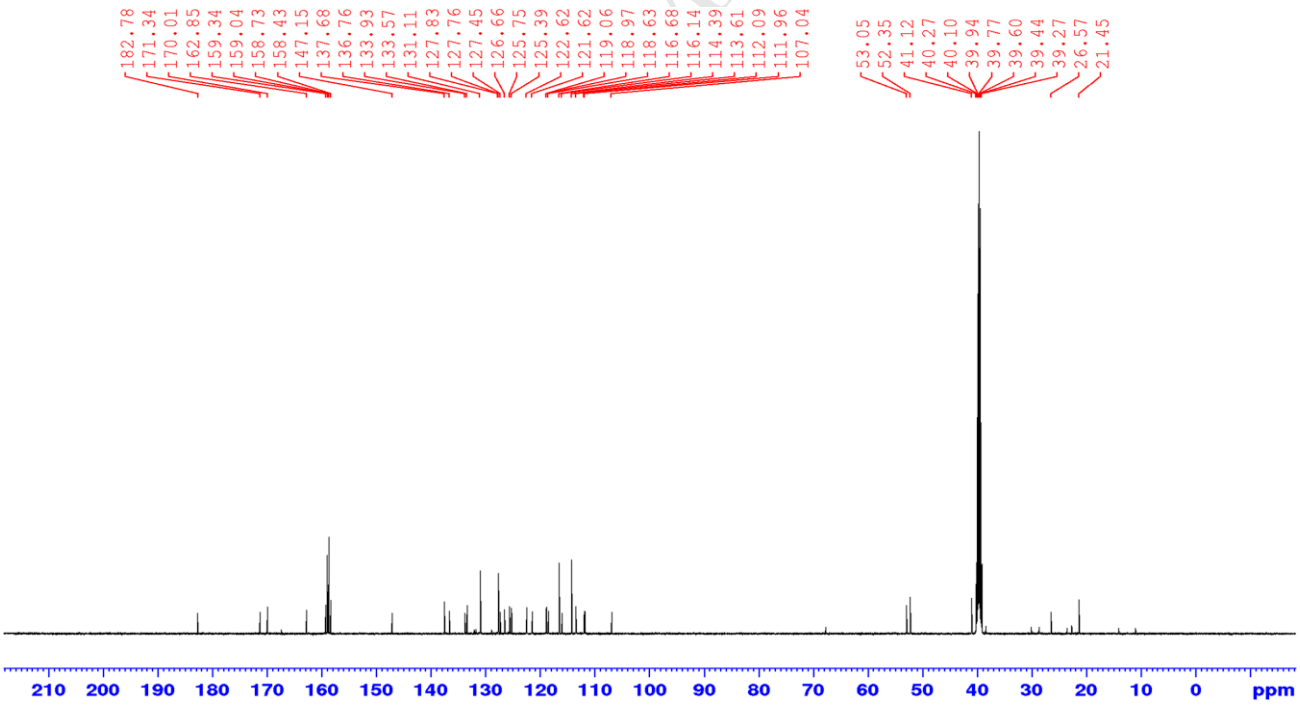

Figure S32. ^{13}C NMR spectrum of compound 6b.

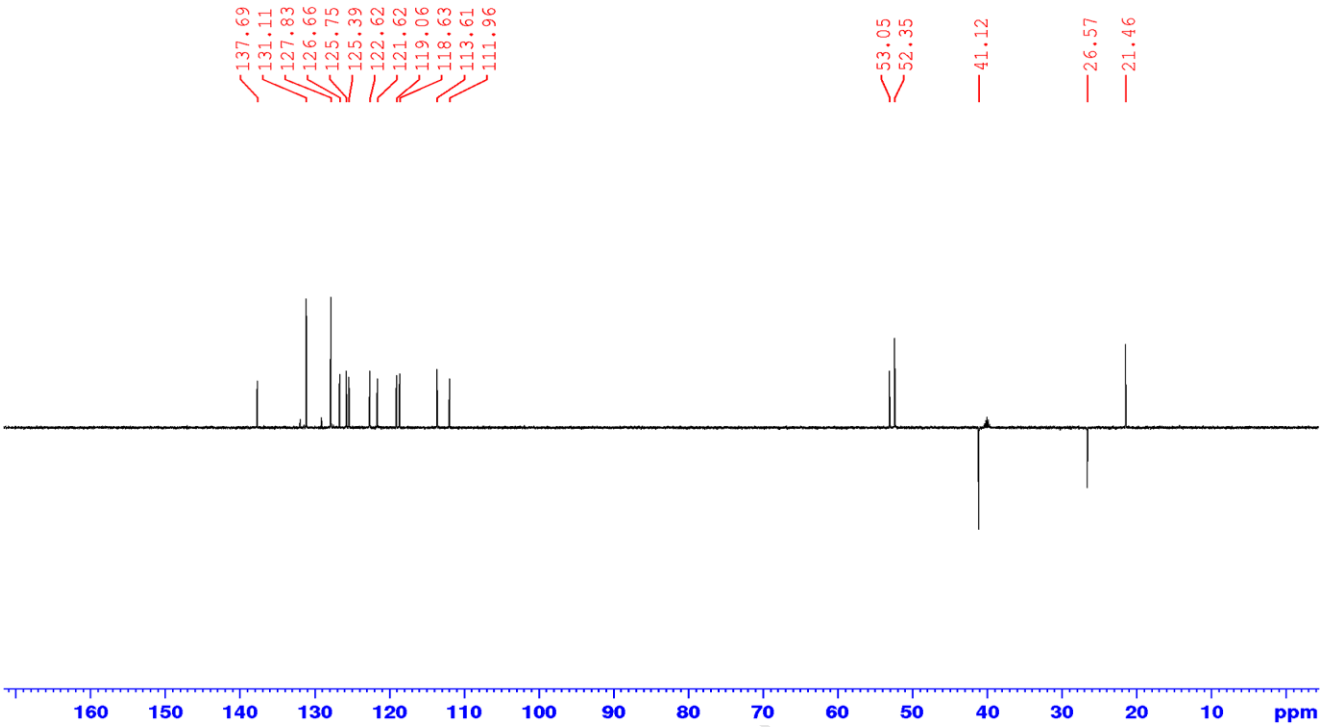

Figure S33. DEPT-135 NMR spectrum of compound 6b

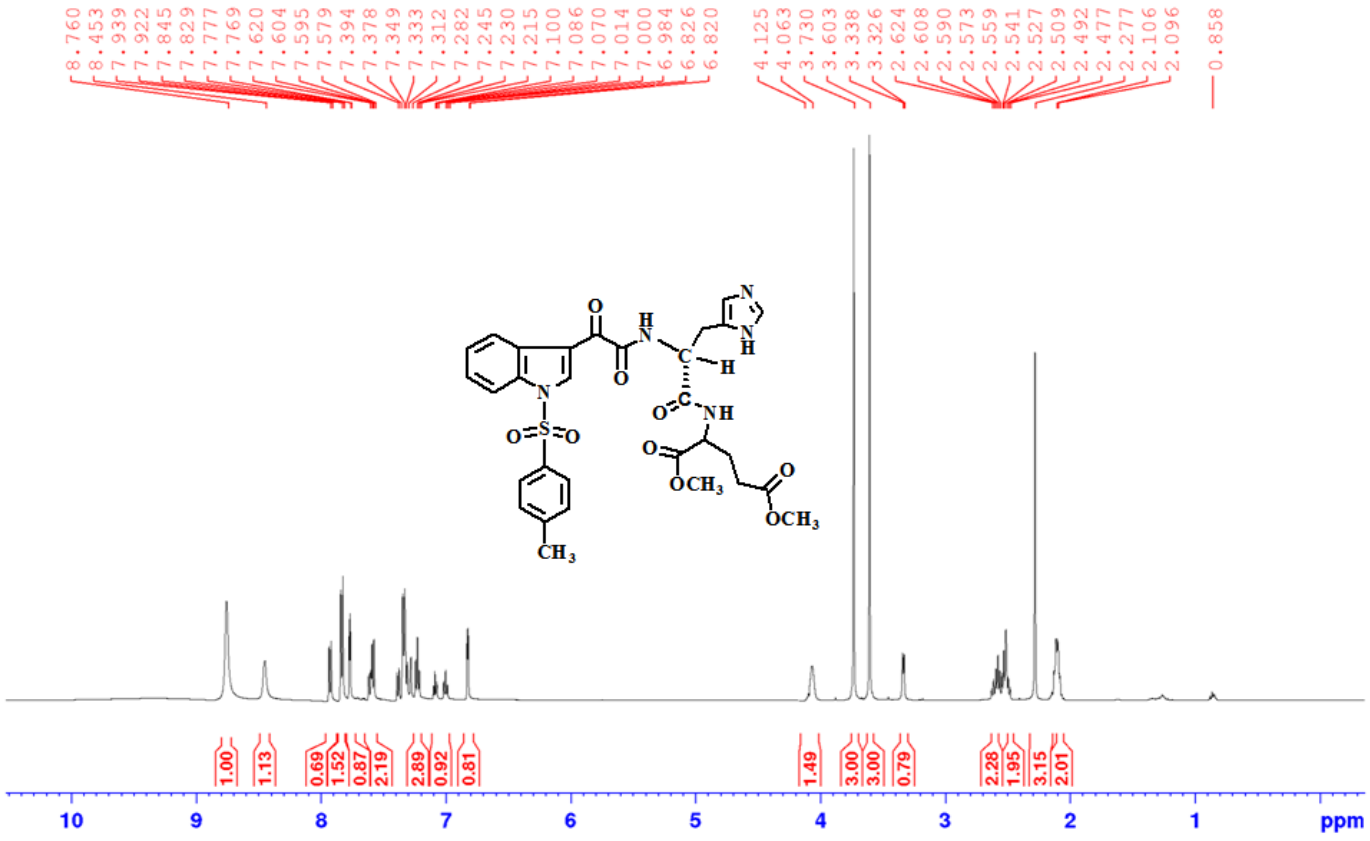

Figure S34. ^{1}H spectrum of compound 6h.

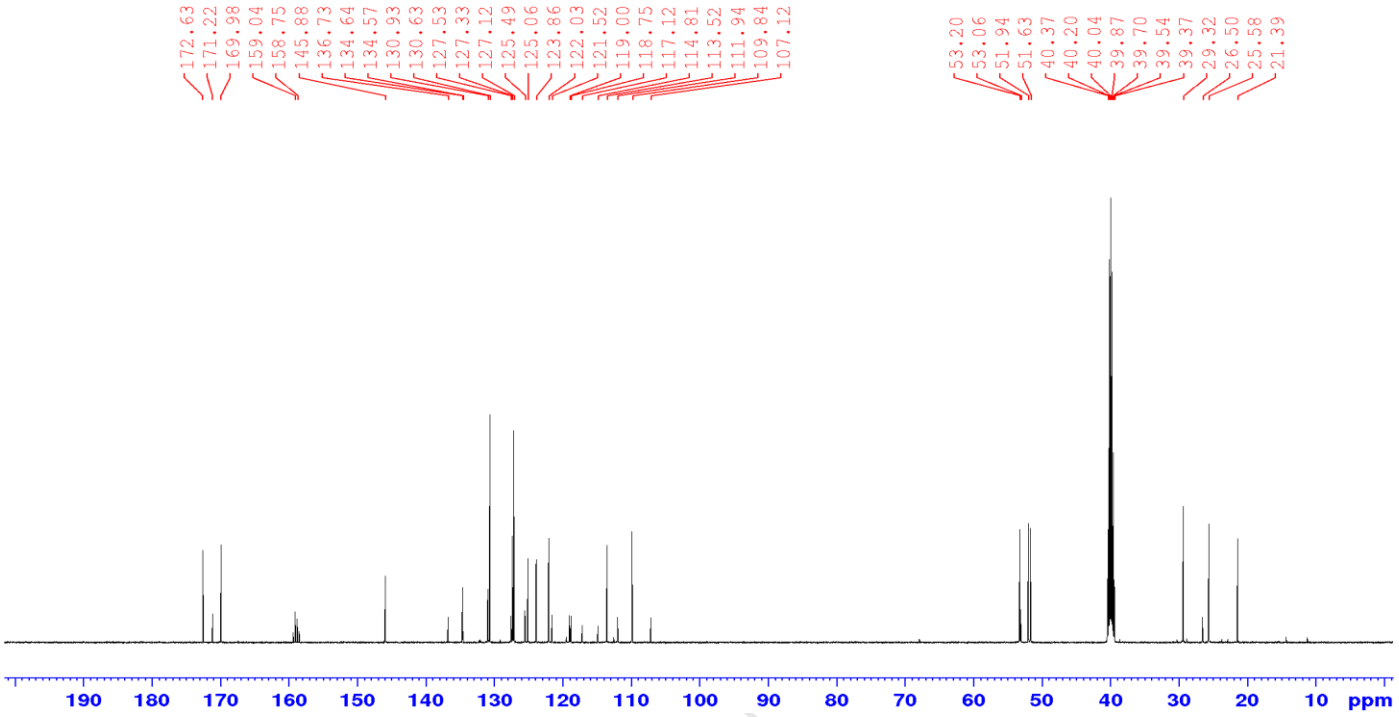

Figure S35. ^{13}C NMR spectrum of compound 6h.

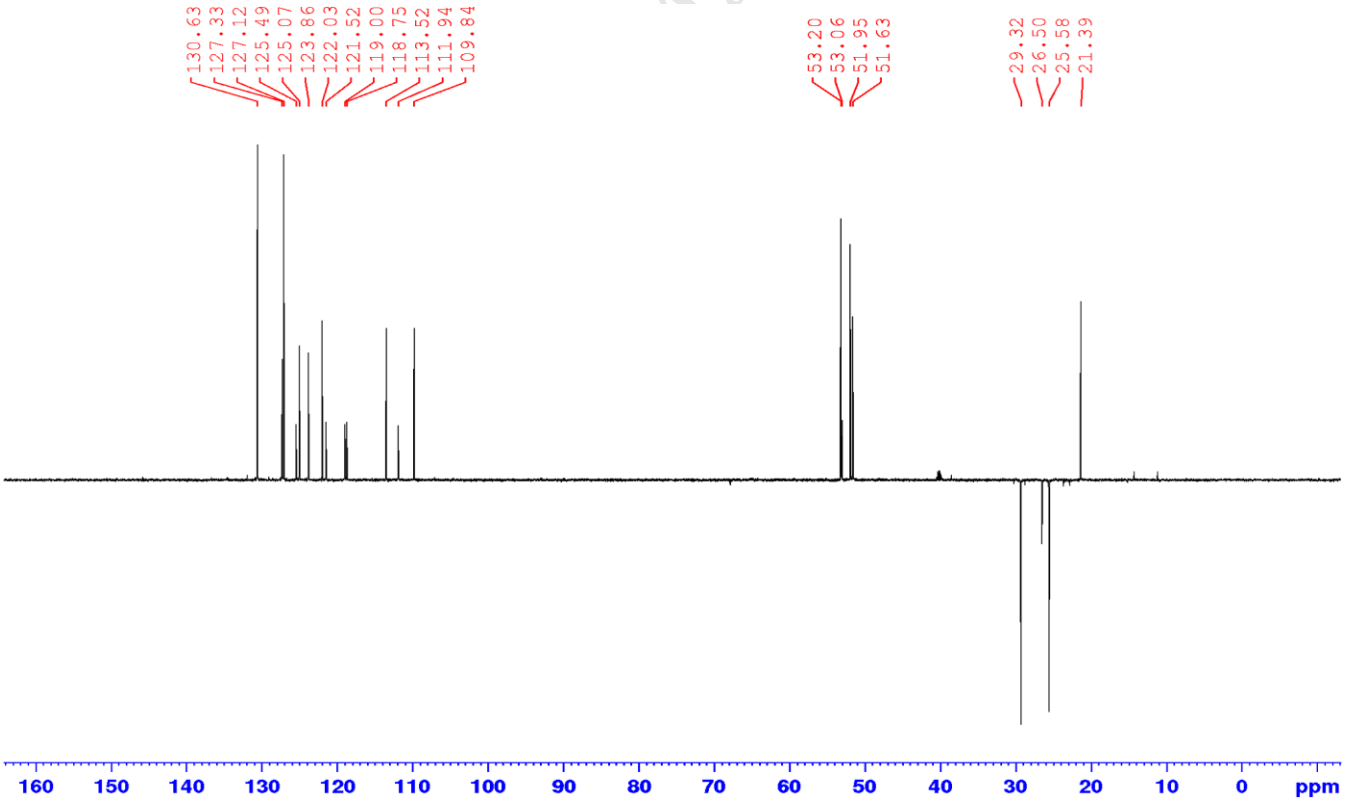

Figure S36. DEPT-135 NMR spectrum of compound 6h.

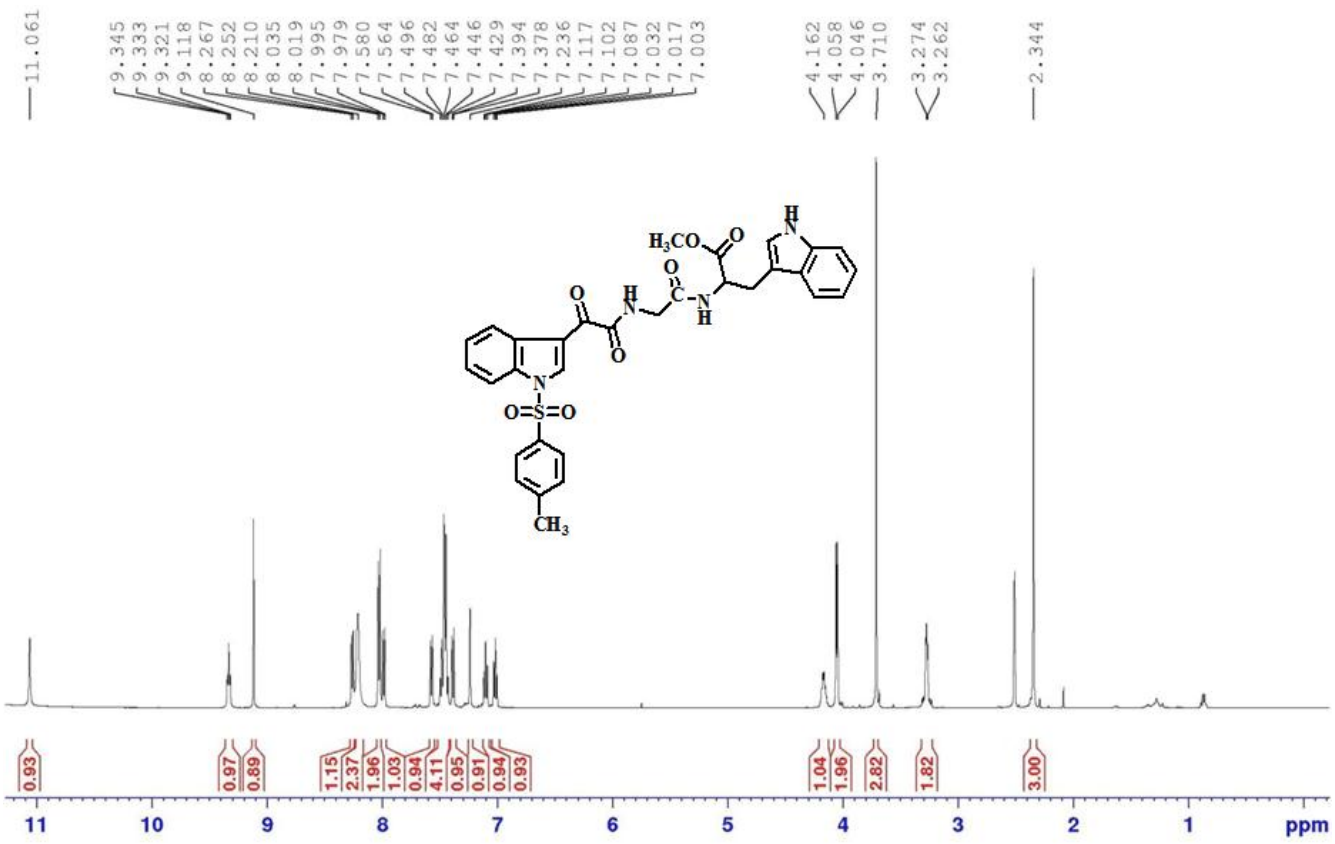

Figure S37. ^{1}H spectrum of compound 6d.

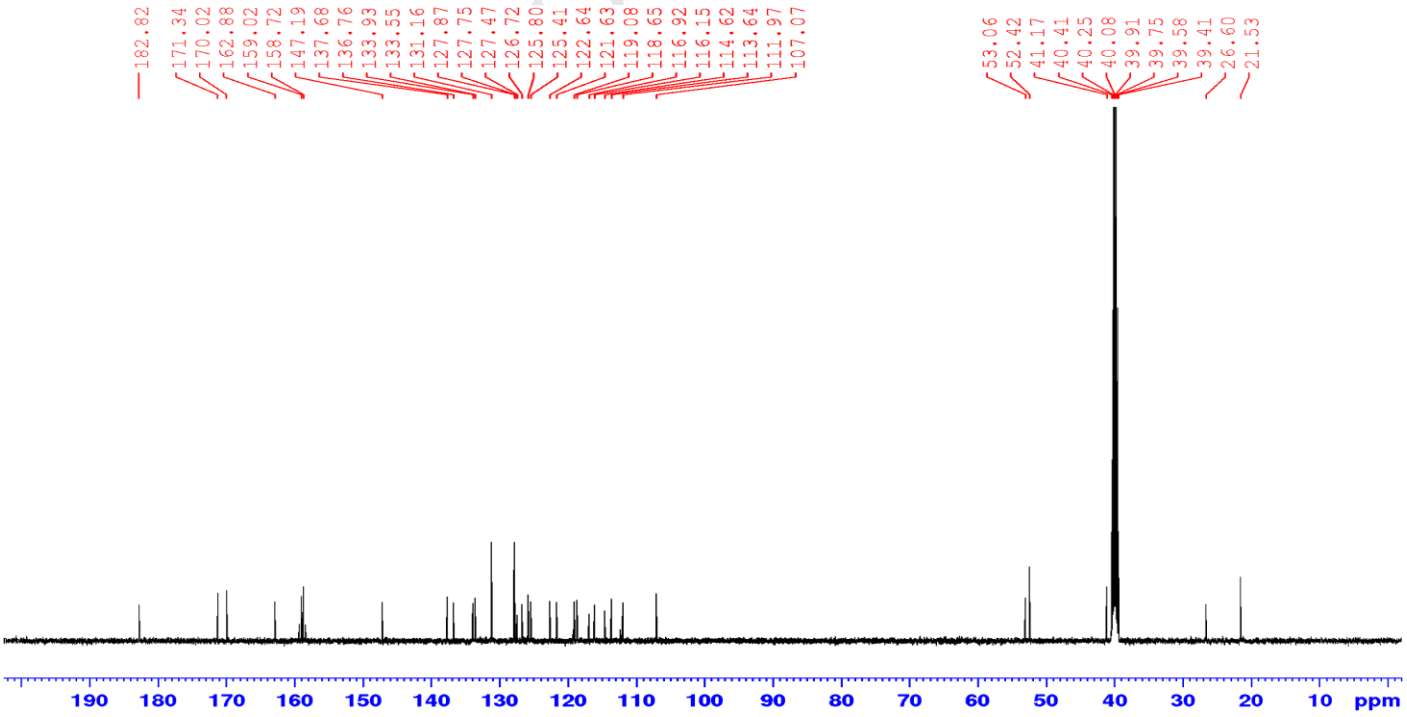

Figure S38. ^{13}C NMR spectrum of compound 6d.

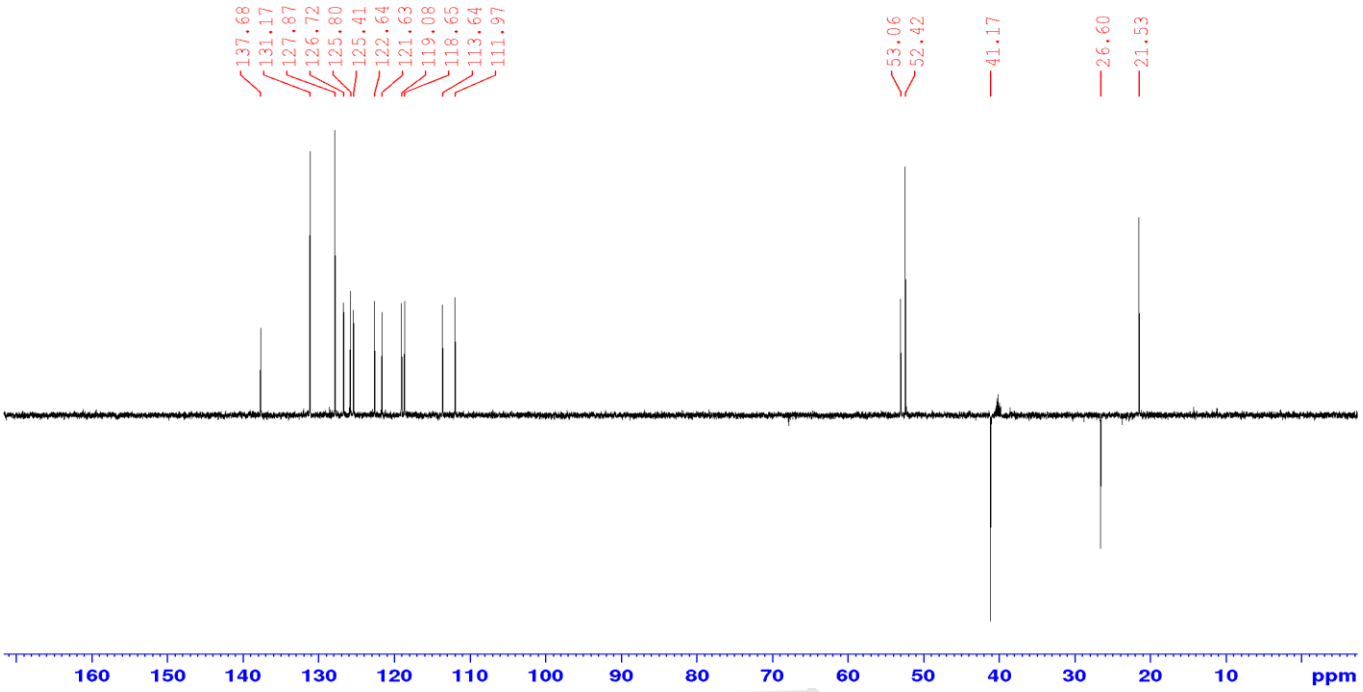

Figure S39. DEPT-135 NMR spectrum of compound 6d.

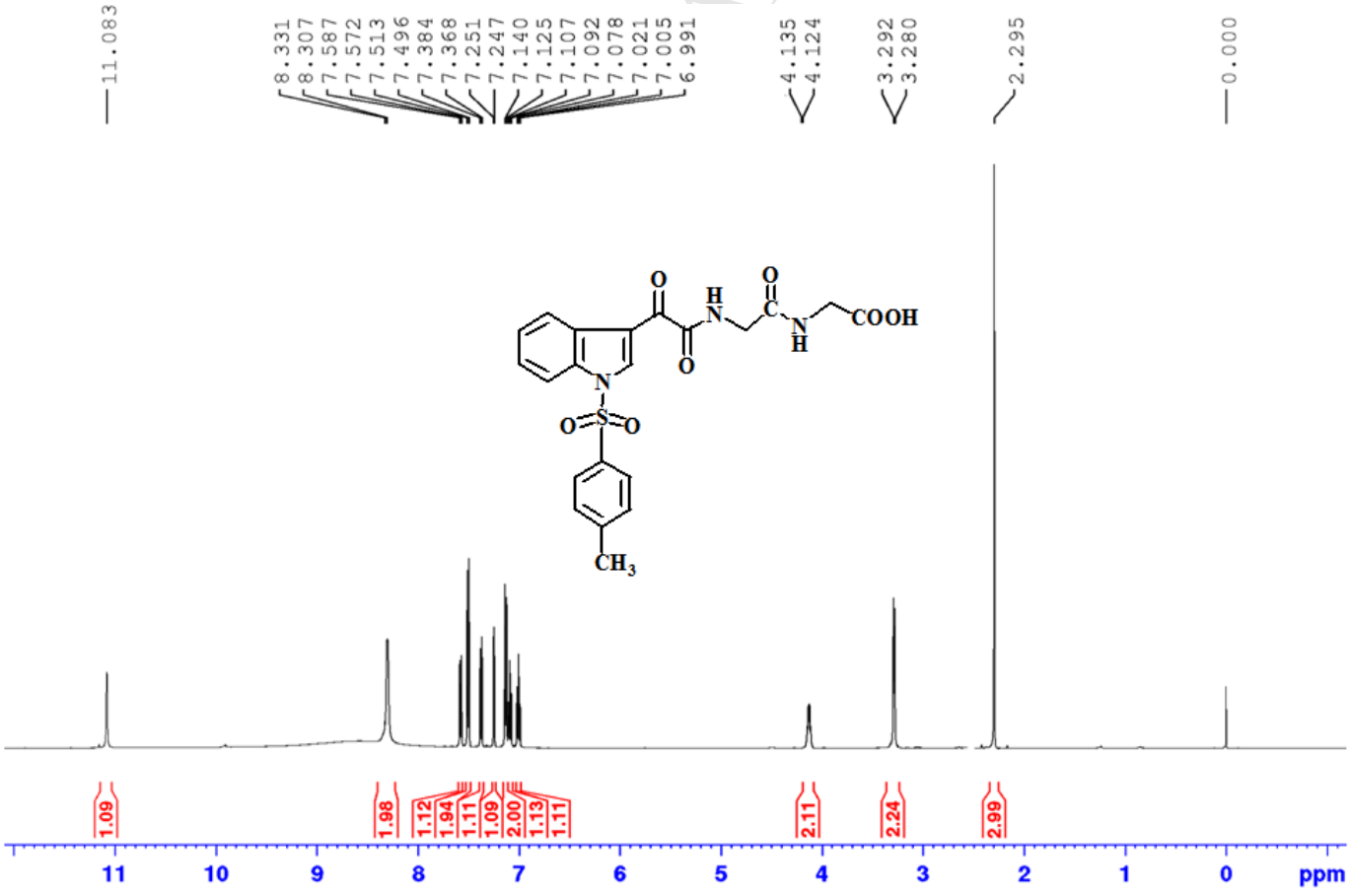

Figure S40. ^{1}H spectrum of compound 7i.

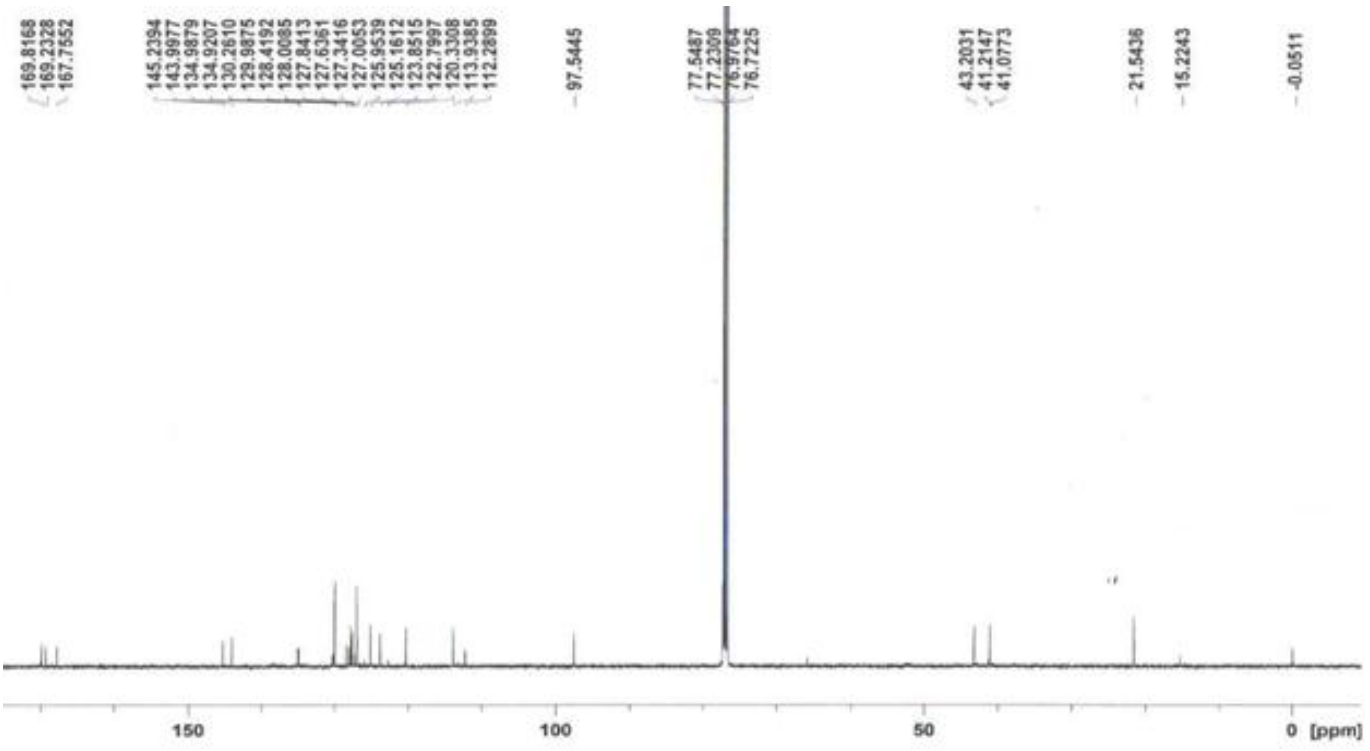

Figure S41. ^{13}C NMR spectrum of compound 7i.

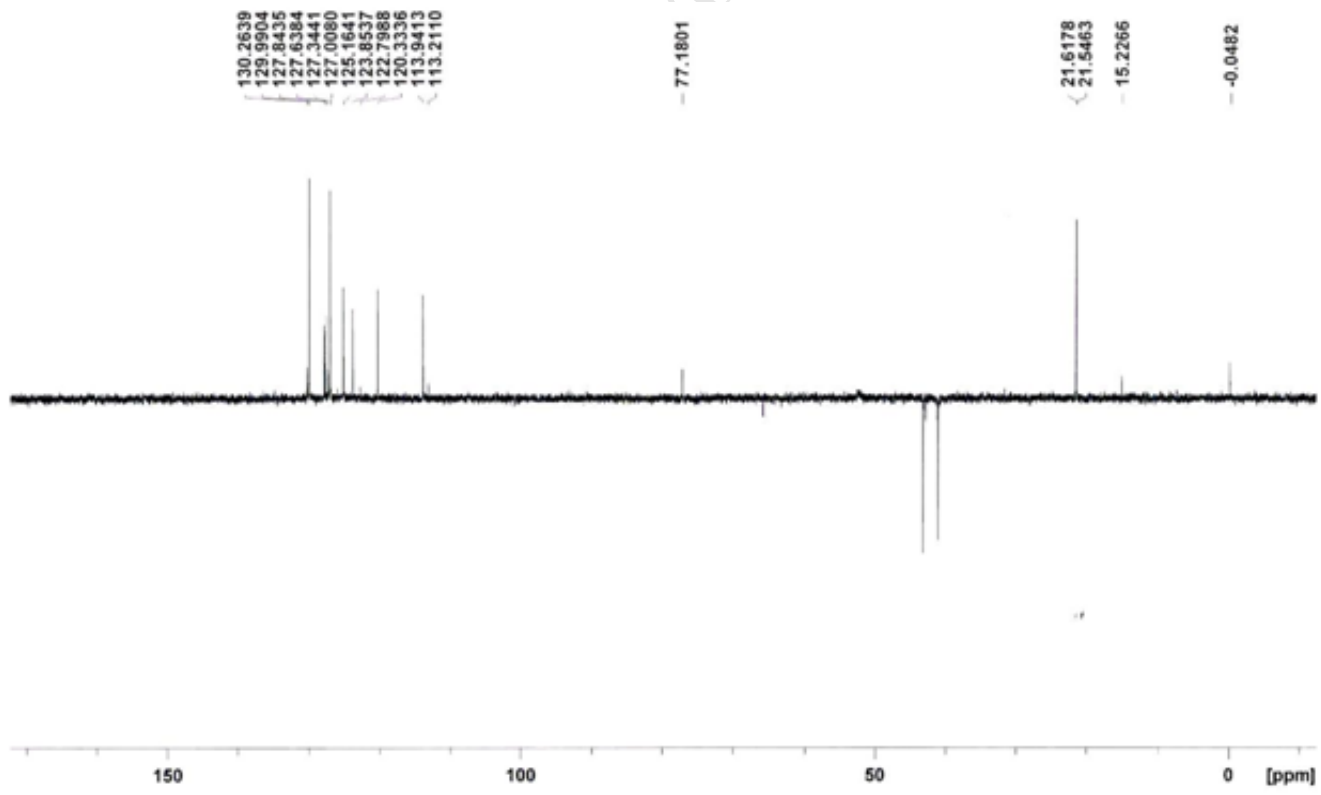

Figure S42. DEPT-135 NMR spectrum of compound 7i.

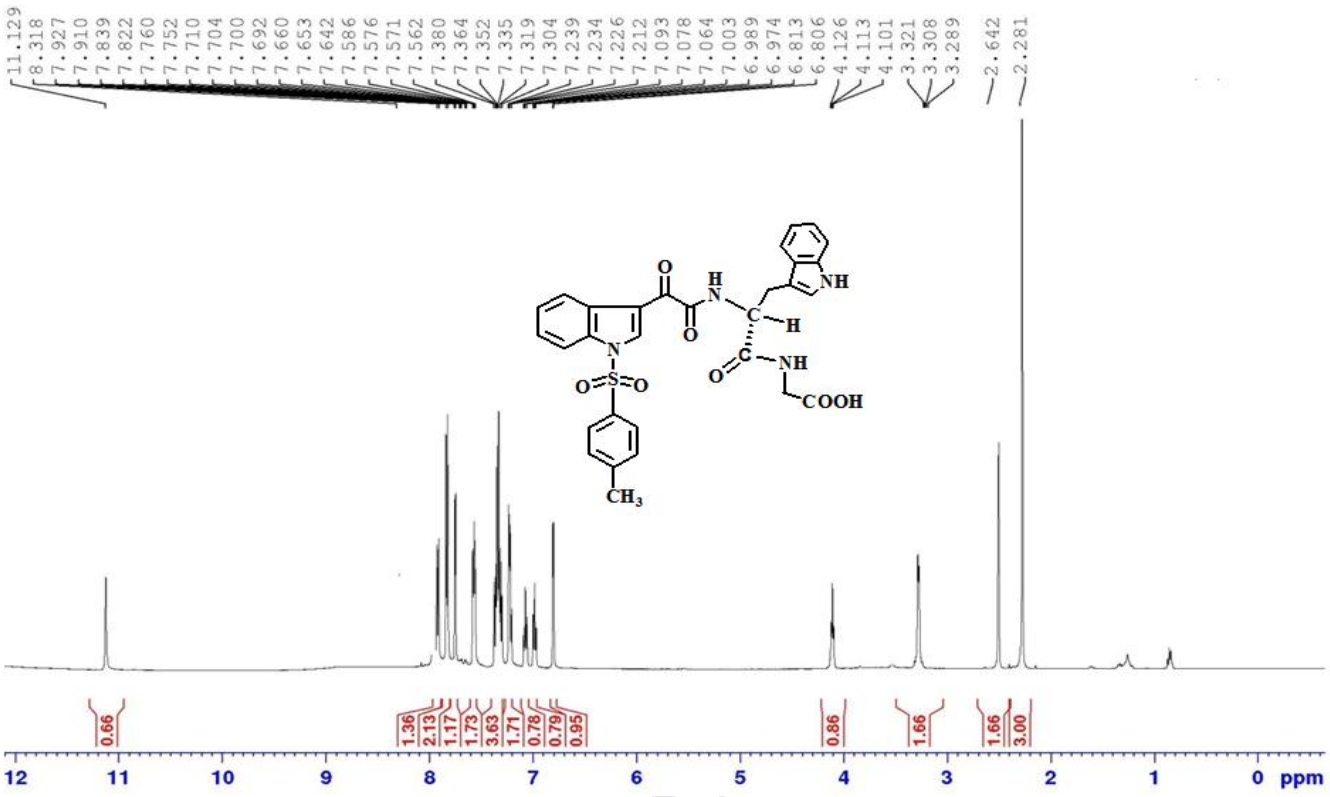

Figure S43. ^{1}H spectrum of compound 7b.

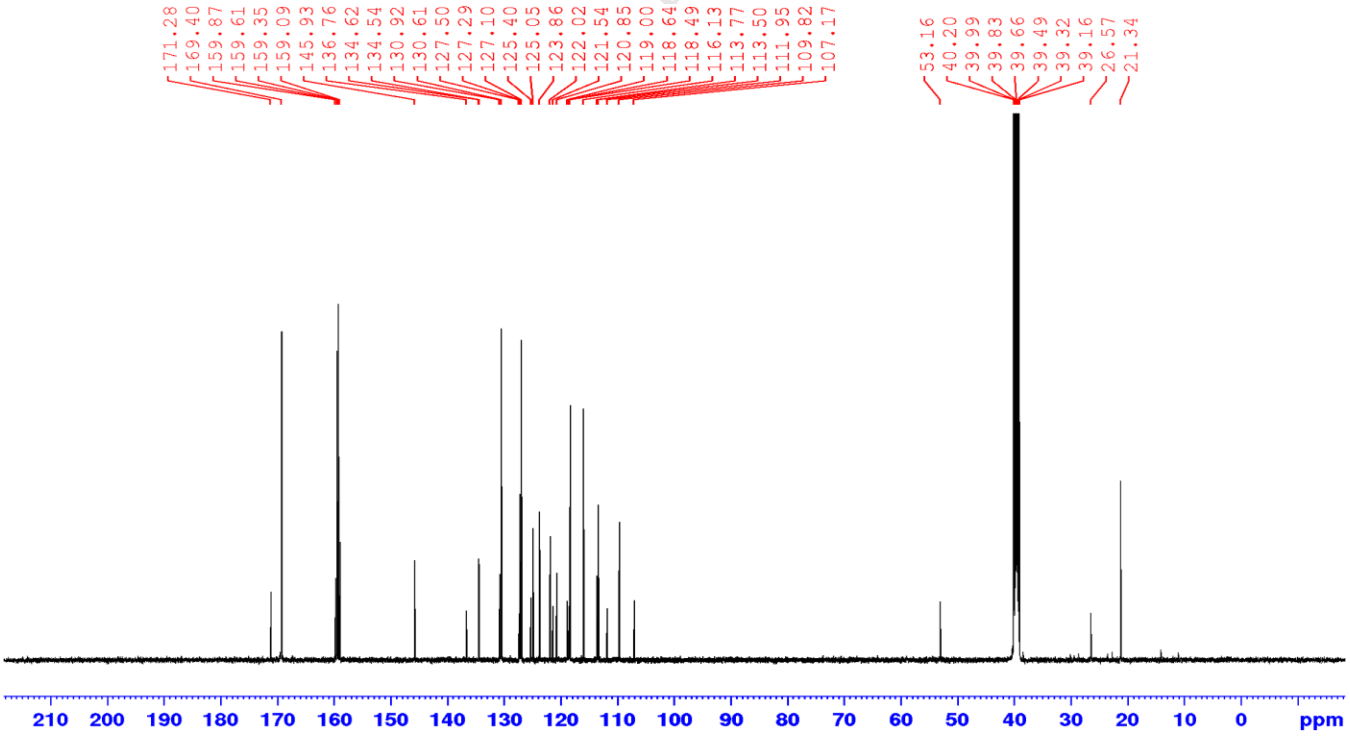

Figure S44. ^{13}C NMR spectrum of compound 7b.

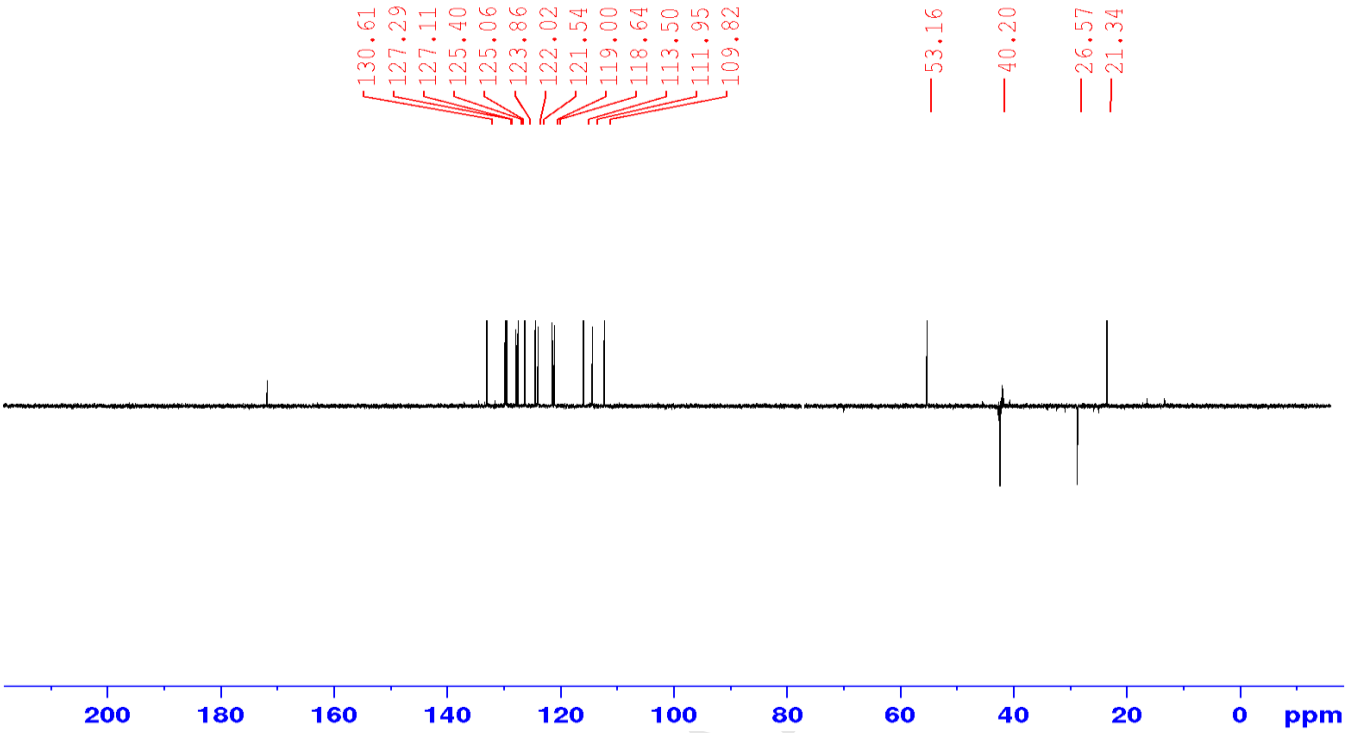

Figure S45. DEPT-135 NMR spectrum of compound 7b

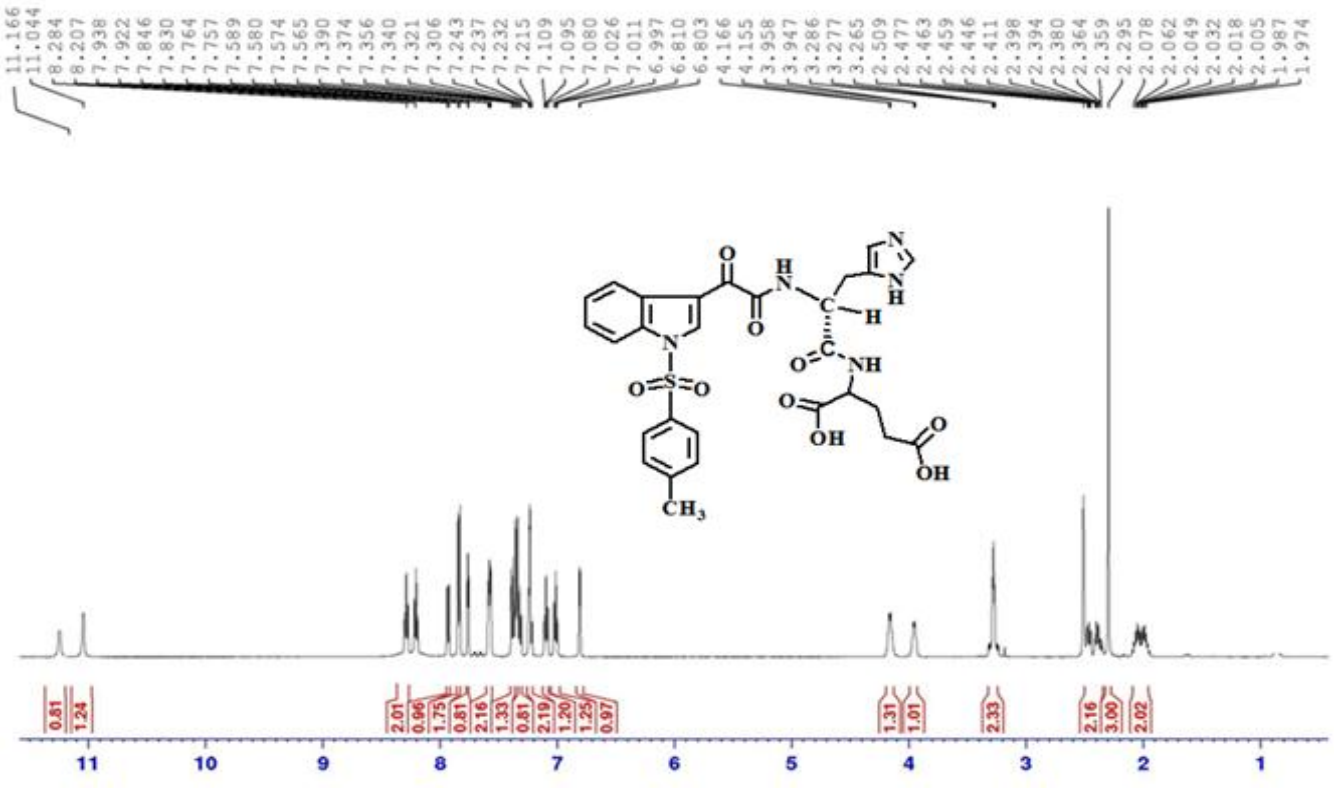

Figure S46. ^{1}H spectrum of compound 7h

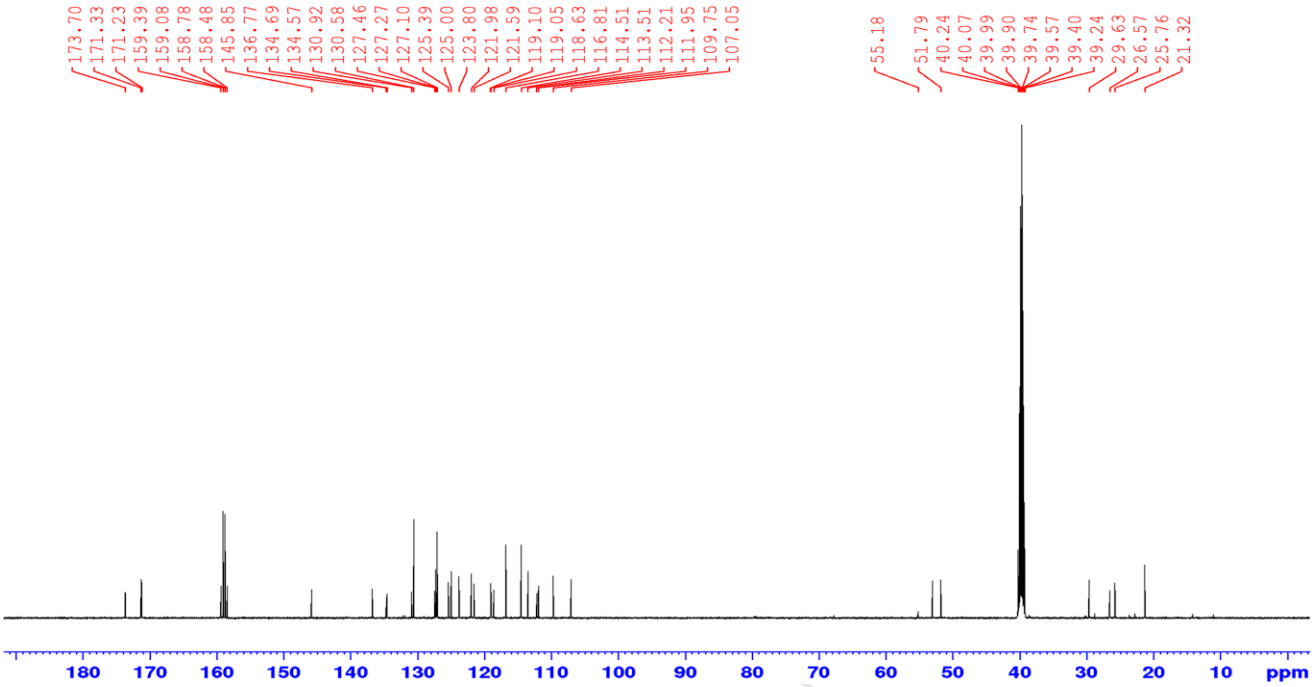

Figure S47. ^{13}C NMR spectrum of compound 7h.

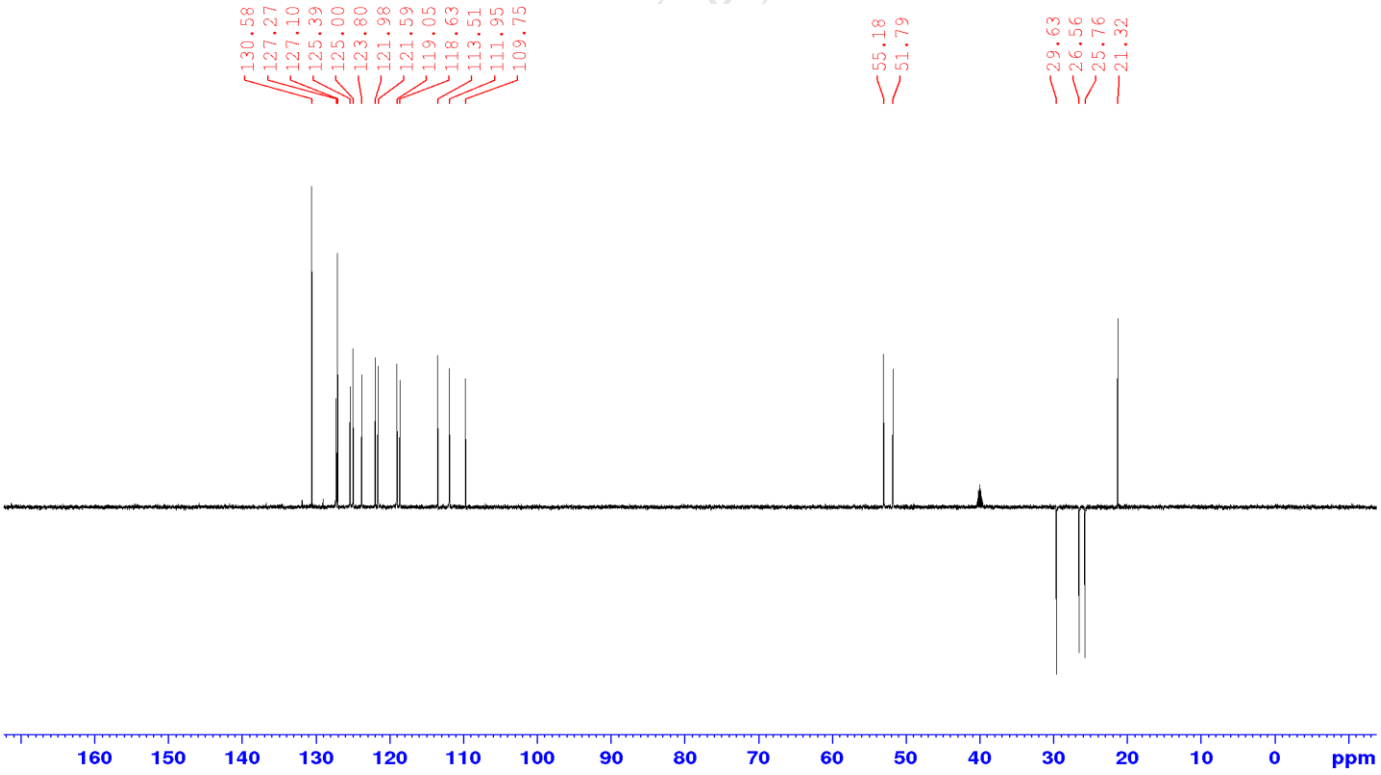

Figure S48. DEPT-135 NMR spectrum of compound 7h.

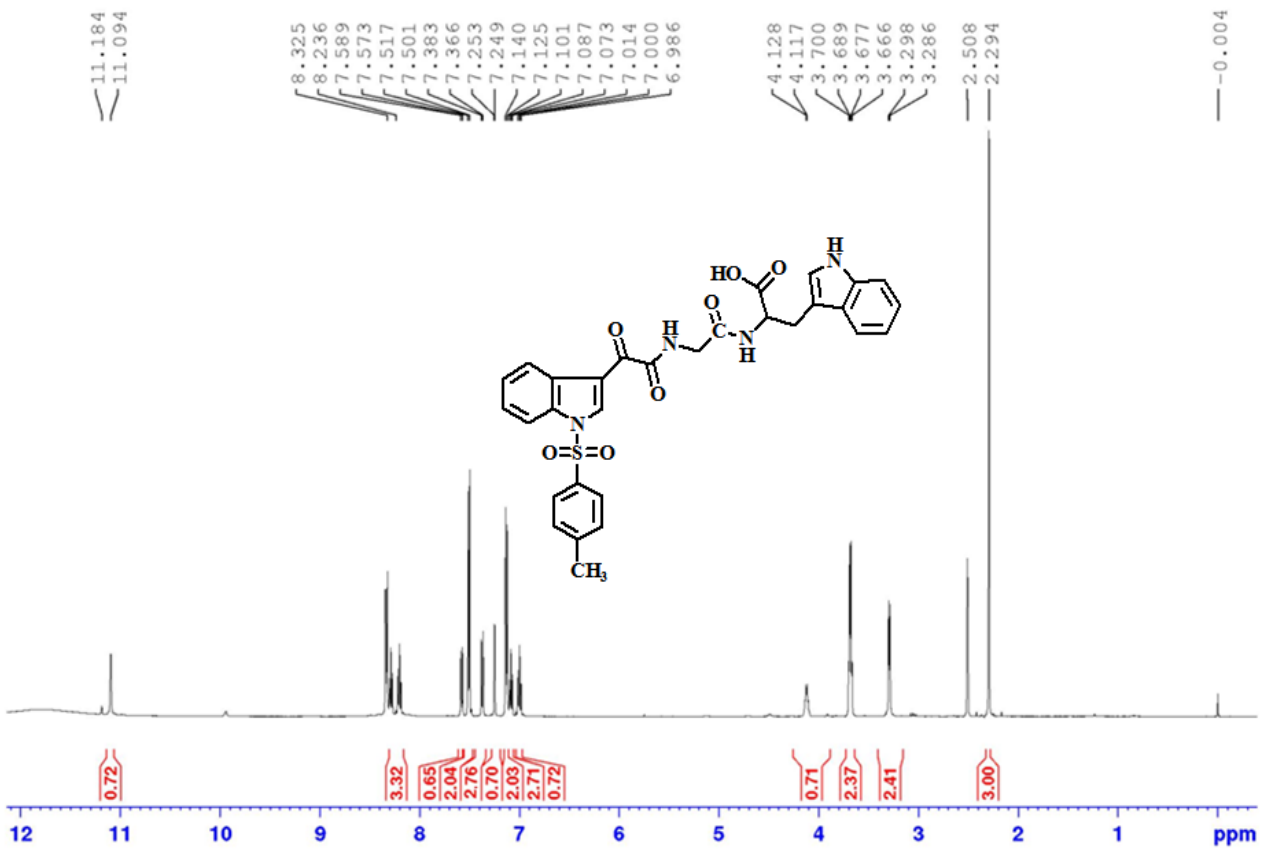

Figure S49. ^{1}H spectrum of compound 7d.

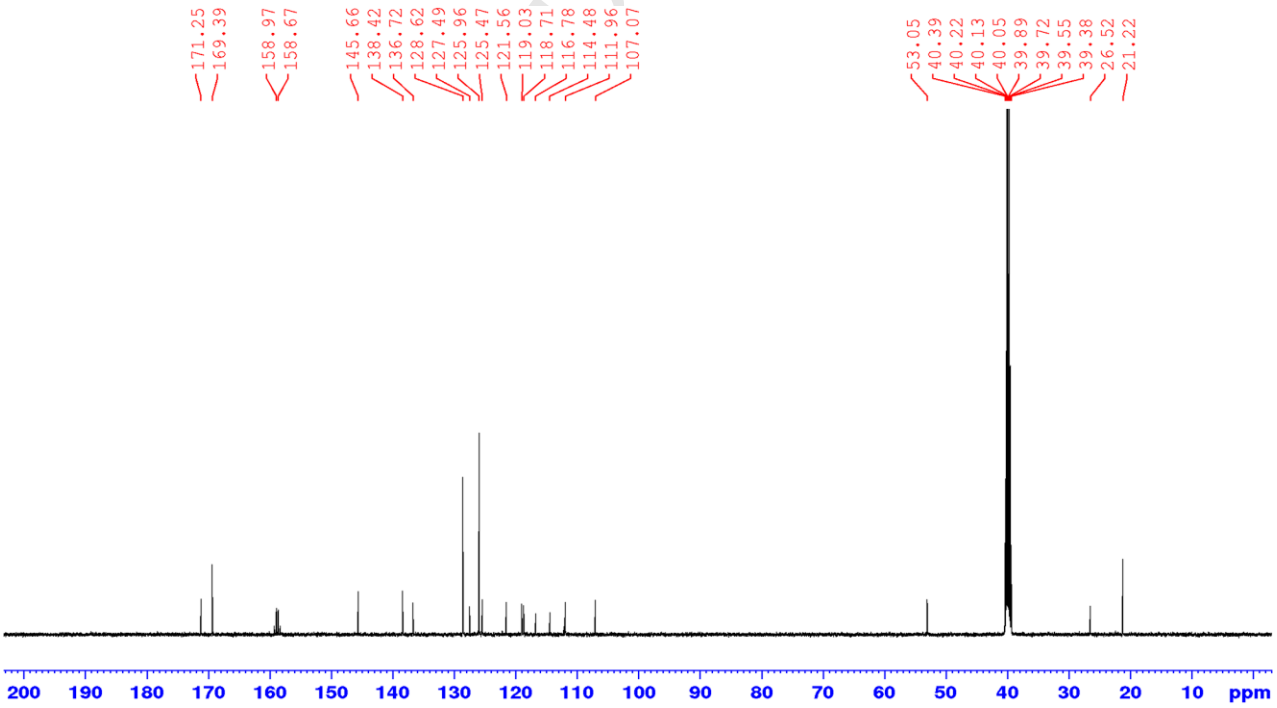

Figure S50. ^{13}C NMR spectrum of compound 7d.

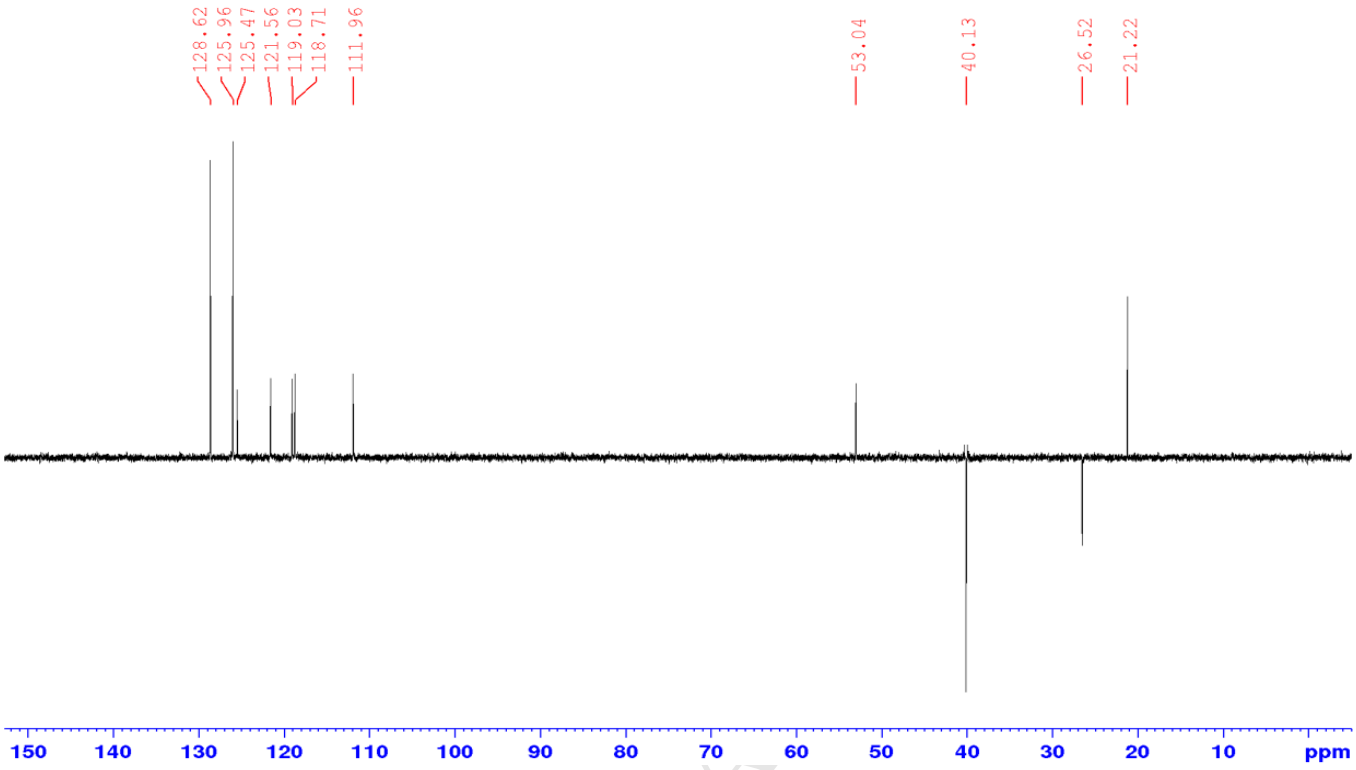

Figure S51. DEPT-135 NMR spectrum of compound 7d.

HRMS of the compounds:

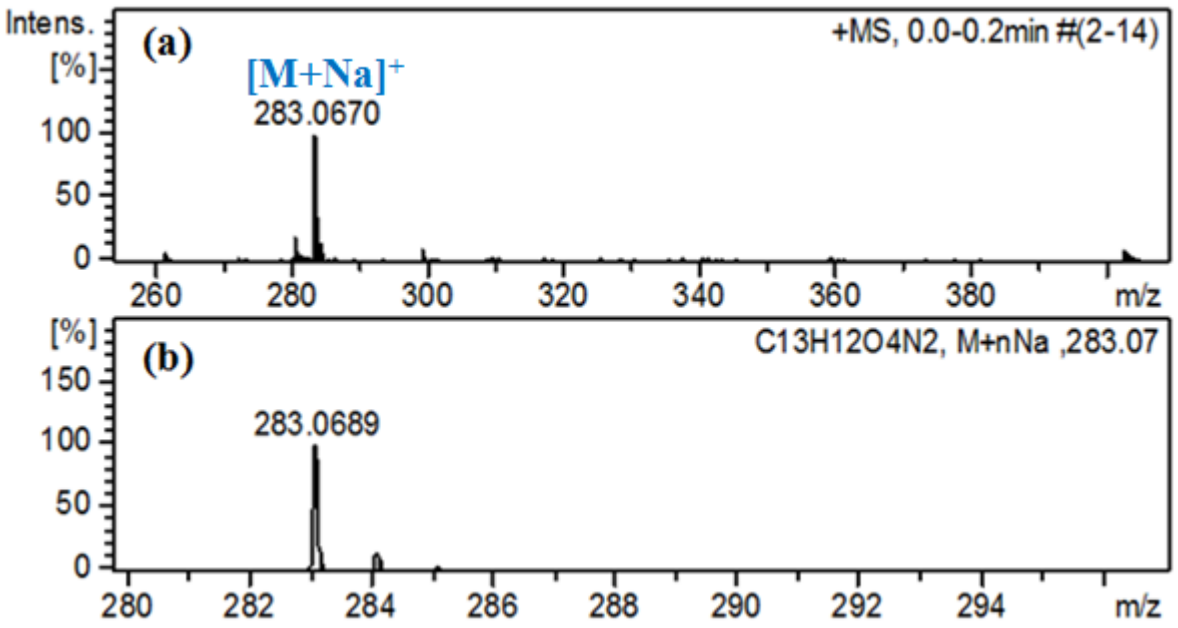

Figure S52. a) High resolution mass spectrum of compound **10**, b) simulated mass spectrum of **10**.

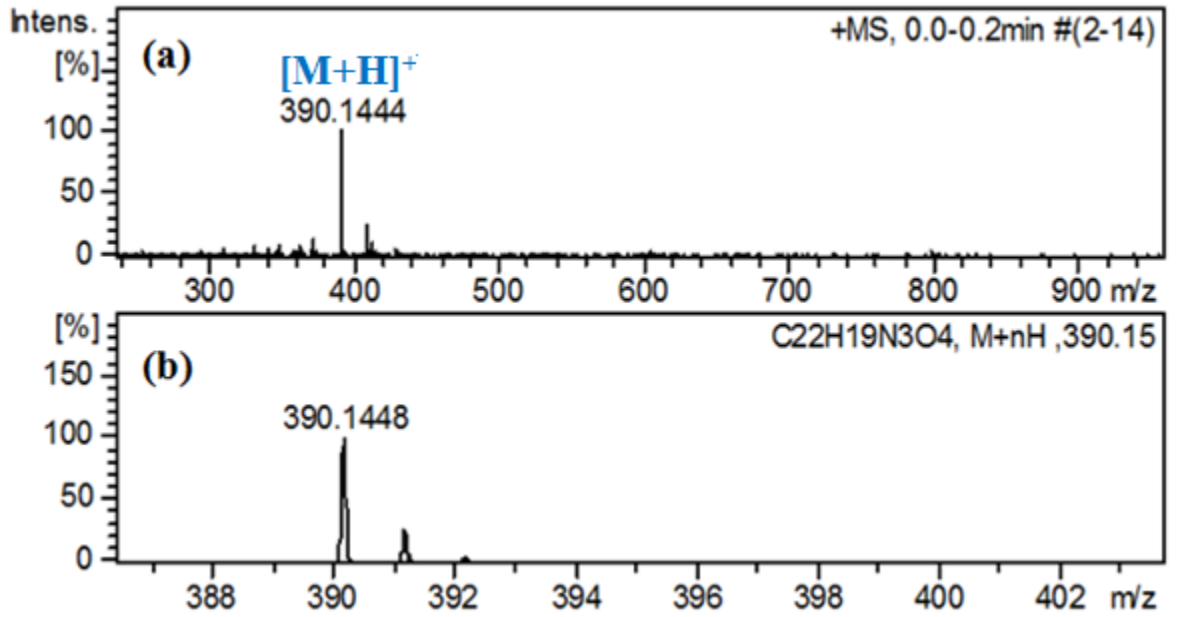

Figure S53 a) High resolution mass spectrum of compound **11**, b) simulated mass spectrum of **11**.

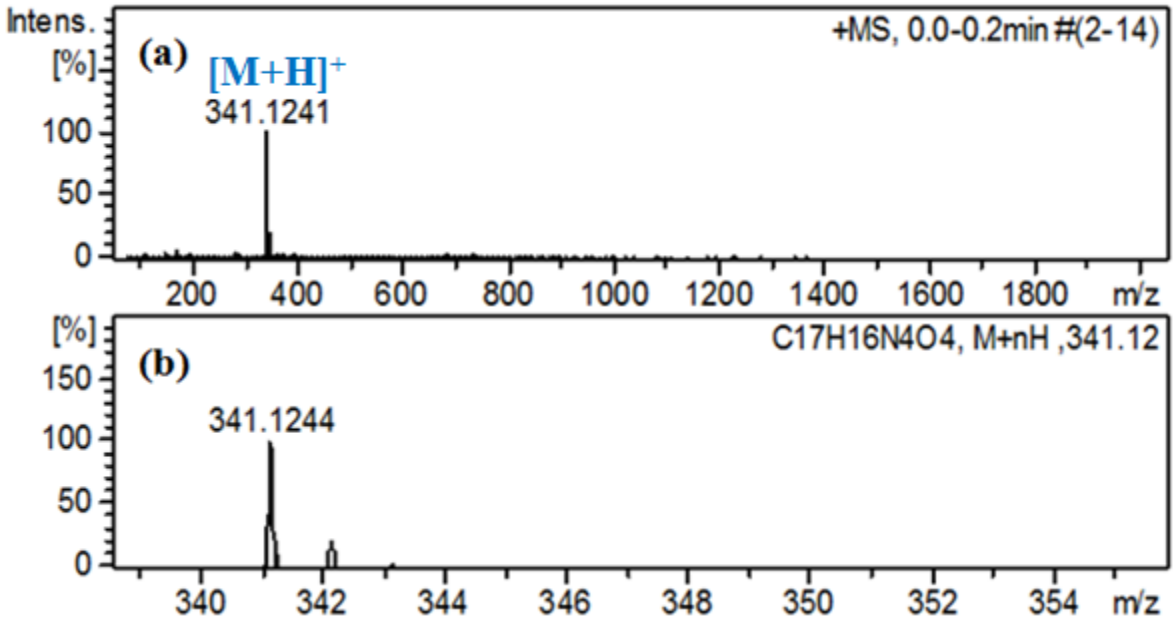

Figure S54 a) High resolution mass spectrum of compound **12**, b) simulated mass spectrum of **12**.

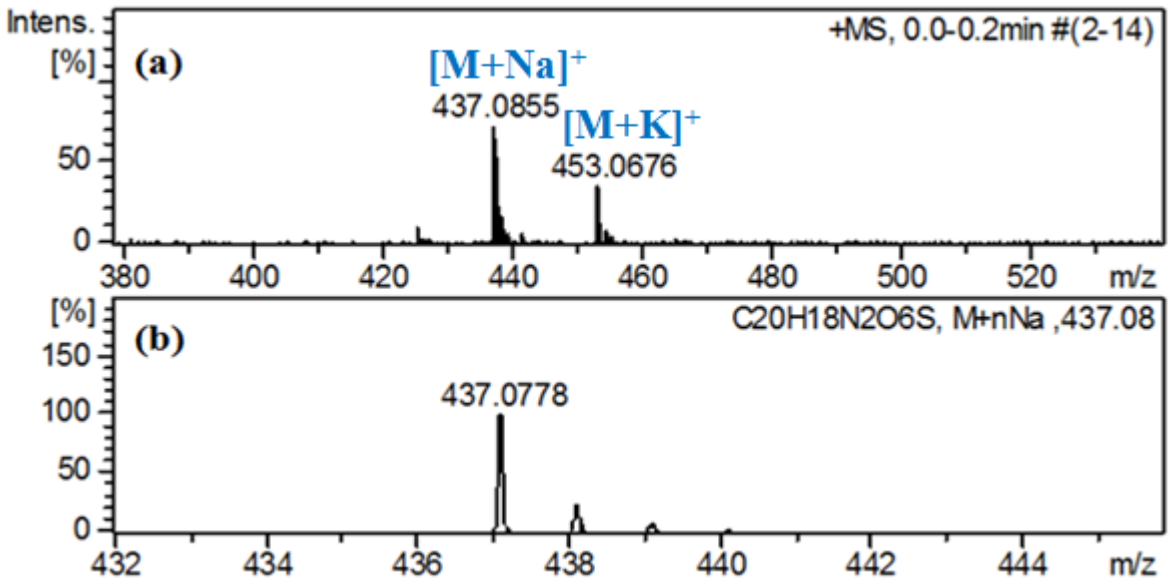

Figure S55 a) High resolution mass spectrum of compound **13**, b) simulated mass spectrum of **13**.

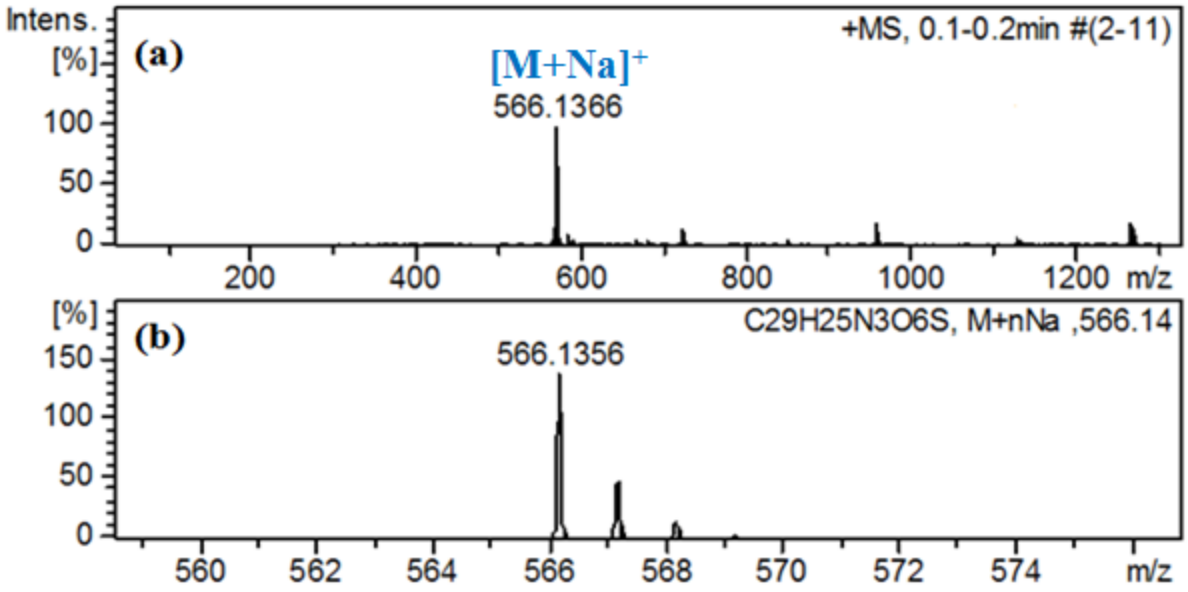

Figure S56 a) High resolution mass spectrum of compound **14**, b) simulated mass spectrum of **14**.

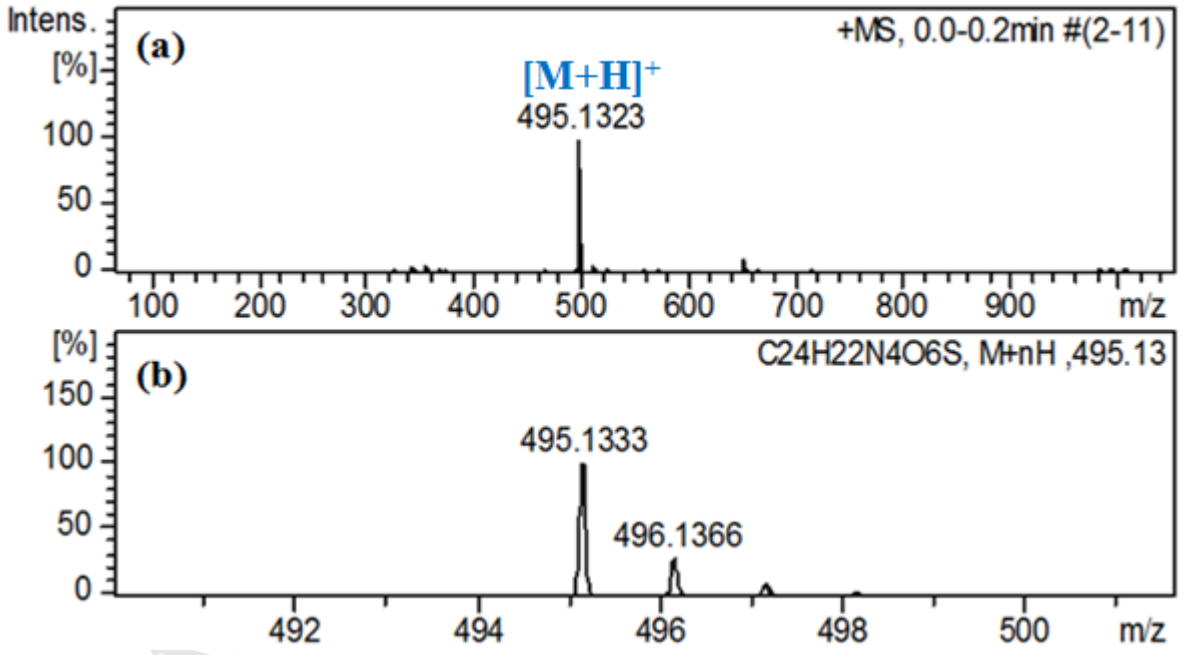

Figure S57 a) High resolution mass spectrum of compound **15**, b) simulated mass spectrum of **15.**

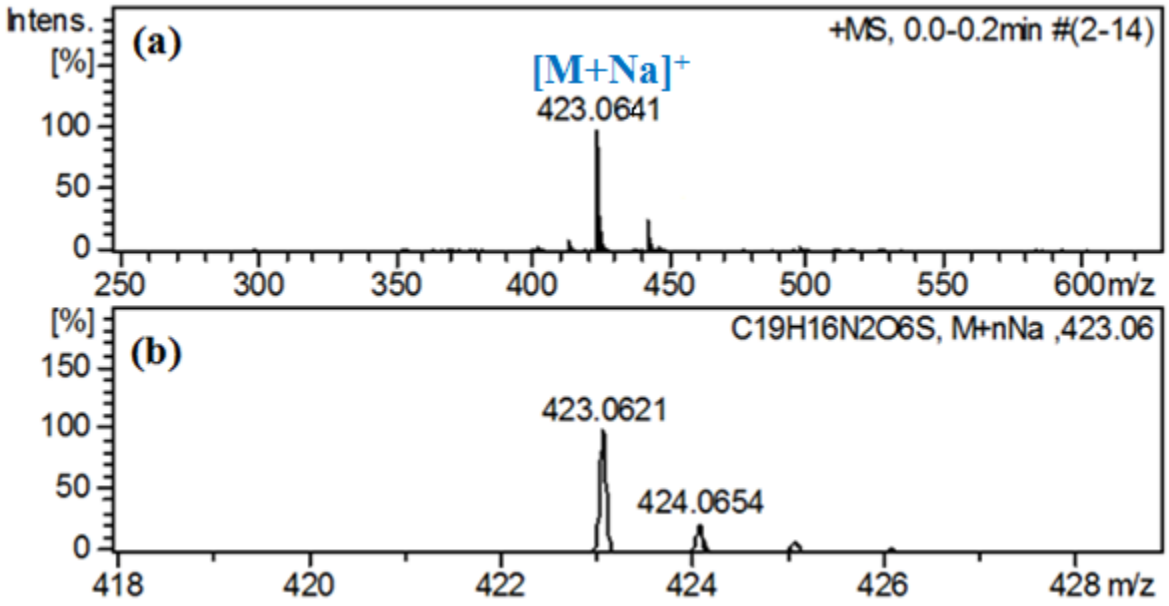

Figure S58 a) High resolution mass spectrum of compound **16**, b) simulated mass spectrum of **16**.

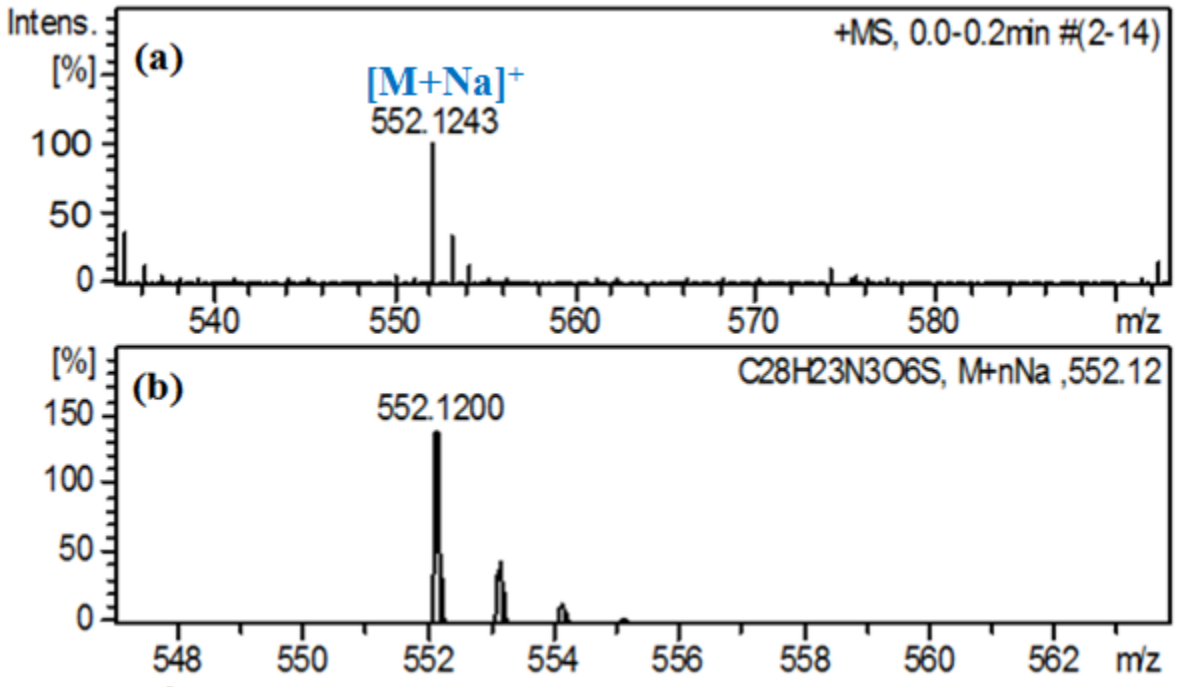

Figure S59 a) High resolution mass spectrum of compound **17**, b) simulated mass spectrum of **17**.

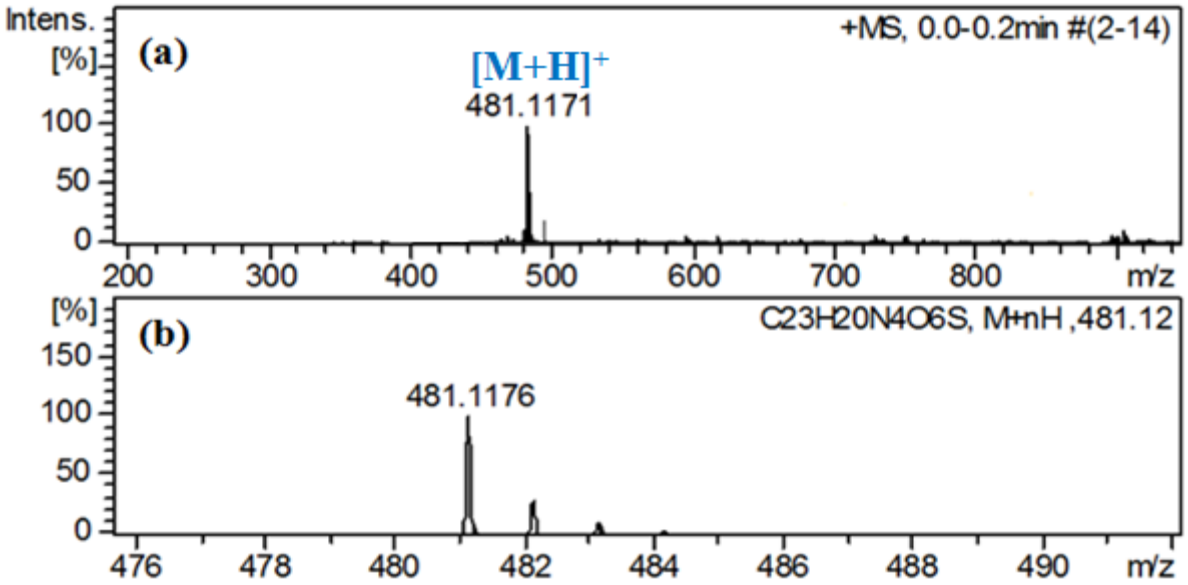

Figure S60 a) High resolution mass spectrum of compound **18**, b) simulated mass spectrum of **18**.

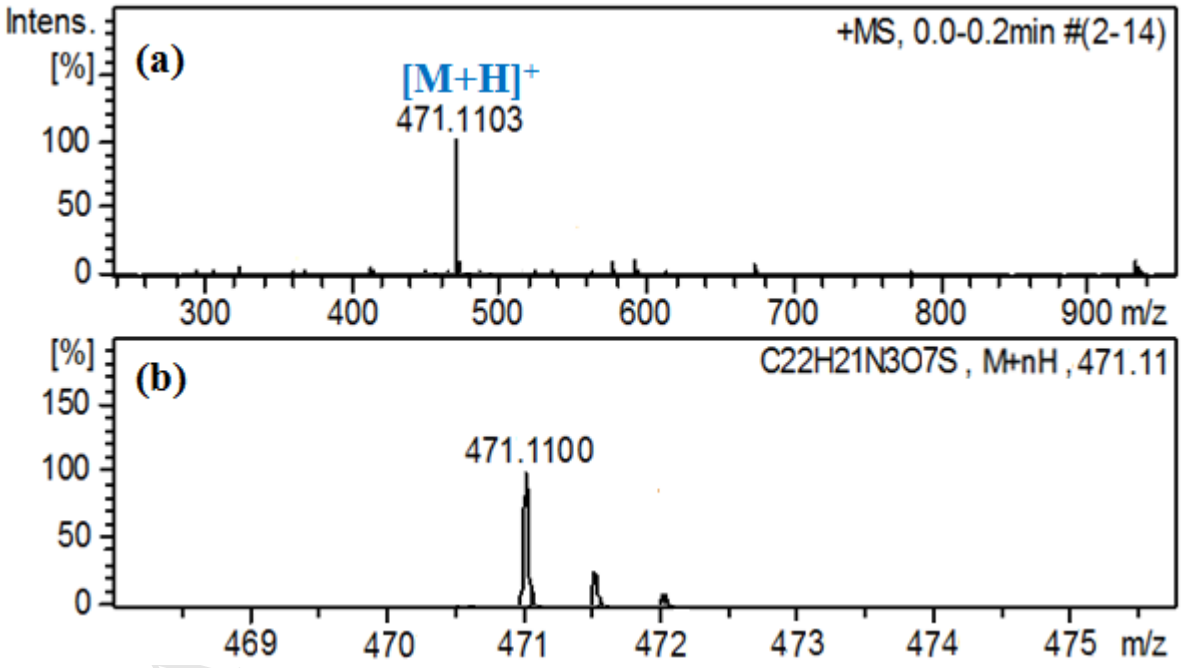

Figure S61. a) High resolution mass spectrum of compound **6i**, b) simulated mass spectrum of **6i**

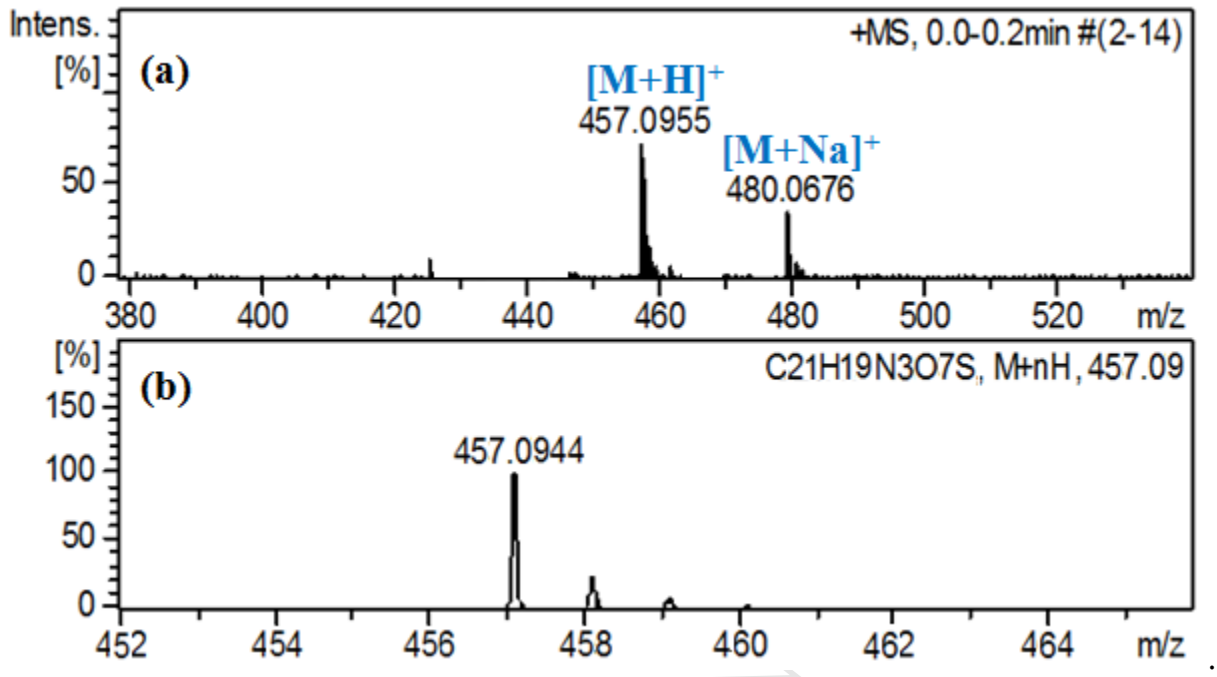

Figure S62. a) High resolution mass spectrum of compound **7i**, b) simulated mass spectrum of **7i**

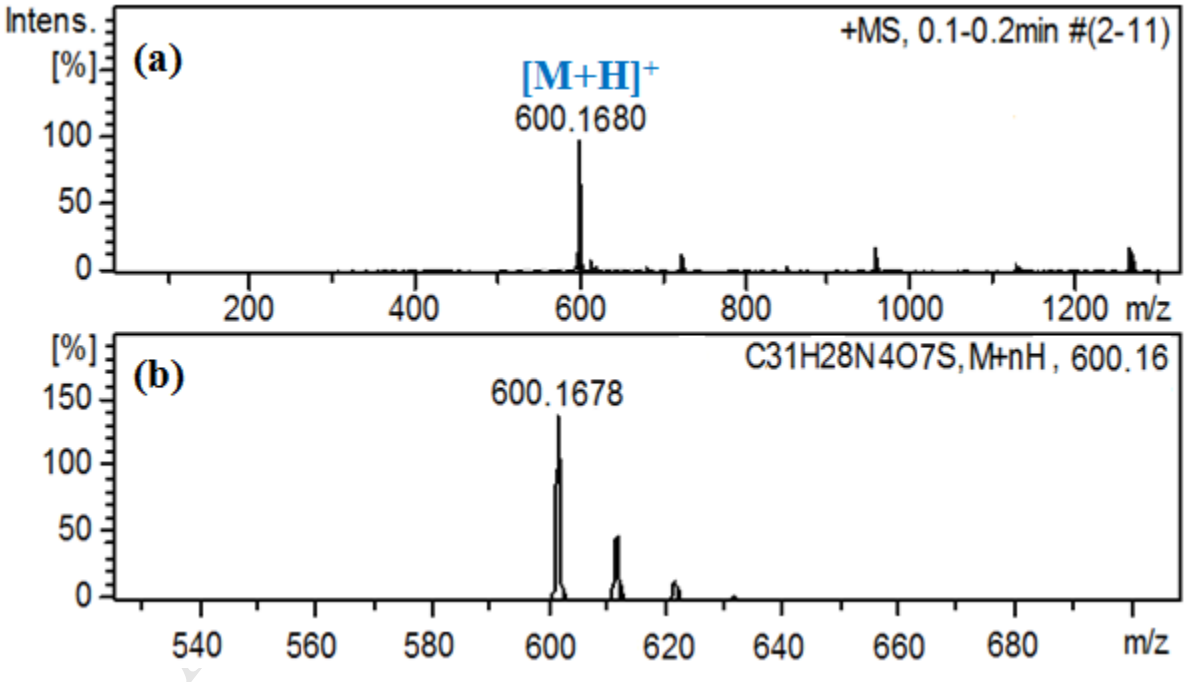

Figure S63. a) High resolution mass spectrum of compound **6b**, b) simulated mass spectrum of **6b.**

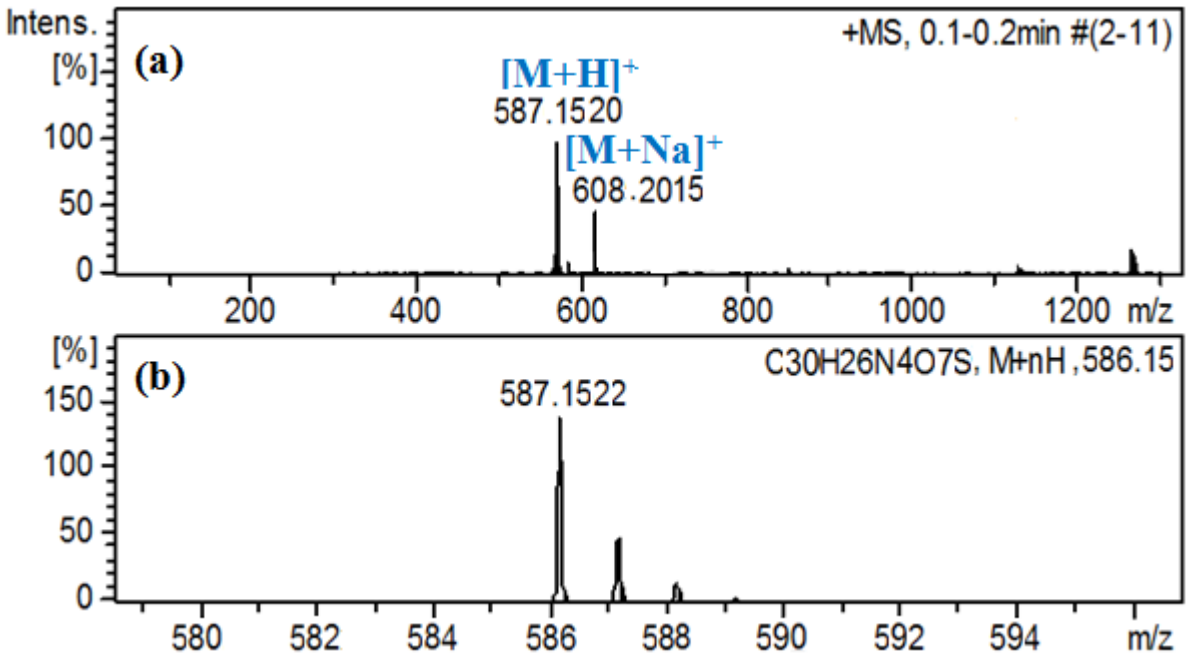

Figure S64. a) High resolution mass spectrum of compound **7b**, b) simulated mass spectrum of **7b.**

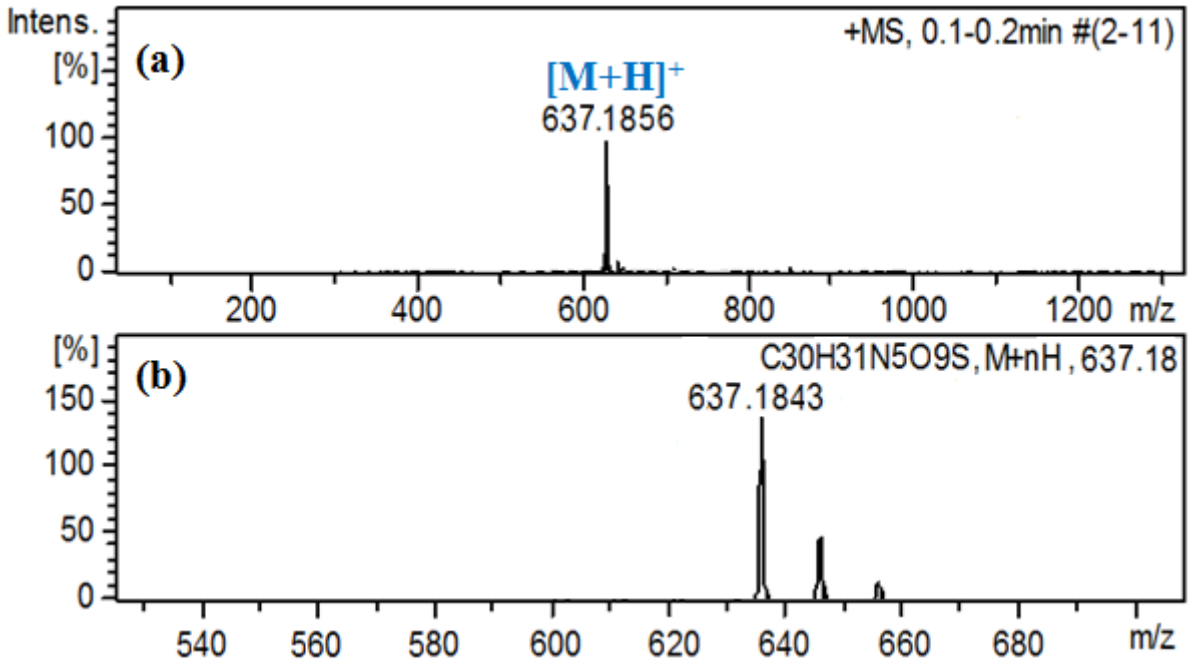

Figure S65. a) High resolution mass spectrum of compound **6h**, b) simulated mass spectrum of **6h.**

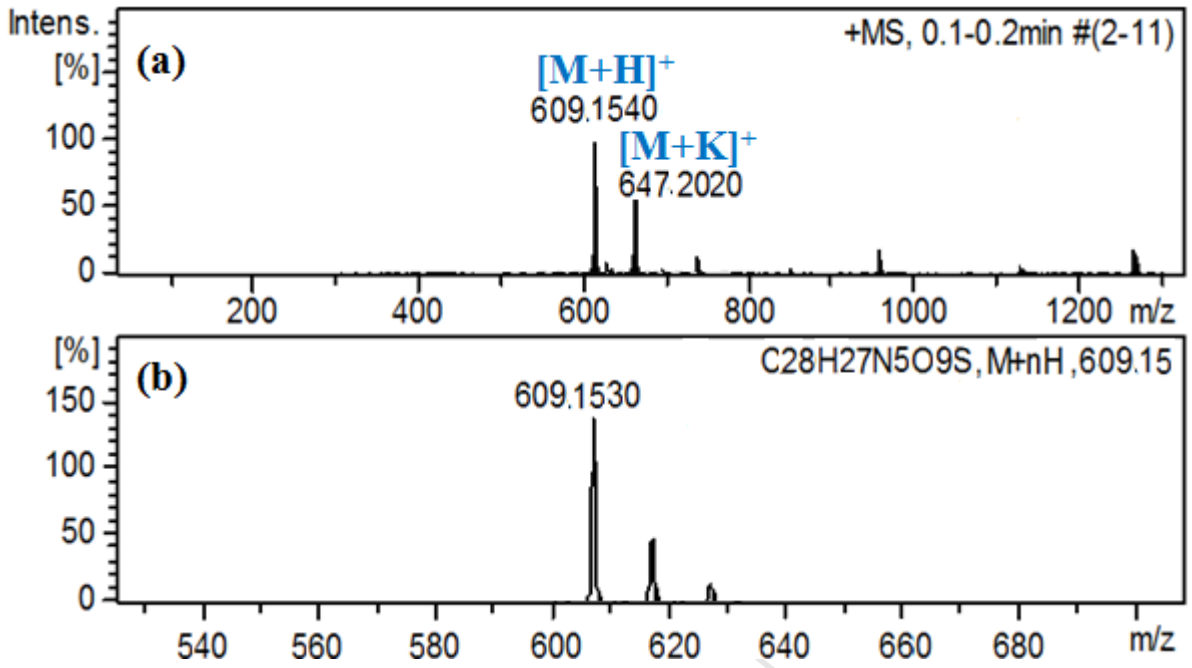

Figure S66. a) High resolution mass spectrum of compound **7h**, b) simulated mass spectrum of **7h.**

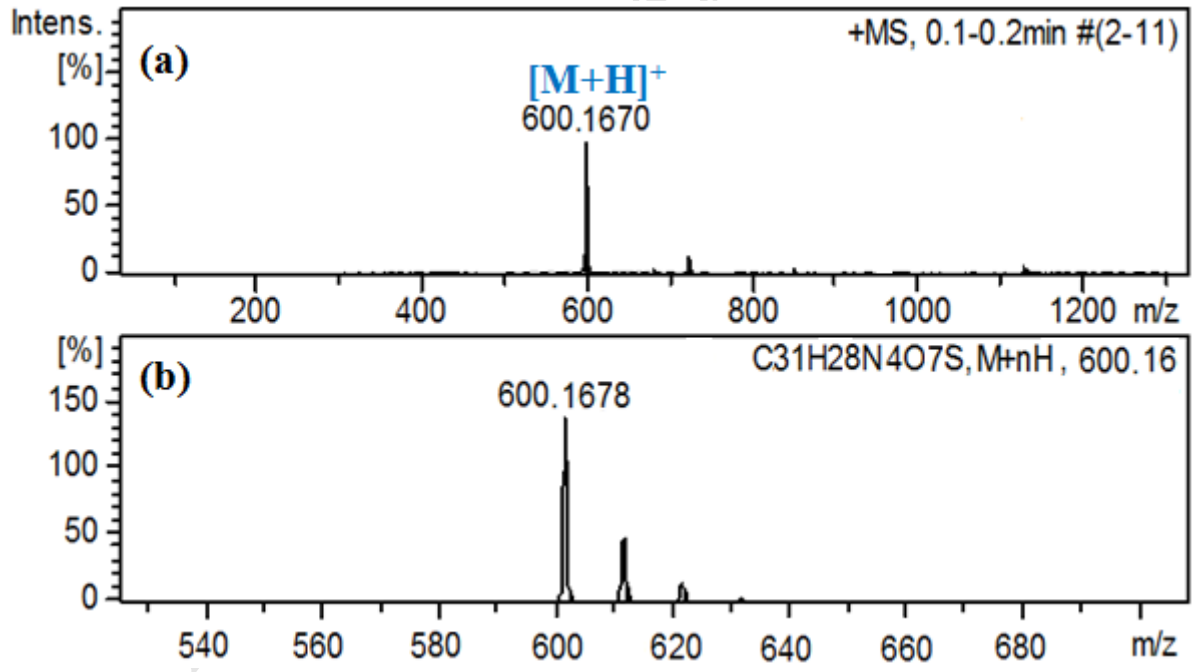

Figure S67. a) High resolution mass spectrum of compound **6d**, b) simulated mass spectrum of **6d.**

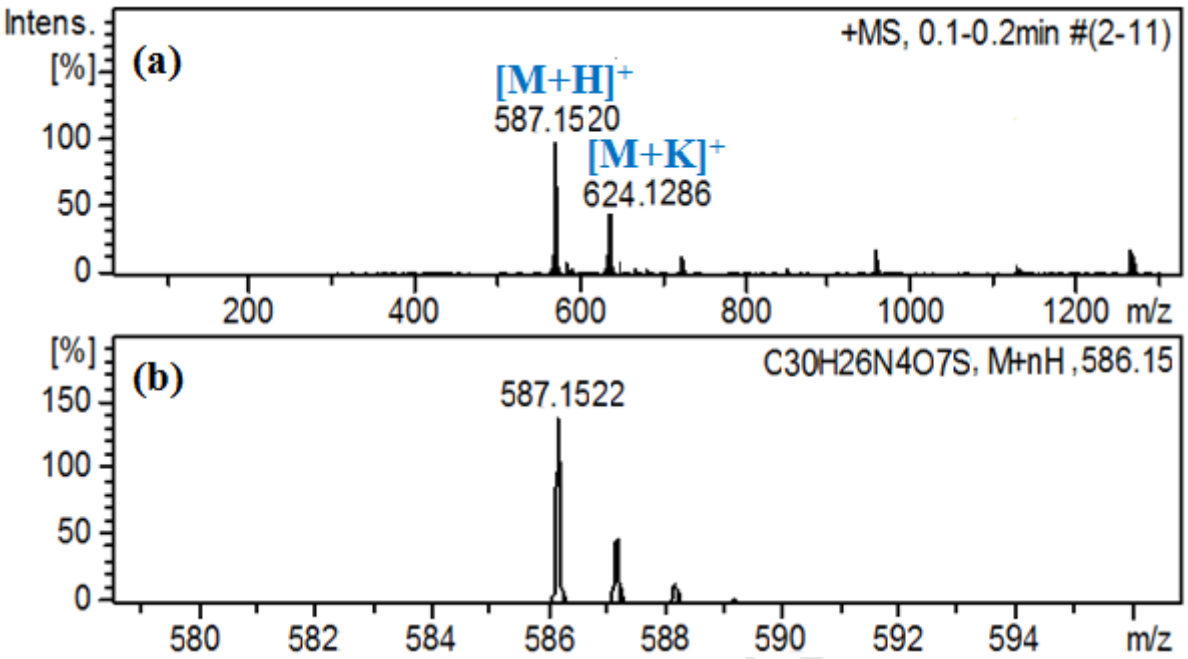

Figure S68. a) High resolution mass spectrum of compound **7d**, b) simulated mass spectrum of **7d.**

HPLC analysis of compounds 7.

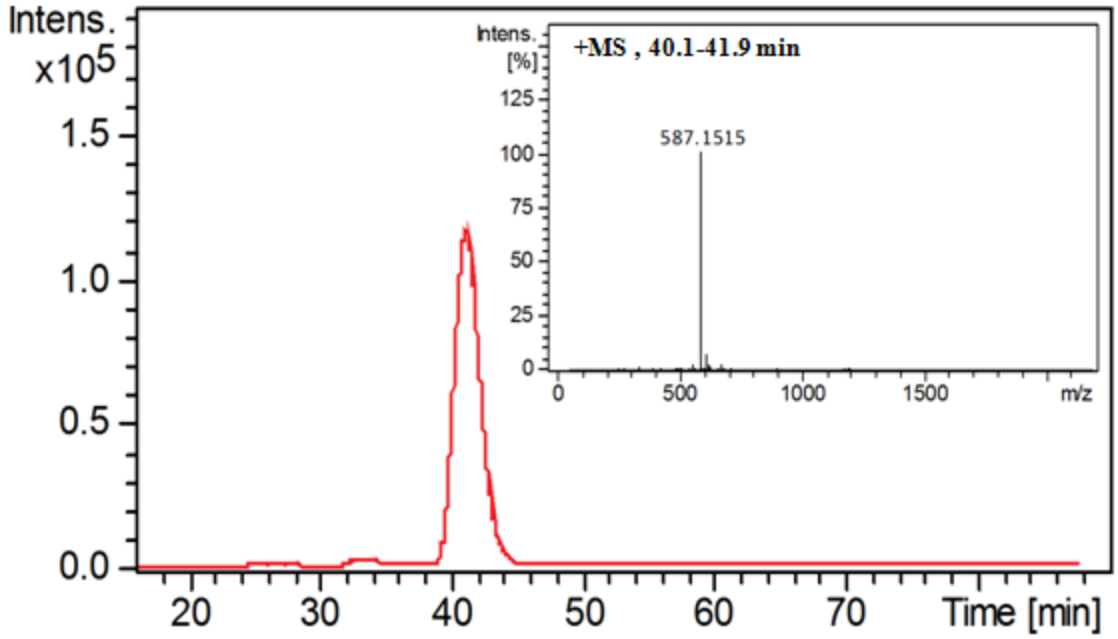

Figure S69. LC chromatogram of compound **7d** (55% ACN + 45% H_2O). Inset: Mass peak corresponding to the LC chromatogram.

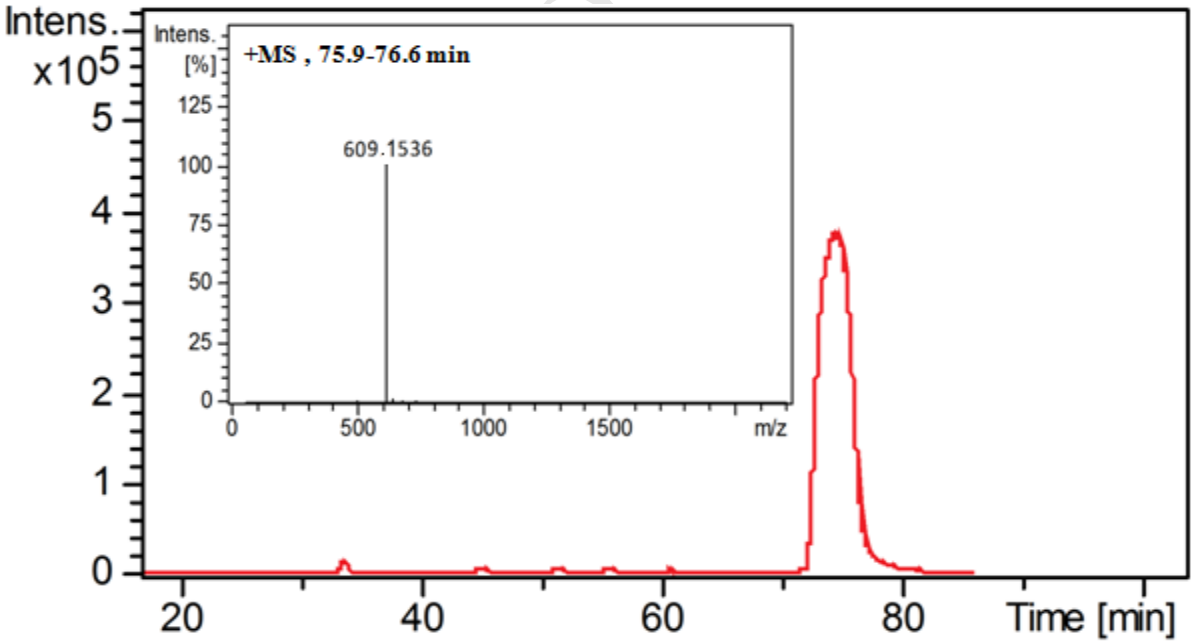

Figure S70. LC chromatogram of compound **7h** (55% ACN + 45% H_2O). Inset: Mass peak corresponding to the LC chromatogram.

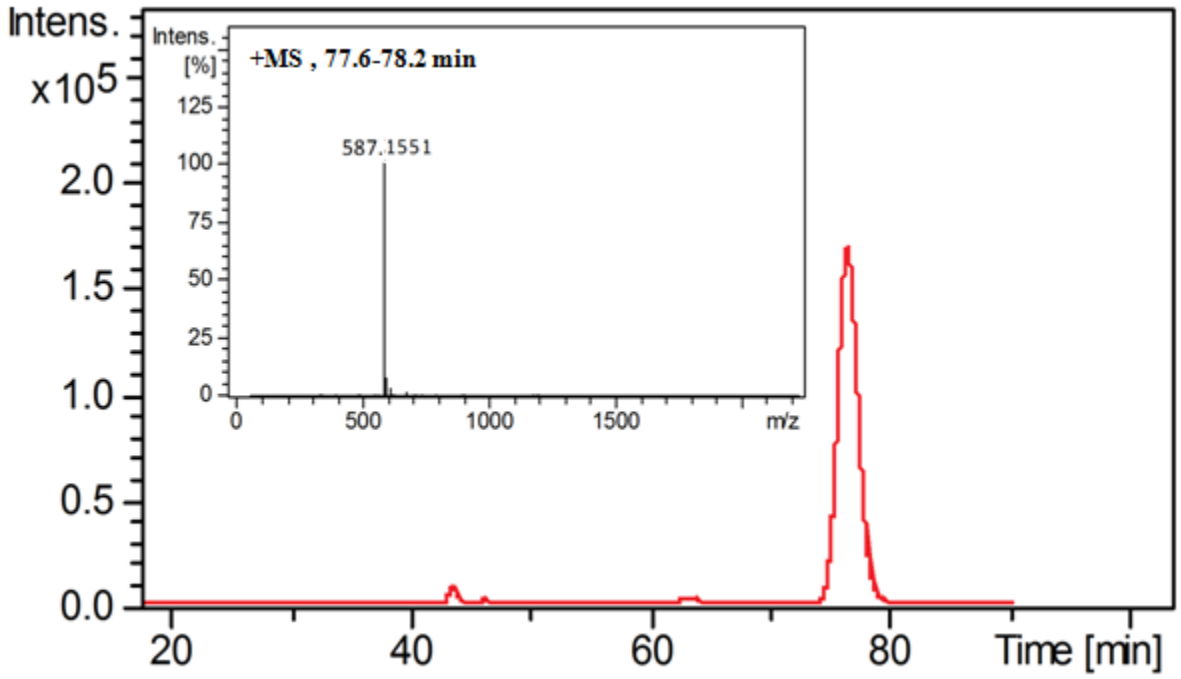

Figure S71. LC chromatogram of compound **7b** (55% ACN + 45% H_2O). Inset: Mass peak corresponding to the LC chromatogram.

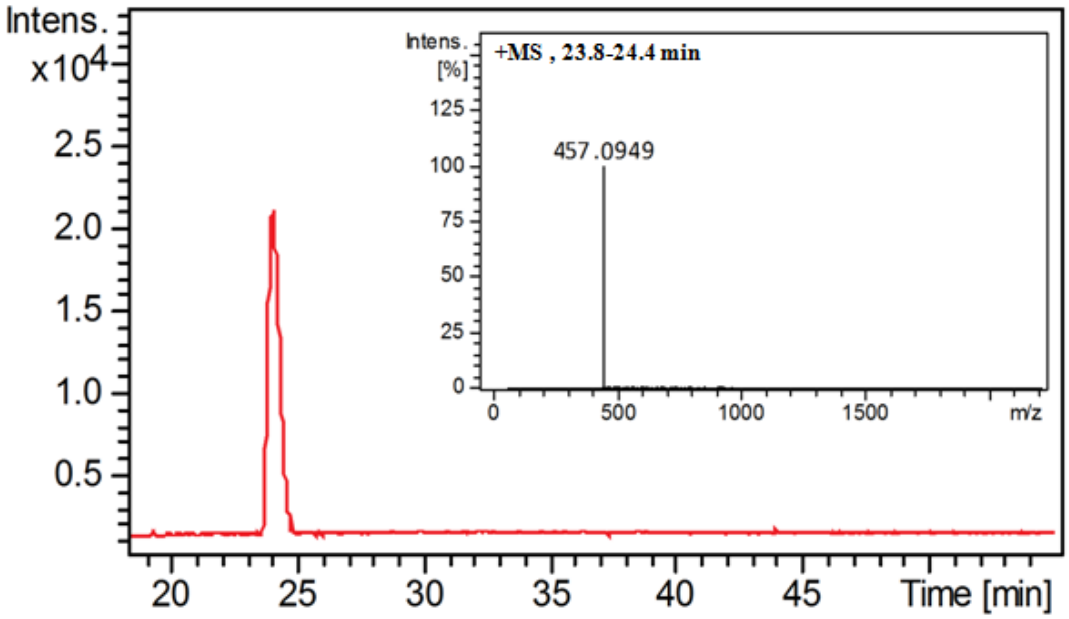

Figure S72. LC chromatogram of compound **7i** (55% ACN + 45% H_2O). Inset: Mass peak corresponding to the LC chromatogram.

Docking Images of compounds docked in the active site of 5-LOX enzyme:

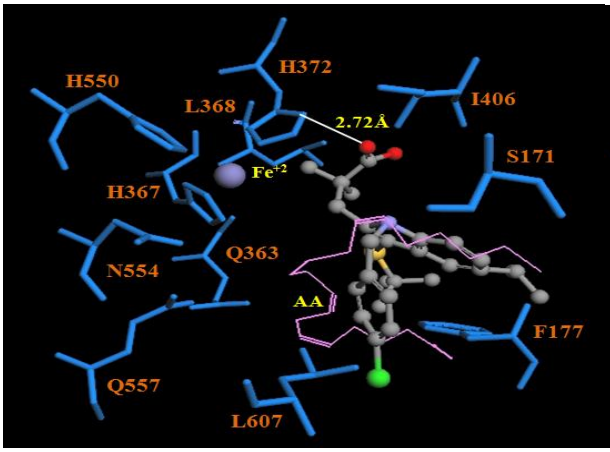

Figure S73. MK-886 docked in the active site of 5-LOX

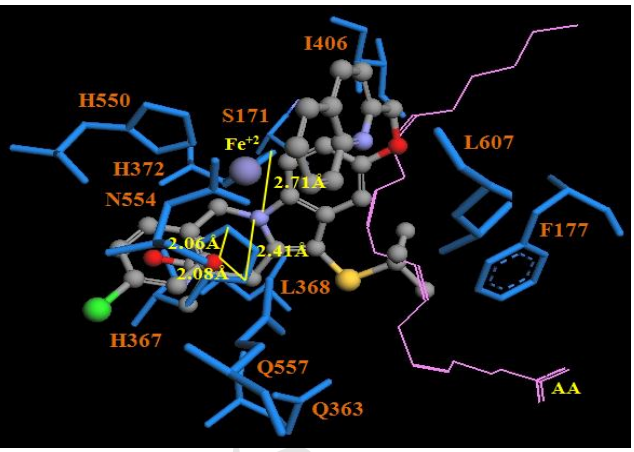

Figure S74. MK-0591 docked in the active site of 5-LOX (PDB ID 3V99)

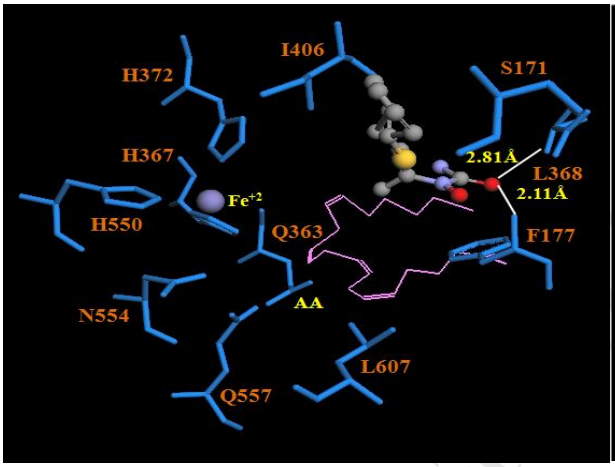

Figure S75. ZILEUTON docked in the active site of 5-LOX)

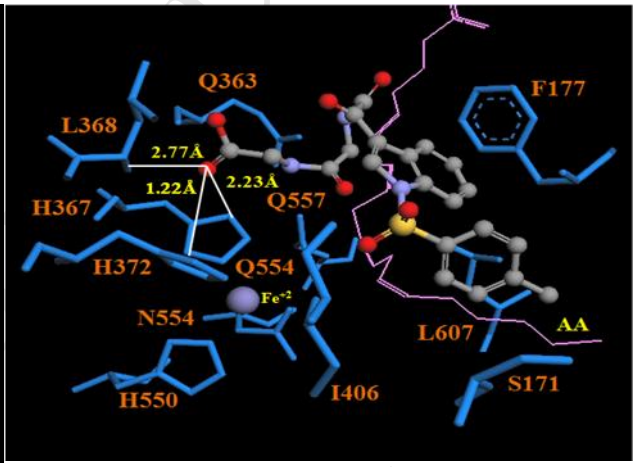

Figure S76. 7i docked in the active site of 5-LOX (PDB ID 3V99)

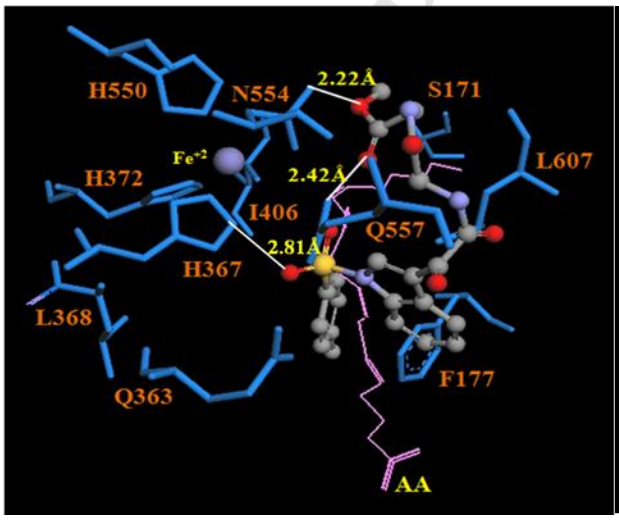

Figure S77.6i docked in the active site of 5-LOX (PDB ID 3V99)

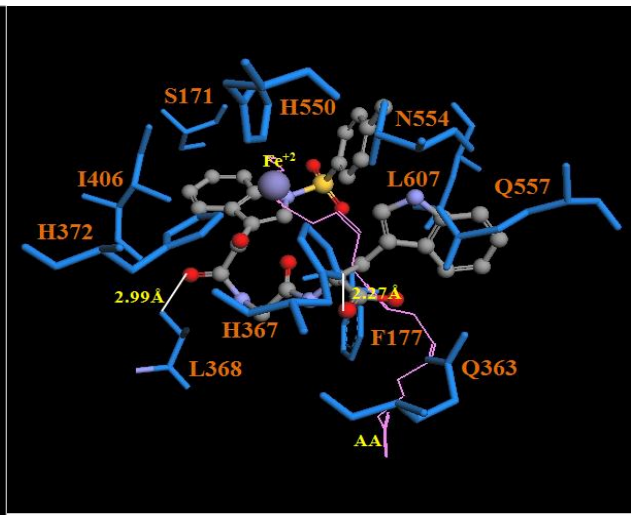

Figure S78.7c docked in the active site of 5-LOX (PDB ID 3V99)

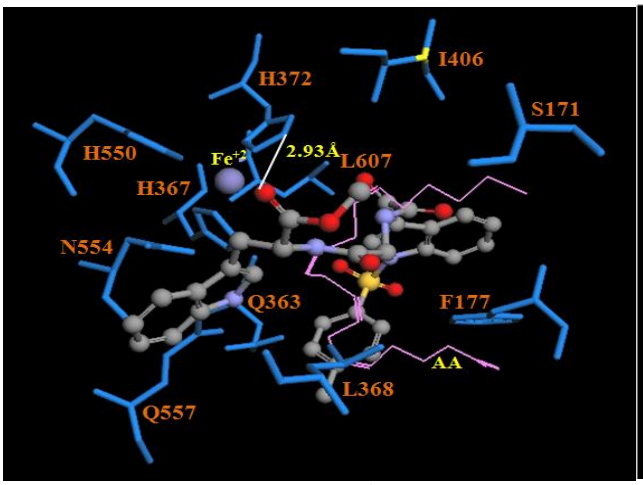

Figure S79.6c docked in the active site of 5-LOX (PDB ID 3V99)

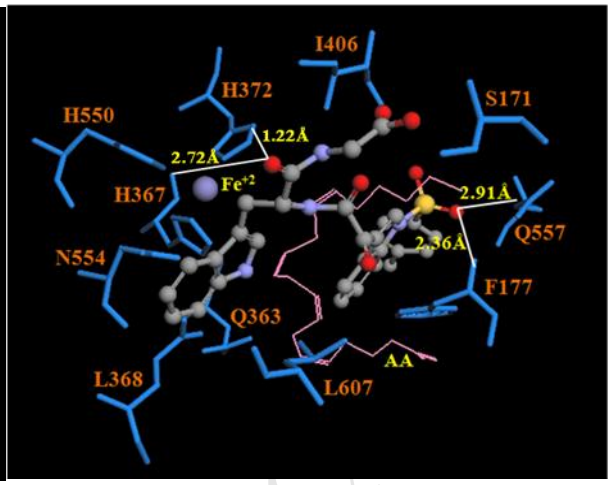

Figure S80.7a docked in the active site of 5-LOX (PDB ID 3V99)

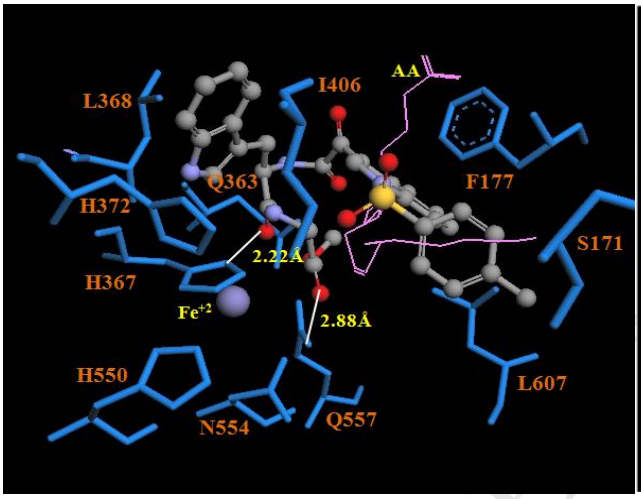

Figure S81.6a docked in the active site of 5-LOX (PDB ID 3V99)

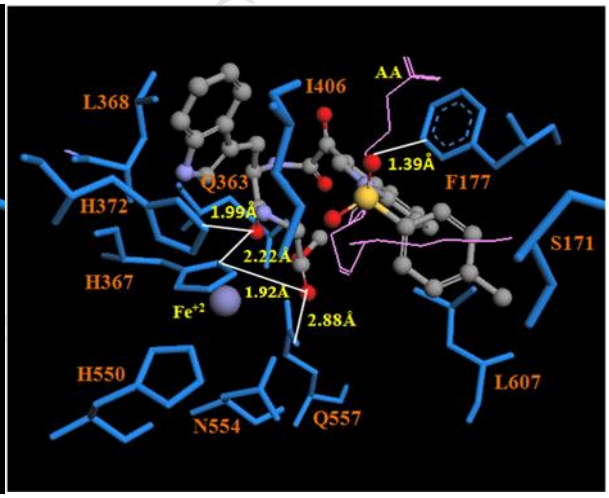

Figure S82.7e docked in the active site of 5-LOX (PDB ID 3V99)

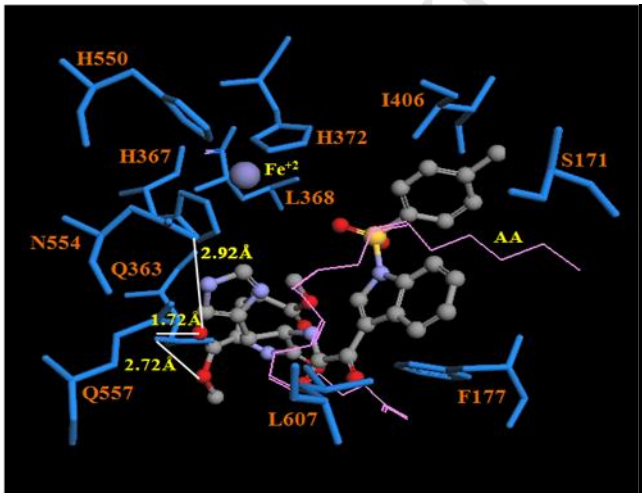

Figure S83.6e docked in the active site of 5-LOX (PDB ID 3V99)

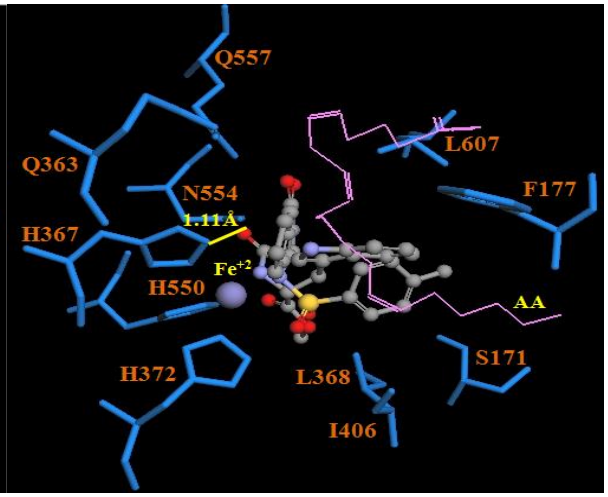

Figure S84.6d docked in the active site of 5-LOX (PDB ID 3V99)

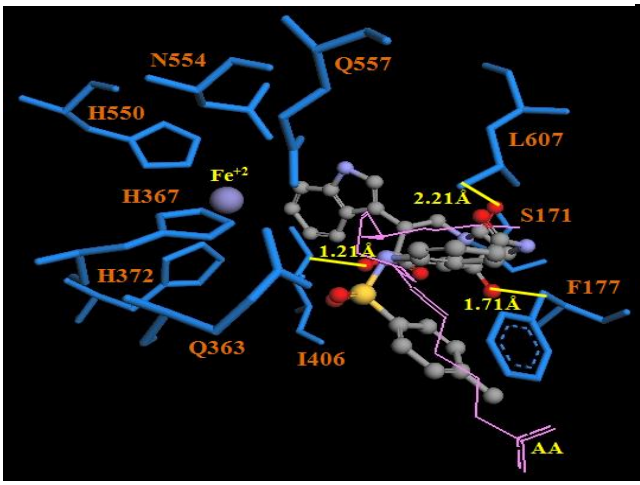

Figure S85.7d docked in the active site of 5-LOX (PDB ID 3V99)

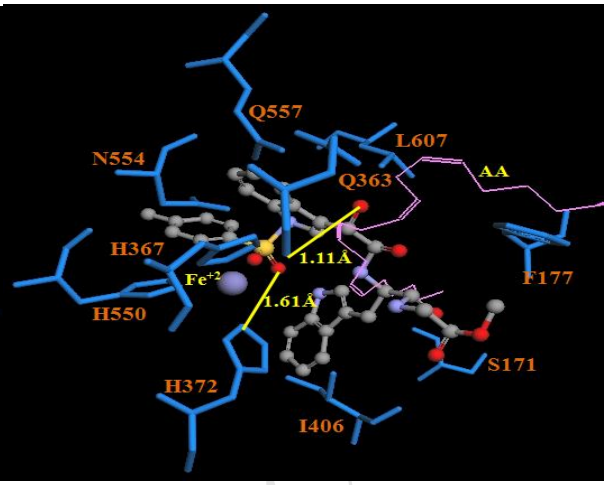

Figure S86.6b docked in the active site of 5-LOX (PDB ID 3V99)

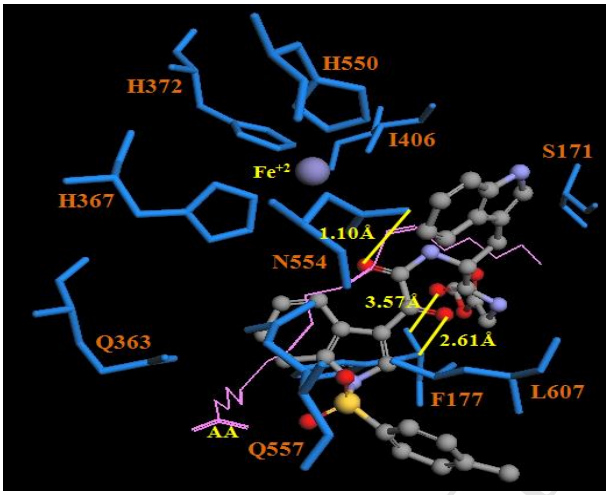

Figure S87.7b docked in the active site of 5-LOX (PDB ID 3V99

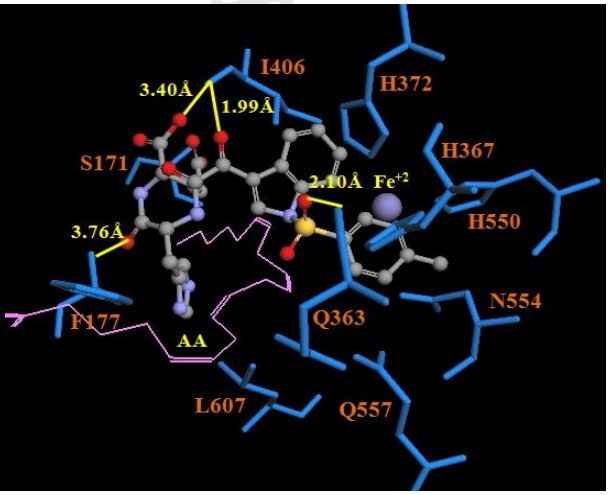

Figure S88.7h docked in the active site of 5-LOX (PDB ID 3V99)

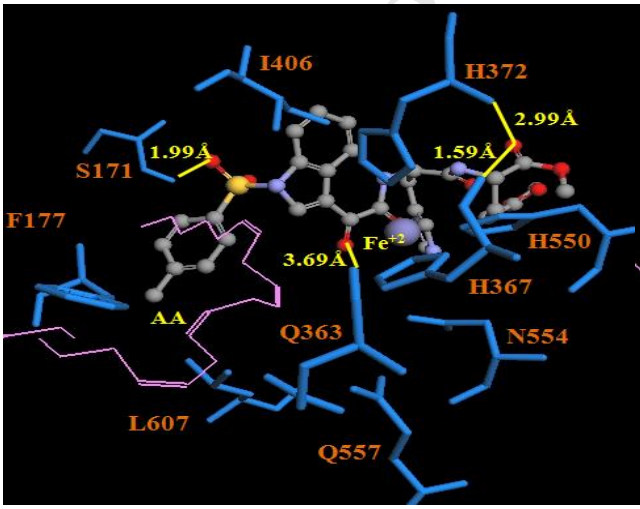

Figure S89.6h docked in the active site of 5-LOX (PDB ID 3V99

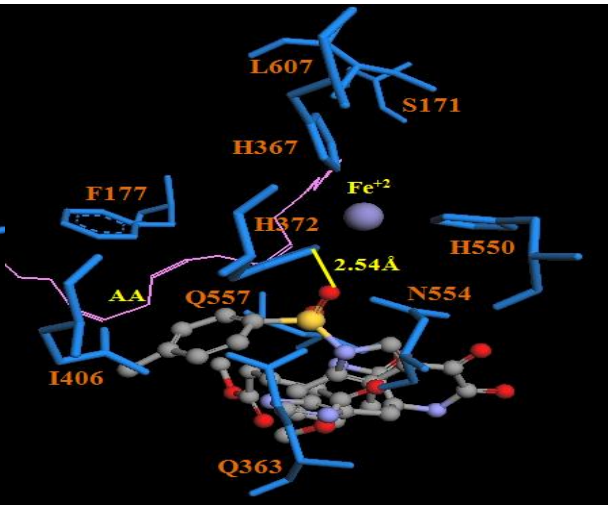

Figure S90.7g docked in the active site of 5-LOX (PDB ID 3V99)

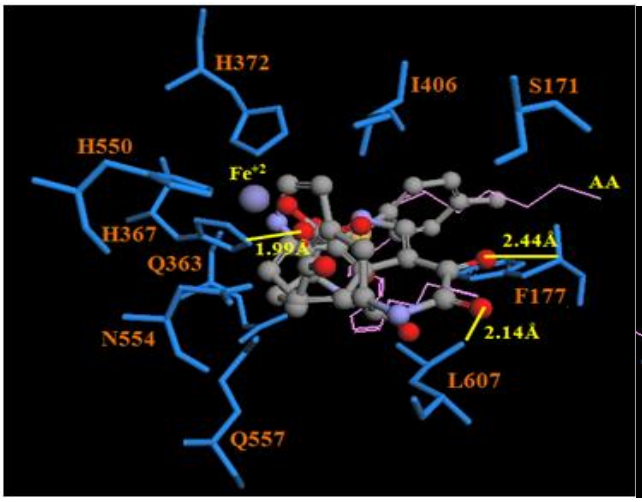

Figure S91.7f docked in the active site of 5-LOX (PDB ID 3V99)

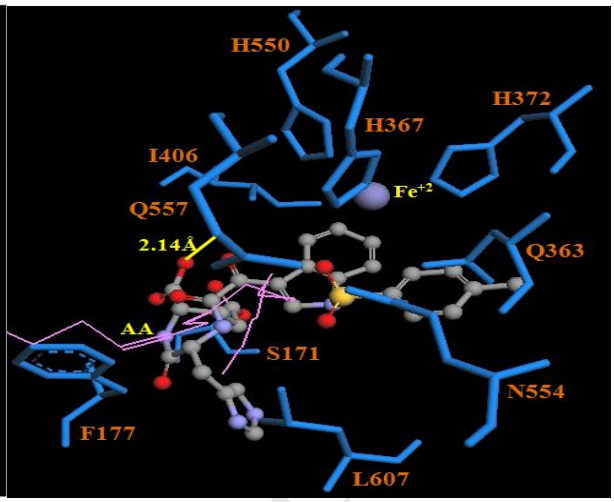

Figure S92.6g docked in the active site of 5-LOX (PDB ID 3V99)

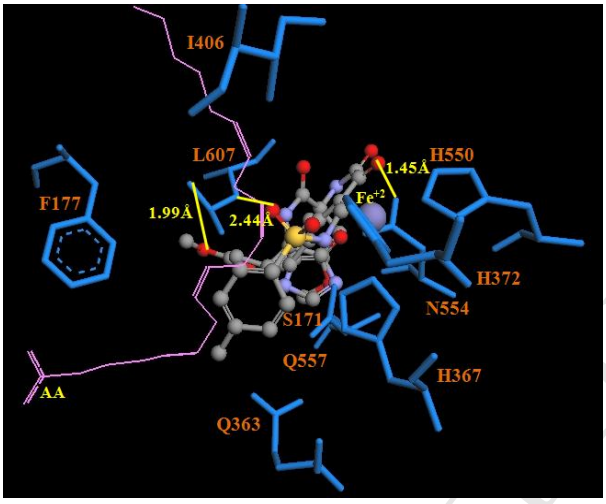

Figure S93.6f docked in the active site of 5-LOX (PDB ID 3V99)

Docking Images of compounds docked in the active site of COX-2 enzyme:

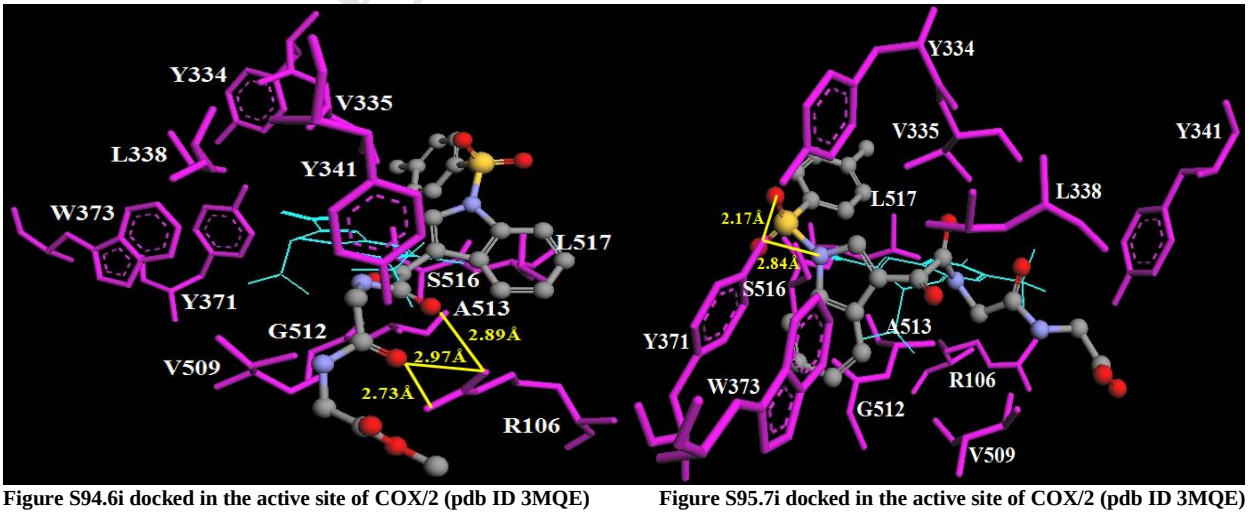

Figure S94.6i docked in the active site of COX/2 (pdb ID 3MQE)

Figure S95.7i docked in the active site of COX/2 (pdb ID 3MQE)

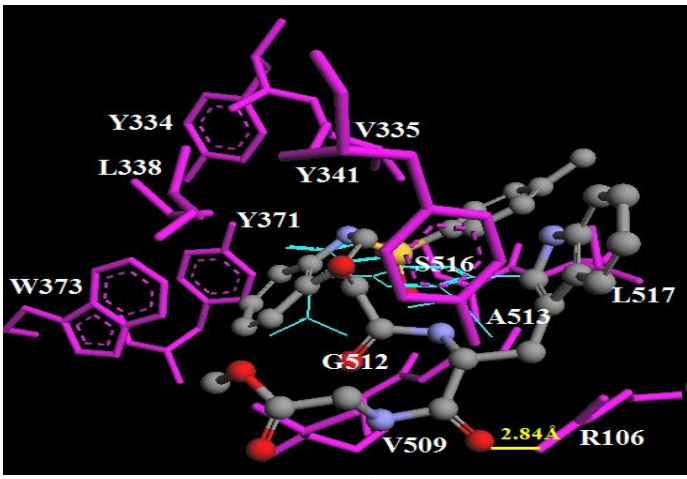

Figure S96.6a docked in the active site of COX/2 (pdb ID 3MQE)

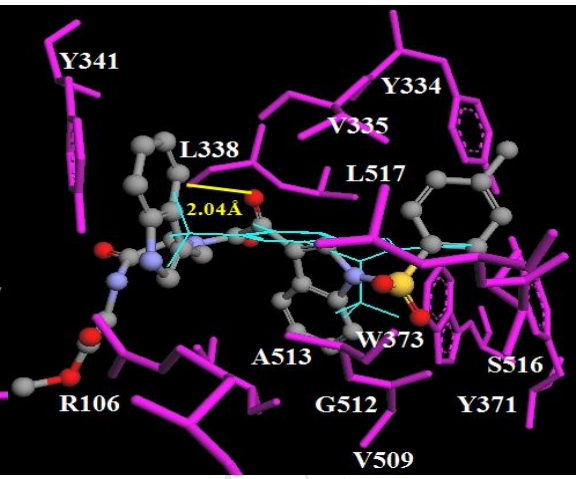

Figure S97.6b docked in the active site of COX/2 (pdb ID 3MQE)

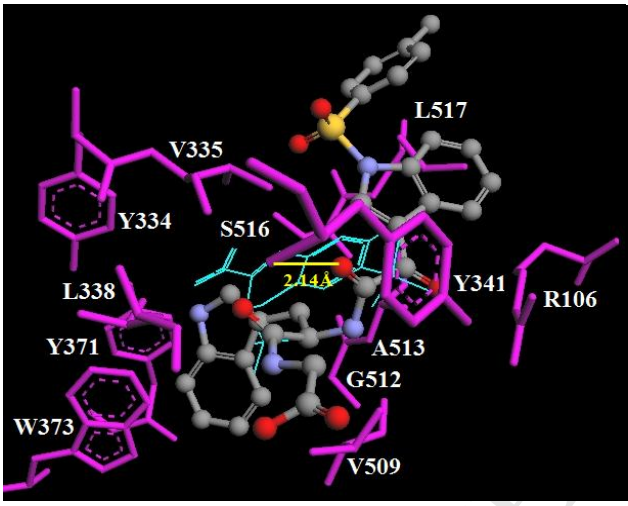

Figure S98.7a docked in the active site of COX/2 (pdb ID 3MQE)

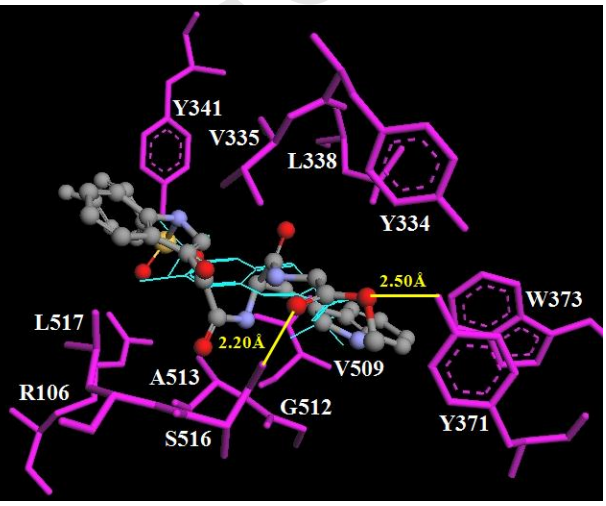

Figure S99.7b docked in the active site of COX/2 (pdb ID 3MQE)

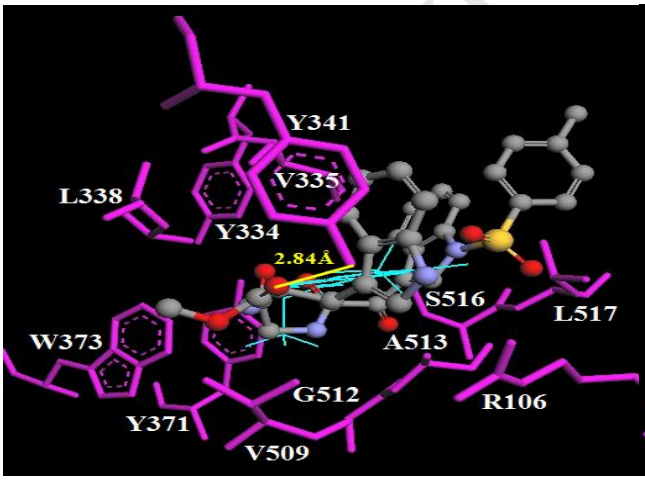

Figure S100.6c docked in the active site of COX/2 (pdb ID 3MQE)

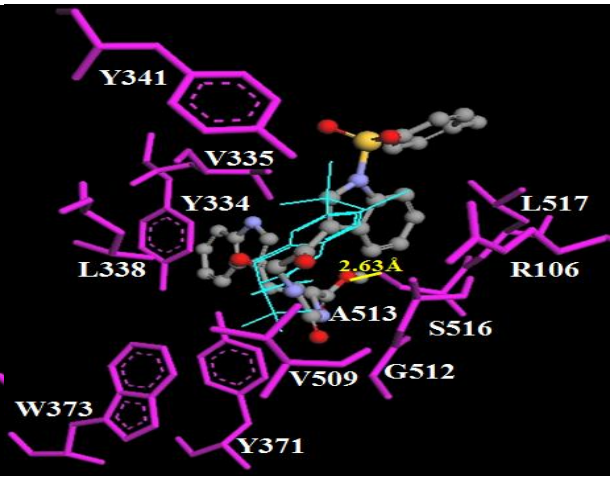

Figure S101.6d docked in the active site of COX/2 (pdb ID 3MQE)

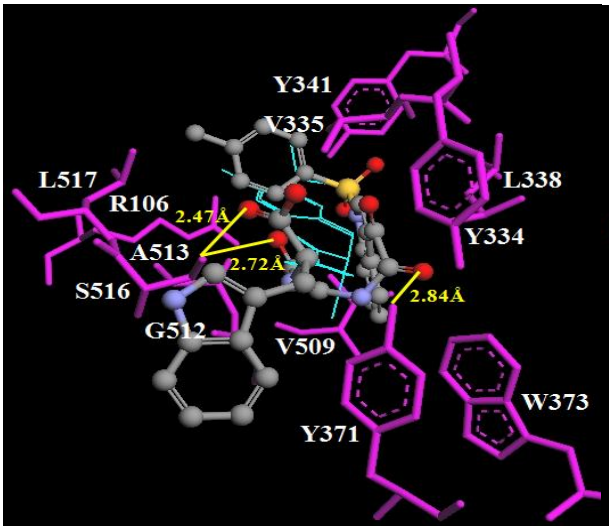

Figure S102.7c docked in the active site of COX/2 (pdb ID 3MQE)

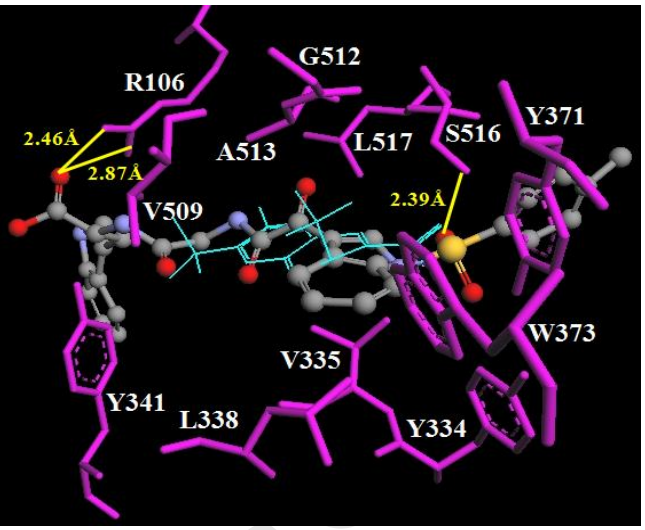

Figure S103.7d docked in the active site of COX/2 (pdb ID 3MQE)

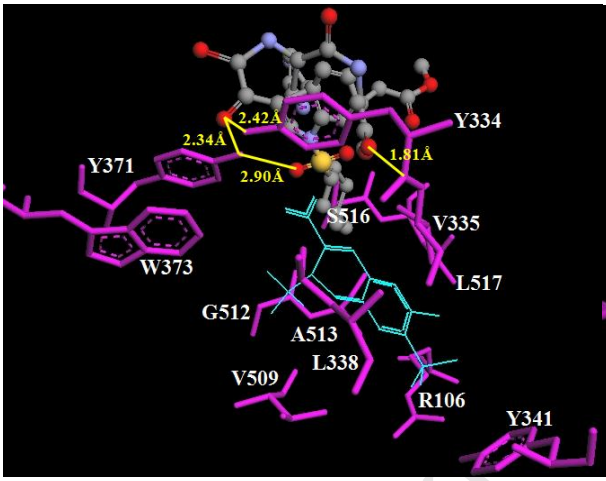

Figure S104.6e docked in the active site of COX/2 (pdb ID 3MQE)

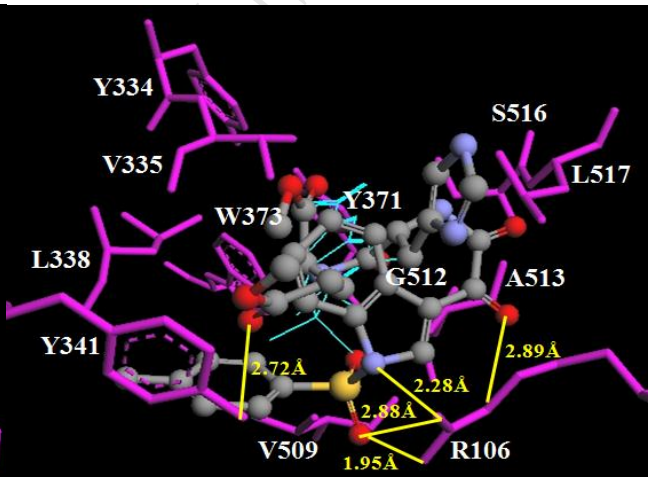

Figure S105.6h docked in the active site of COX/2 (pdb ID 3MQE)

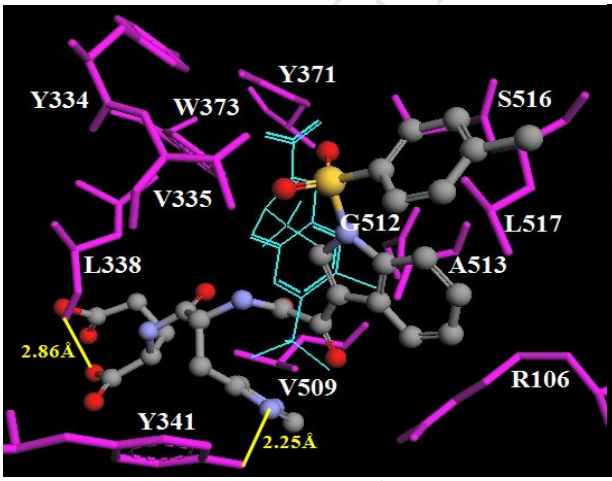

Figure S106.7e docked in the active site of COX/2 (pdb ID 3MQE)

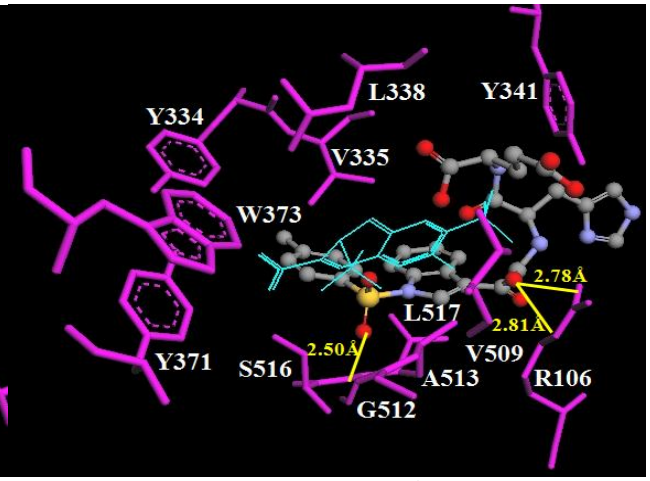

Figure S107.7h docked in the active site of COX/2 (pdb ID 3MQE)

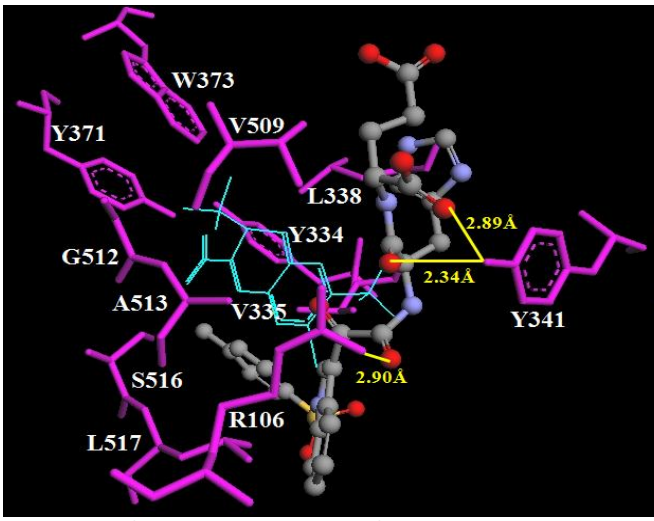

Figure S108.6f docked in the active site of COX/2 (pdb ID 3MQE)

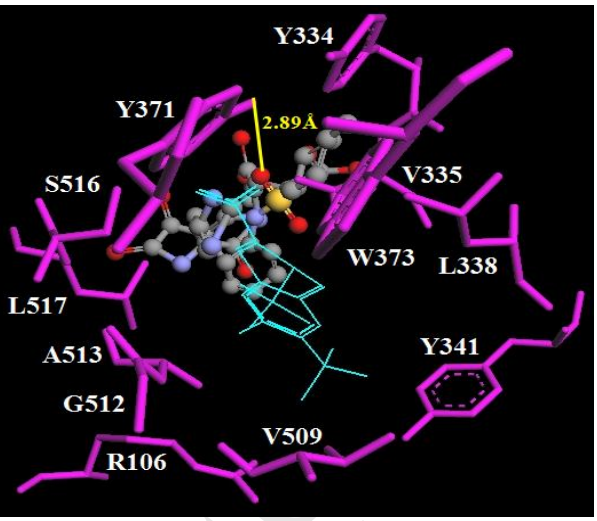

Figure S109.6g docked in the active site of COX/2 (pdb ID 3MQE)

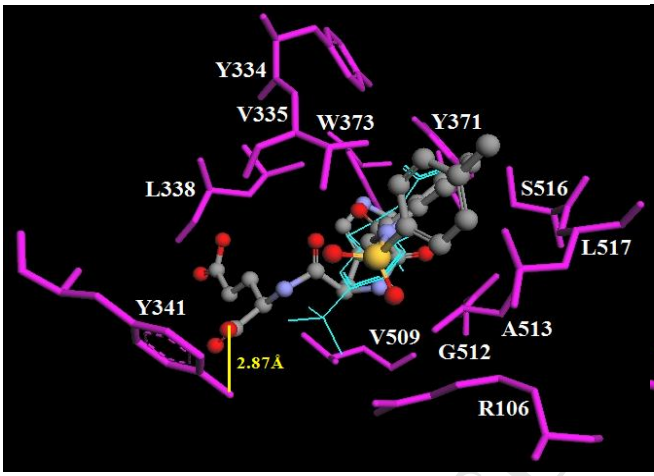

Figure S110.7f docked in the active site of COX/2 (pdb ID 3MQE)

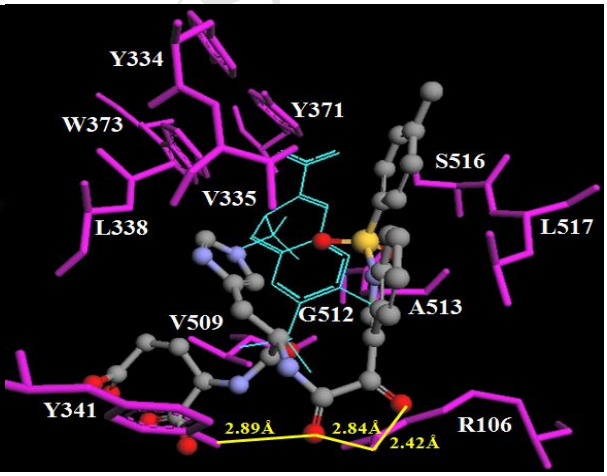

Figure S111.7g docked in the active site of COX/2 (pdb ID 3MQE)

ITC PROFILE

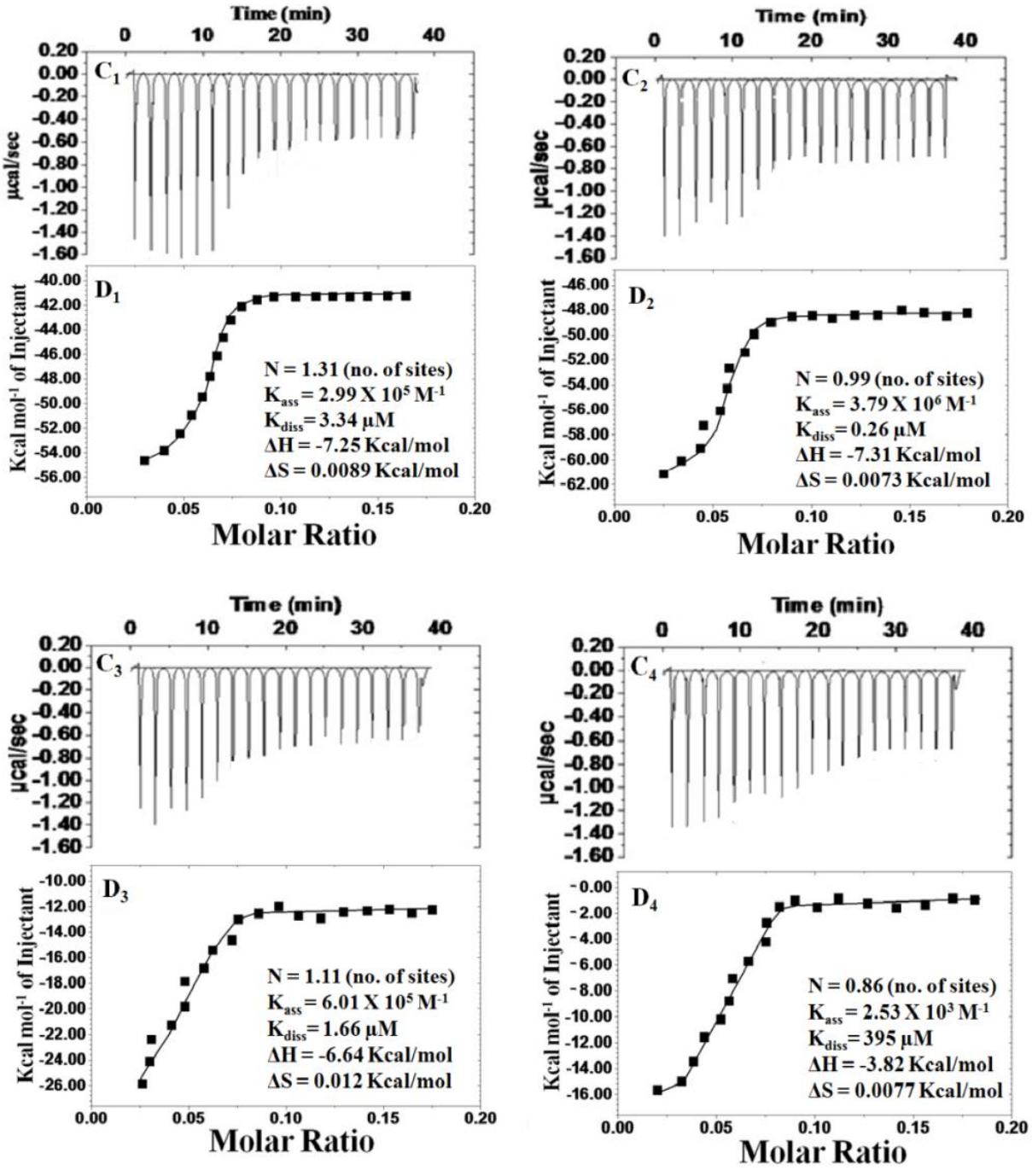

Fig. S112. Thermodynamics of interaction of Compounds 7 with the COX-2 enzyme. C_1, D_1: compound **7b**, C_2, D_2: compound **7d**, C_3, D_3: compound **7h** and C_4, D_4: compound **7i**. A. ITC raw data 19 x 2 µL injections, B. Integrated heat pulse data.

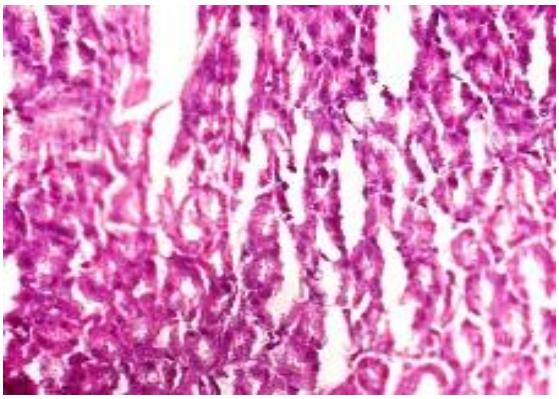

A

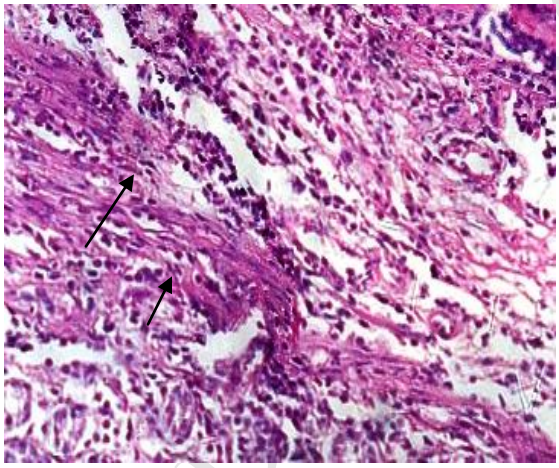

B

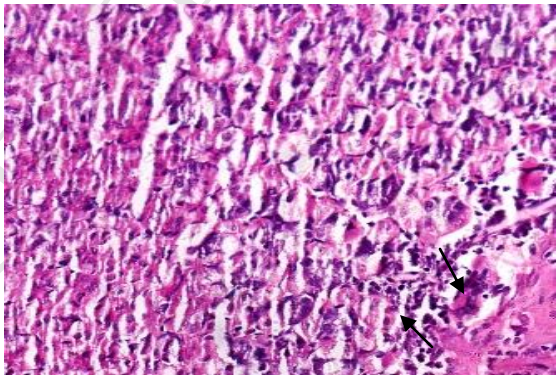

C

Figure S113. Photomicrographs of mice stomach showing normal structure (A), indomethacin treated showing inflammatory cells and extensive areas of necrosis (B) and compound treated showing lesser inflammatory cells and relatively decreased areas of necrosis (C).